UNIVERSITY OF SOUTHAMPTON

Novel Fabrication Techniques For Microfluidic Based *In-Situ* Oceanographic Nutrient Sensors *[e-Prints version]*

by

Iain R. G. Ogilvie

A thesis submitted in partial fulfillment for the degree of Doctor of Philosophy

in the

Faculty of Physical and Applied Sciences

Department of Electronics and Computer Science

September 2012

UNIVERSITY OF SOUTHAMPTON

ABSTRACT

FACULTY OF PHYSICAL AND APPLIED SCIENCES
DEPARTMENT OF ELECTRONICS AND COMPUTER SCIENCE

Doctor of Philosophy

by Iain R. G. Ogilvie

This work presents an investigation into the production of components for *in-situ* oceanographic nutrient sensors. These devices are based on a microfluidic chip platform, taking the lab-on-a-chip (LOC) system concept out of the laboratory and into a real world environment. The systems are designed to provide data on nutrient concentrations in the ocean and as such are built from robust low cost materials designed for deployments from 24 hours to 3 months. This report focuses on the challenges faced in designing a microfluidic system for these harsh deployment situations including a study of the relevant literature to indicate short falls in current technologies.

The aim of this work was to develop the next generation of microfluidic chip based nutrient sensors. A novel solvent vapour bonding technique has been developed for the production of polymer based microfluidic chips which produces robust chips while simultaneously reducing the surface roughness of the substrates during bonding. This has allowed micromilling of polymer substrates to quickly and easily develop new chip designs with optical quality features. The surface reduction technology has enabled development of a method to integrate absorbance cells into tinted PMMA devices which is also discussed. Integration of polymer membranes to produce valve and pump structures is discussed and a novel bonding technique for chemically robust Viton® membranes is demonstrated. The final chapter includes a discussion on system topologies, concentrating on the need for high resolution sampling and the implications on system design that arise. A novel multiplexed stop flow system is demonstrated. Questions about the role of traditional microfluidic components, such as mixers, in high-throughput low temporal response system designs are discussed and a microfluidic mixer suitable for some of these systems demonstrated.

Contents

List of Figures

List of Tables

Nomenclature

AFM	Atomic Force Microscope
APTES	(3-Aminopropyl)triethoxysilane
bar	a unit of pressure equal to 100 kilopascals
CAS number	Chemical Abstracts Service
cm	centimetre
CMM	Centre for Marine Microsystems
COC	cyclic olefin copolymer
CTD	Conductivity, Temperature and Depth
DI water	de-ionised water
dia.	diameter
dm	decimetre
D_m	molecular diffusion constant
e.g.	exempli gratia (for example)
ECS	Electronics and Computer Science
EHD	Electrohydrodynamics
EO	Electro-osmosis
EPSRC	Engineering and Physical Sciences Research Council
ER	electrorheological
FEP	fluorinated ethylene-propylene
FIA	flow-injection analysis
FKM	fluoroelastomer containing vinylidene fluoride monomer
g	grams
GPa	gigapascal
GPTMS	(3-glycidoxypropyl)trimethoxysilane
hr	hour
i.e.	id est (that is)
in-situ	in position
IPMC	ionic polymer-metal composites
IR	Infrared
kg	kilograms
kPa	kilopascal
L	Litre

LCD	Liquid crystal display
LCW	Liquid Core Waveguide
LD	Limit of Detection
LED	Light Emitting Diode
LOC	Lab on a Chip
LSI	Large Scale Integration
m	metre
mm	millimetre
MEMS	Micro-Electro-Mechanical Systems
mg	milligrams
MHD	Magnetohydrodynamics
MilliQ	deionized water, typically 18.2 MΩ ·cm
min	minute
ml	millilitre
mol	mole
MPa	megapascal
ms	millisecond
MSF	Multiplexed Stop Flow
mW	milliwatt
N	Newtons
NERC	Natural Environment Research Council
Ni	Nickel
nm	nanometre
NOC	National Oceanography Centre
PC	Personal Computer
PCB	Printed Circuit Board
PCI	Peripheral Component Interconnect
PDMS	Polydimethylsiloxane
Pe	Peclet Number
PEEK	Polyether ether ketone
PET	Polyethylene terephthalate
PFPE	perfluoropolyether
pH	a measure acidity
PMMA	Poly(methyl methacrylate)
PMMA-PGMA	poly(methyl methacrylateb-glycidyl methacrylate)
PP	Polypropylene
psi	pounds per square inch
PTFE	polytetrafluoroethylene
PU	PolyUrethane
Re	Reynolds number
R_t	A measure of surface roughness indicating the maximum height of the profile

s	second
SAR	Split and Re-combine
SEM	Scanning Electron Microscope
Si	Silicon
SIA	sequential injection analysis
SFA	segmented flow analysis
t_d	molecular diffusion time
Tg	Glass transition temperature
TMSPMA	3-(trimethoxysilyl) propyl methacrylate
t_r	residence time
UV	Ultraviolet
V	velocity
v/v	volume concentration
WMO	World Meteorological Organisation
λ	Darcy friction factor
μ	Fluid dynamic viscosity
μl	microlitre
μm	micron
μTAS	Micro Total Analysis System
ρ	Density
ϕ	concentration OR diameter
$\sim$	approximately
$\ll$	much smaller than
$\gg$	much greater than
$<$	smaller than
$>$	greater than
£	Pound sterling
°C	Degrees Celcius
%	percent
2.5D	refers to laminar multilayer constuction

Declaration of Authorship

I, IAIN RODNEY GEORGE OGILVIE declare that the thesis entitled
NOVEL FABRICATION TECHNIQUES FOR MICROFLUIDIC BASED IN-SITU OCEANOGRAPHIC NUTRIENT SENSORS
and the work presented in the thesis are both my own, and have been generated by me as the result of my own original research. I confirm that:

- this work was done wholly or mainly while in candidature for a research degree at this University;
- where any part of this thesis has previously been submitted for a degree or any other qualification at this University or any other institution, this has been clearly stated;
- where I have consulted the published work of others, this is always clearly attributed;
- where I have quoted from the work of others, the source is always given. With the exception of such quotations, this thesis is entirely my own work;
- I have acknowledged all main sources of help;
- where the thesis is based on work done by myself jointly with others, I have made clear exactly what was done by others and what I have contributed myself;
- parts of this work have been published as detailed in section 1.4

Signed:

Date: 1st September 2012

Acknowledgements

First I would like to recognise the guidance and support provided throughout this study by my three supervisors, Prof. M. Kraft, Dr. M. Mowlem and Dr. N. Harris. Special mention must also be made of Prof. H. Morgan who has provided regular guidance and many much needed challenges which have helped drive the work forward.

Further academic support has been provided by the post-doctoral researchers of the Centre of Marine Microsystems (CMM), especially Dr. C. Floquet and Dr. V. Sieben without whom this research would have not been possible. Working alongside these research fellows has provided the much needed encouragement and guidance essesntial to PhD study. Without their advice on time management, practical methodology and their contributions towards the improvement of written pieces this work would have failed at many of the early hurdles. Practical support has been provided by CMM technicians Lee Fowler and Rob Brown who have given more than just their practical skill, going out of their way to work long hours and provide technical feedback to ensure continual improvement of design work. The Engineering and Physical Sciences Research Council (E.P.S.R.C), Natural Environment Research Council (N.E.R.C) and School of Electronics and Computer Science (E.C.S) are also acknowledged for the funding required for this research.

Finally I would like to thank my friends, family and especially my wife who have provided love and support through many struggles faced during this study. Their encouragement, the provision of technical advice and continual supply of chocolate cake have certainly eased the burden.

- *À fin* -
"To the end"
(Ogilvie Clan Motto)

Chapter 1

Introduction

1.1 Project Description

The purpose of this study is to produce components for *in-situ* oceanographic nutrient sensor systems from robust low cost materials. These systems are used to measure the concentration of chemicals through wet chemical analysis (herein referred to as wet chemical sensors). Fluid handling components required on these devices include; mixers, pumps, valves and optical detection chambers. This report gives a brief review of the literature highlighting microfluidic devices that can be used to create these *in-situ* nutrient sensors and outlines the current contributions made by the author to this discipline. Many parts of the included work are essential for the creation of real world devices and enabling the development of future technologies.

This work was carried out at the Centre for Marine Microsystems (CMM) which is a part of the National Oceanography Centre (NOC) Southampton, UK. At CMM the team develops sensors for oceanographic applications which has allowed this author to explore the discipline while surrounded by experts in the field. This experience has aided the developments featured herein, especially in gaining knowledge and experience in the field while working with macro-systems.

If the final product is to be considered, then the desired outcome of this project is a microfluidic chip with integrated valves and pumps produced in robust, chemically resistant materials. The ability to handle all of the chemicals needed for oceanographic sensing is a key requirement in order that these chips can be used in real world environments. The system must also be physically robust as sensors often need to be deployed at depths of several thousand metres subjecting components to extreme pressures. Essentially this work is concerned with developing a platform to allow multiple nutrient sensor systems to be realised and as such scalability and flexibility are essential to the platforms success. The platform must also allow multiple chemical and control processes as well as the integration of external components where required. By addressing these issues the

developments contained within this document form the basis of the next generation of sensor systems and allow for even further development.

This thesis contains seven chapters: an introduction to the field of nutrient sensors in the ocean, a chapter on the development of a robust system platform, a chapter on the integration of an absorbance flow cell, a chapter on the integration of membranes to form valves and pumps, a chapter demonstrating these developments in the form of a high temporal response system, and a conclusion chapter. The four core chapters are based upon refereed journal publications.

1.2 Previous Work at CMM

Nutrient concentrations in the ocean have been studied since the early 20^{th} century as determination of these chemical concentrations aids understanding of the life-cycle processes taking place in the locale (Atkins (1923)). Traditionally bottled samples are taken and analysed in a laboratory either on-board ship or upon return to land. Recent developments have placed systems into the environment to provide better resolution and improved sample reliability where the time to analysis is short reducing sample degradation. Further reduction in size and cost of these systems will allow greater scope for collection of data and understanding of the ocean system processes.

Currently in development at CMM are a variety of sensors using colourimetric absorbance measurements to determine concentration of nutrients. These are outlined in the next chapter. Prior to this work the main focus of the research was into macro-scale systems (optofluidic channels >1 mm) built from commercial and custom built components joined with tubes, typically 0.6 or 0.8 mm internal diameter. This work has enabled the development of physically smaller devices operating in the microfluidic regime using smaller sample volumes.

A brief description previous development work at CMM is given in Appendix B.2.

1.3 Scope of Thesis: Development of a robust platform for colourimetric microfluidic nutrient sensor systems

To allow a greater scope of information to be gathered with oceanographic nutrient sensors they must be robust, portable and low cost (Patey et al. (2008)). The aim of this project is to address these issues by placing the analysis of the sample upon a microfluidic Lab-On-Chip platform. A number of nutrient detection chemistries have been considered and demonstration of phosphate measurement is used to highlight the benefits of moving to the new platform.

The first issue addressed was the lack of truly robust system platforms. In this work 'robust' is defined such that the system can withstand cyclic immersion in seawater to depths of 6000 m for a period greater than 3 months. During this time its performance and preferably its physical structure should not degrade such that reliable data continues to be returned. Also it should ideally remain in salvageable condition if lost at sea and subsequently recovered. The integration of many system components onto a single platform was essential; much of the delicacy within the previous generation systems is due to the interconnects and need for mechanical supports. In chapter 3 the manufacturing method presented allows for devices with integral connectors and the integration of channel structures (mixers, optical cells etc.) onto a single platform. Much of the robustness comes from the tough plastic substrates and also the reduction in the number of tubular interconnects. There is also provision for the integration of commercial valves while allowing for on-chip components where possible. This has been utilised in several published systems (Sieben et al. (2010), Floquet et al. (2011), Beaton et al. (2011)).

The second issue addressed was the integration of an absorbance flow cell for measurement of fluid optical properties. This was enabled by the robust platform developed in this work. In macro-scale systems the optical components are separate devices but integration onto the platform reduces system volume and cost. A solution is presented in chapter 4 which is simple to fabricate and does not affect the robustness of the rest of the system. The concept is scalable and as such has been adapted to multiple chemistries within the scope of the desired nutrients. It is also a low-cost method of providing the functionality as it requires little additional micromilling and does not require expensive commercial components.

The third consideration was the integration of membranes onto the system platform. These must be formed from an elastomer which is chemically robust (to handle all of the desired reagent chemistries) while flexible enough to seal with samples containing particles. A fluoropolymer Viton® material was chosen because of it chemical robustness and mechanical properties. The integration method is discussed in chapter 5 along with demonstration of valves manufactured in this material upon a systems platform compatible with that shown previously.

Finally all of these technologies were proved together through the production of a new system architecture. This was achieved by building and testing a multiplexed stop-flow system which can make measurements at a rate of >4 min^{-1} compared to $\sim$10 /hour for previous systems (Sieben et al. (2010)). This was only possible with the use of on-chip valves and provides a significant performance improvement over the previous generation of systems. Demonstration of this system and a comparison push-pull system is shown in chapter 6.

As such my thesis was broken down into four progressive sections which follow the development of the system components and demonstrate their use in a complete system.

1.3.1 Research Novelty

The novel aspects of the research presented in this document are: the fabrication of microfluidic devices in PMMA using a solvent vapour bonding process; the reduction of surface roughness in polymer substrates (PMMA and COC) through solvent vapour treatment; integration of optical absorbance cells into tinted PMMA devices; a method to integrate Viton® membranes into PMMA and COC devices; and a novel approach to sensor system design - the Multiplexed Stop Flow (MSF) system.

1.4 Publications and contributions

The work described herein was carried out between October 2007 and March 2011 within the Centre for Marine Microsystems (CMM) at the National Oceanography Centre (NOC) Southampton in collaboration with the Electronics and Computer Science (ECS) department of the University of Southampton, UK. Funding for this research has been provided by NERC, EPSRC and the seventh European Framework Programme.

This thesis is the result of my own work and I have attempted to include notes where research was done in collaboration. The content is based on the publications listed below. My contribution to each is given in Table 1.1. The full reference for each publication is given in the following bibliography.

1.4.1 Bibliography

Journal Papers

Iain R. G. Ogilvie, Vincent J. Sieben, Matthew C. Mowlem, and Hywel Morgan. Temporal optimization of microfluidic colorimetric sensors by use of multiplexed stop-flow architecture. *Analytical Chemistry*, 83(12):48144821, 2011. DOI: 10.1021/ac200463y

Iain R. G. Ogilvie, Vincent J. Sieben, Barbara Cortese, Matthew C. Mowlem, and Hywel Morgan. Chemically resistant microfluidic valves from viton® membranes bonded to coc and pmma. *Lab on a Chip*, 11(14):24552459, 2011. DOI: 10.1039/C1LC20069K

Alexander D. Beaton, Vincent J. Sieben, Cedric F. A. Floquet, Edward M. Waugh, Samer Abi Kaed Bey, **Iain R. G. Ogilvie**, Matthew C. Mowlem, and Hywel Morgan. An automated microfluidic colourimetric sensor applied in situ to determine nitrite concentration. *Sensors and Actuators B: Chemical*, 156(2):10091014, 2011. DOI: 10.1016/j.snb.2011.02.042

Cedric F. A. Floquet, Vincent J. Sieben, Ambra Milani, Etienne P. Joly, **Iain R. G. Ogilvie**, Hywel Morgan, and Matthew C. Mowlem. Nanomolar detection with high sen-

TABLE 1.1: Publications

Title	Type	My Contribution
Temporal optimisation of microfluidic colourimetric sensors by use of multiplexed stop-flow architecture Appendix A.4	Journal Article	Co-Author
Chemically resistant microfluidic valves from Viton® membranes bonded to COC and PMMA Appendix A.3	Technical Note	Lead Author
An automated microfluidic colorimetric sensor applied in situ to determine nitrite concentration Appendix A.5	Journal Article	Secondary Author
Nanomolar detection with high sensitivity microfluidic absorption cells manufactured in tinted PMMA for chemical analysis Appendix A.2	Technical Note	Secondary Author
Low-cost high sensitivity opto-fluidic absorption cell for chemical and biochemical analysis manufactured from coloured materials	Patent	Co-Inventor
Autonomous microfluidic sensors for nutrient detection: Applied to nitrite, nitrate, phosphate, manganese and iron Appendix A.8	Conference Paper	Secondary Author
Solvent processing of pmma and coc chips for bonding devices with optical quality surfaces Appendix A.7	Conference Paper	Lead Author
Reduction of Surface roughness for optical quality microfluidic devices in PMMA and COC Appendix A.1	Journal Article	Lead Author
Solvent Vapor Bonding and Surface Treatement Methods	Patent	Primary Inventor
Microfluidic colourimetric chemical analysis system: Application to nitrite detection Appendix A.6	Journal Article	Secondary Author

sitivity microfluidic absorption cells manufactured in tinted pmma for chemical analysis. *Talanta*, 84(1):235239, 2011. DOI: 10.1016/j.talanta.2010.12.026.

Iain R. G. Ogilvie, Vincent J. Sieben, Cedric F. A. Floquet, Robert Zmijan, Matthew C. Mowlem, and Hywel Morgan. Reduction of Surface roughness for optical quality

microfluidic devices in PMMA and COC, *Journal of Micromechanics and Microengineering*, 20, 065016, 2010. DOI: 10.1088/0960-1317/20/6/065016.

Vincent J. Sieben, Cedric F. A. Floquet, **Iain R. G. Ogilvie**, Matthew C. Mowlem, and Hywel Morgan. Microfluidic colourimetric chemical analysis system: Application to nitrite detection. *Analytical Methods*, 2:484491, 2010. DOI: 10.1039/c002672g.

Conference Proceedings

Vincent J. Sieben, Alexander D. Beaton, Cedric F. A. Floquet, Samer Abi Kaed Bey, **Iain R. G. Ogilvie**, Edward M. Waugh, Matthew C. Mowlem, and Hywel Morgan. Autonomous microfluidic sensors for nutrient detection: Applied to nitrite, nitrate, phosphate, manganese and iron, *Proceedings of MicroTAS 2010*, Groningen (The Netherlands), 3-7 October 2010, pp. 1016-1018.

Iain R. G. Ogilvie, Vincent J. Sieben, Cedric F. A. Floquet, Robert Zmijan, Matthew C. Mowlem, and Hywel Morgan. Solvent processing of pmma and coc chips for bonding devices with optical quality surfaces, *Proceedings of MicroTAS 2010*, Groningen (The Netherlands), 3-7 October 2010, pp. 1244-1246.

Patents

PCT/GB2011/050198: Cedric F. A. Floquet, Vincent J. Sieben, **Iain R. G. Ogilvie**, Hywel Morgan, and Matthew C. Mowlem. "Low-cost high sensitivity opto-fluidic absorption cell for chemical and biochemical analysis manufactured from coloured materials", filed February 2010.

US Application: 13/106,488: **Iain R. G. Ogilvie**, Vincent J. Sieben, Cedric F. A. Floquet, Matthew C. Mowlem, and Hywel Morgan. "Solvent Vapor Bonding and Surface Treatement Methods", filed May, 2011.

Chapter 2

Background

2.1 Sensors systems for the Ocean

2.1.1 Global System Models

If one is to believe the popular media then the future of humanity is very bleak. Recent Hollywood productions (such as *The Age of Stupid*, *The 11^{t}h Hour*, *The Day After Tomorrow* and *An Inconvenient Truth* among others) indicate that humanity has caused irreparable damage to the planet on which we live. Although these films often appear to have been produced with little regard to scientific literature, the fact that the subject matter is given attention shows that environmental issues are now important mainstream concerns.

Short and long term computer models exist for the prediction of weather allowing accurate forecasts to be made. Weather stations around the world collect data to a common standard governed by the World Meteorological Organisation (WMO) which is then distributed to weather forecasters. The Met Office in the UK is one such forecaster which runs continuous computer simulations based on the data provided in order to improve their model and predict future weather conditions. There are thousands of weather stations around the world (WMO) and the Met Office has been keeping records for over a hundred years. Consequently the combined human experience in this area is large and helps to give confidence in the computational models which output the forecasting data.

The oceans cover $\sim 2/3$ of the world's surface and although it is possible to understand the larger scale phenomena, such as ocean currents and large scale surface temperature variations, small scale effects are more difficult to model (WMO). The difficulties are two fold; firstly the physical scale of phenomena, such as algae blooms, may require metre length scale resolution and sub-hour time scale to accurately record them (Flewelling et al. (2005)). To understand the processes that occur within these sub-systems and the

effects they have on ocean systems as a whole there is a requirement to make constant measurements of a number of factors (temperature, salinity, pH, dissolved oxygen, nutrient concentrations etc.) at a variety of locations and depths across the ocean (Sellner et al. (2003)). Resolution of these factors at metre length and sub-hour time scales is currently very difficult and often prohibitively expensive (Rudnick et al. (2004)). However, to fully assess the future of our world we need to attempt to understand all of the sub-systems and their effects on the global ecosystem.

2.1.2 Collection of Data

Permanent fixed structures such as buoys can be used as deployment platforms for low-power sensors where suitable power installations (such as solar) are in place (WMO). These are well placed to collect data about water temperature and details on current flow direction and speed. Using buoys in this way provides thousands of deployment opportunities worldwide (WMO).

Other methods of deploying sensors to gather data involve some form of vehicle. The highest cost version of this is towing sensors behind scientific vessels. This allows high power instruments to be used but the high cost of running the ship makes this data rather expensive. For example the annual running cost of the four NERC scientific research vessels is approximately £13.5m per annum, or £9k per day per vessel, without including the capital costs or cost of the scientists and equipment for this time (NERC Accounts 2010). There are also semi-permanent installations on commercial and private vessels that are used to gather data (Petersen et al. (2003), Hydes et al. (2009), Chelsea Instruments, The International Seakeepers Society). These are often utilised in areas of great scientific interest or on commercial shipping routes. These systems are convenient because they gather data while the vessel is in motion with limited user intervention. However they are limited to deployments along shipping routes which are not necessarily of scientific interest.

Smaller vessels include gliders and the Argo float network (Rudnick et al. (2004), Gould et al. (2004)). Gliders use minimal buoyancy engine based propulsion to move very slowly through the water which conserves energy. They follow ocean streams, surfacing to transmit data and for physical collection at the end of their deployment (Rudnick et al. (2004)). These vehicles can cover hundreds of miles if required and allow the scientist to record data along a set route. Alternatively the Argo float network is a series of floating platforms which cycle their depth and float around the world on the ocean currents (Argo). These again transmit data when surfaced allowing remote deployment of sensors without user intervention. Another advantage of these systems is their relatively low cost; ~$15k at the time of writing (Argo). Consequently over 3000 Argo floats have been deployed in the ocean to date (Argo). Although convenient to gather un-manned data, both of these vehicles are limited in the amount of power they are able to provide

(limited by the on-board battery capacity) and their maximum payload (limited by the buoyancy change).

With the deployment opportunities in mind, optimisation of sensor systems to reduce physical size, reagent usage per sample and power consumption is required to reduce the cost per sample and allow large scale remote deployment of sensors for data collection.

2.1.3 Current Commercial Systems

This section contains a brief overview of commercially available sensor systems. The appearance of wet chemical sensors in scientific literature is discussed in chapter 6. There are a number of integrated oceanographic sensor systems that are available commercially for monitoring environmental conditions. Generally their size is much larger than potential LOC systems making them bench top solutions.

Flow through sensor stations for installation on ships and yachts measure the environment using water pumped from outside the hull (Chelsea Instruments, The International Seakeepers Society). Conventional macro sensors are used to measure water temperature, conductivity, concentration of Chlorophyll-a (Chelsea Instruments) as well as air temperature, salinity and acidity (pH) (The International Seakeepers Society). Data is then stored or transmitted to a remote data node on-board the vessel. The systems are around 1 m high and 0.5 m wide and deep, weighing 30-100 kilograms. Similar systems have been positioned along estuaries and water ways as well as at coastal stations (Southern California Coastal Ocean Observing System).

The are five commercial suppliers providing *in-situ* seawater monitoring systems. Sea-Bird Electronics Inc. produce systems for measuring conductivity, temperature and depth (CTD) as well as systems for sampling. These are around 100 mm in diameter, 0.5 m long and are able to provide on-board logging for other sensors if required. These systems can be towed behind a ship or submerged to depth to obtain samples that can be analysed in the lab. WET Labs also produce a CTD system alongside wet chemical analysers. These are capable of measuring dissolved oxygen, chlorophyll fluorescence and phosphate concentration. The systems are quite large; for example the phosphate system is 0.18 m diameter and 0.56 m long. It is capable of 2 measurements per hour which restricts the possible spacial resolution on moving deployments. WET Labs also manufacture the SubChemPak Analyzer for SubChem Systems Inc.. This system is designed for rapid *in-situ* measurement of dissolved Nitrogen species, Phosphate, Silicate and Iron upto 200 m depth. The system draws upto 80 W and is 0.6 m long and 0.12 m in diameter. Systea produce three *in-situ* deployable systems; Water in-situ analyzer (WIZ), Nutrients probe analyzer (NPA Pro.) and Deep-sea Probe Analyzer (DPA Pro.). These systems are capable of measuring Phosphate and Nitrogen species. The NPA is designed for deployment on buoys whereas the larger DPA is enclosed in pressure

housings for deeper deployments. The WIZ uses a smaller detection volume so reduces physical size while retaining the capability to take 1000 measurements as can the NPA and DPA. In contrast to the other systems which are wet chemical based, Satlantic Inc. build the ISUS and SUNA Nitrate sensor systems which measure concentration using a UV light absorption method. They are able to measure in the range of 500 nM to 2 mM with an accuracy of ± 2 μM. The systems are capable of deployments upto 100m, are 0.6 m long, approximately 0.1 m in diameter and weigh under 5 kg.

2.1.4 Nutrients of interest

Table 2.1 contains a list of the nutrients for which sensors are in development at CMM. Reagent details are provided to indicate materials compatibility issues which arise when building these wet chemical sensors.

TABLE 2.1: Nutrient species of interest for Wet Chemical Sensors

Nutrient	Reagent	Operating pH	Sample : Reagent	Measurement Wavelength	Reference
Nitrite/ Nitrate	Griess	pH 1-2	1:1	525 nm	Sieben et al. (2010)
Iron	Ferrozine	pH 5.5	50:1	562 nm	Stookey (1970)
Manganese	PAN	pH 10	16:3	569 nm	Chin et al. (1992)
Ammonia	OPA + sulphite	pH 11	2:1:1	375 nm	Amornthammarong et al. (2006)
Phosphate	'yellow method' ammonium molybdate ammonium metavanadate hydrochloric acid	-	-	380 nm	Bowden et al. (2002b)
Phosphate	'blue method'	-	-	715 nm or 900 nm	Murphy and Riley (1962)

As illustrated in Table 2.1 the systems are required to tolerate a wide range of acids and alkali chemicals. The materials must also be transparent to light from ultraviolet (UV) to infra red (IR).

2.1.5 Wet Chemical Sensor Operation overview

Wet chemical sensors use simple operations to perform very precise analysis of a sample (Figure 2.1). The sample is pumped into the system and mixed with a reagent which reacts with the chemical species of interest. This reaction causes a change in the optical

properties of the sample either through the formation of a dye or a change in the fluorescent properties. The next stage is optical detection which involves measuring either the absorption or fluorescence of the reacted sample stream. Comparison to the optical properties of the sample without the reagent, a blank or a standard gives a quantitative value for the chemical content.

The choice of procedure is dependent upon the specific chemistry of the nutrient, reagent used and the physical properties of the product. The chemistry of the contents inside the detection chamber is varied using a series of pumps and valves. Storage of the reagents, blanks and standards requires a flexible chamber (to allow for volumetric change) for which CMM utilise ethylene-vinyl-acetate reagent storage bags (Oxford Nutrition). Some of the reagents are also toxic so the reagent storage bags can be used to collect the waste where it cannot be vented to the surrounding environment.

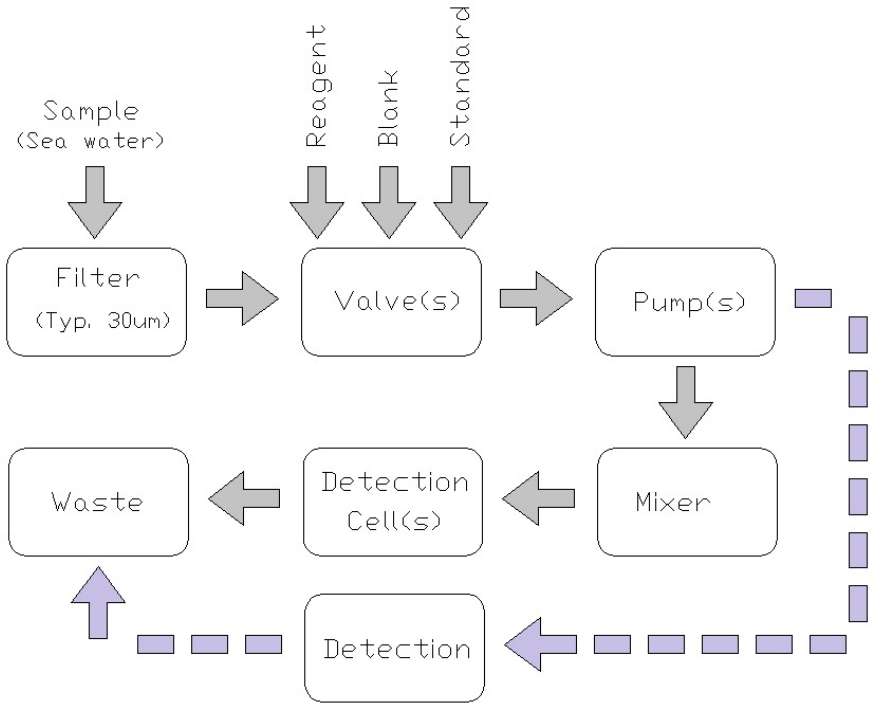

FIGURE 2.1: System diagram for typical wet chemical sensors used to measure the quantity of a nutrient in a fluid sample

The performance of devices is limited in some way by the fluidics of the system. A common problem is dead volume in the system. These are volumes in the system where fluid flows very slowly or is temporarily trapped. If present in the flow path for the sample this causes some portion of the previous sample to recirculate or reside in the system long after it should have been flushed through the system. As these dead volumes diffuse into the fluid stream they affect the chemistry of the current sample distorting the time history (i.e. causing unwanted integration in the measurement). In this way dead volumes affect the temporal performance of the system directly. As a compensatory measure the system can be flushed between samples to reduce the effects. Further flushing is re-

quired during each of the sample steps as the dead volumes need to be normalised to the current fluid being measured. This creates a delay before each reading can be made. In turn this increases sample size, time taken to make a measurement and reagent/blank/-standard consumption and storage requirements. By limiting dead volumes, and total system volume, these factors can be minimised. The move to microfluidic devices for these systems is therefore an obvious one.

2.2 Microfabrication and microfluidics

2.2.1 Miniaturisation:Micro Total Analysis Systems and Lab On Chip

With the advent of micro-fabrication techniques allowing the production of microprocessors in the 1970s, researchers produced microscale mechanical and fluidic devices using similar processes (Esashi et al. (1989)). These MicroElectroMechanical Systems (MEMS) are used for a variety of tasks, often as sensors built into electronic chips producing devices such as gyroscopes and accelerometers (Kraft et al. (1998), Xie and Fedder (2003)).

As well as enabling micro scale mechanical designs, the ability to manipulate fluids on such a small scale through these devices has allowed researchers to produce a Lab On Chip (LOC) solution to enable the analysis of small volumes of fluid. The ideal LOC device should emulate the functionality of laboratory equipment while *in-situ*. However many current generation devices are better described as Chip-In-Lab; the functionality of the system usually depends on bulky external equipment coupled into the fluidic chip (Weibel et al. (2005), Sieben et al. (2007), Taberham et al. (2008)). Ideally these systems would be stand alone and any external connections would be only for sample input, system waste output and a data stream creating a Micro Total Analysis System (μTAS).

Sensor systems for long term remote deployments are ideal candidates for the μTAS philosophy. Low power, simplicity and robustness are key in making these tools available to scientists around the world in order to improve the knowledge base associated with ocean nutrients.

2.2.2 Using Microfluidics In The Ocean

The ocean is a variable environment and as such systems designed to be operated within it must be robust. Rapid prototyping techniques for LOC systems are being developed for robust polymers to minimise development times. The techniques should also allow ease of commercialisation through current large scale manufacturing methods. These

prototyping techniques are detailed in chapter 3. By designing for mass production the scientific community is moving towards large scale distribution of devices at low cost.

There are further advantages which emerge with reduction of fluid volume within the system. The primary lower limit of the sample volume is the minimum system detection volume (dependant upon the detection method chosen to obtain the required sensitivity). Next is the required sample/reagent ratio. Optimisation of these factors enables the smallest reagent volume for measurement of each sample, in turn allowing more samples to be taken for the given reagent storage capacity. More samples can be taken without human intervention increasing the length of deployments for a given sampling rate, reducing the cost per sample. Reduction in reagent and sample use per measurement also reduces the volume of waste produced which is often dominant in space restricted applications. These considerations are discussed in further detail in chapter 6.

2.2.3 Microfluidic Fluid Interactions: Governing equations

2.2.3.1 General Equations

In microfluidic systems there are a number of governing equations which indicate how fluid will behave. The Reynolds number (Re) is used to determine whether the flow will be laminar or turbulent. It is given by equation 2.1 (Reynolds (1883), Douglas et al. (2001))

$$Re = \frac{\rho L V}{\mu} \tag{2.1}$$

Where ρ is the density of the fluid, V the velocity, L is a characteristic dimension of the channel and μ is the dynamic viscosity of the fluid. This dimensionless number is a measure of the ratio between the inertial forces and the viscous forces in the fluid channel. L is usually defined as the diameter of circular channels but in microfluidic devices, where channels are usually rectangular due to laminar construction, the channel width is used.

In conventional fluid theory, when the Reynolds numbers is below 2300 the flow is defined as laminar and above 4000 is turbulent. Between 2300 and 4000 the flow may be either, or a combination of, laminar or turbulent (Douglas et al. (2001)). In microfluidics, where Re<100 the flow is laminar but when $1 \ll \mathrm{Re} < 100$ inertial forces are still significant. When $\mathrm{Re} \ll 1$ viscous forces dominate and the flow is known as 'creeping' (Tabeling (2006)).

Comparing the performance of microfluidic devices may require calculation of the pressure drop (δP) across a device. Using the Darcy-Weisbach equation it is possible to calculate the pressure drop due to friction though a length of pipe (Douglas et al. (2001)).

This can be useful as it gives an indication of the magnitude of the pressure drop when dealing with complicated designs. The Darcy Weisbach equation is given by equation 2.2.

$$\delta P = \lambda \frac{L}{D} . \frac{\rho V^2}{2} \tag{2.2}$$

Where λ is the Darcy friction factor, L the length of pipe, D the diameter, ρ the density of the fluid and V is the velocity. For laminar flow regimes λ is defined as;

$$\lambda = \frac{64}{Re} \tag{2.3}$$

For turbulent flow regimes Moody diagrams are available which give values for λ which have been measured by experimentation (Douglas et al. (2001)).

2.2.3.2 Diffusion and Mixing

When studying microfluidic mixers it is useful to know how the flow conditions will affect mixing. The Peclet number is a dimensionless number which relates the rate of advection of a flow to its rate of diffusion. It is defined by equation 2.4 (Douglas et al. (2001))

$$Pe = \frac{LV}{D} \tag{2.4}$$

This equation is valid for cases of mass diffusion but not thermal diffusion. L is the characteristic length, V the velocity of the fluid and D the mass diffusivity. When the Peclet number is high (>1000) mass transport in the flow is convection dominated. Lower values indicate that it is diffusion dominated.

In microfluidic devices the Reynolds number is usually lower than 100 indicating laminar flow and a diffusion dominated regime for mass transport. However, the flow conditions can be encountered that result in a high Peclet number and that mixing will be driven by the fluid convection. This paradox shows that these equations merely give an indication of what will be happening in the fluid flow and are not definitive. An example of this is given in Appendix B.1.

A description of the mathematics of diffusion is given by Ficks first law (Fick (1855)) which relates the diffusive flux to the concentration field. In microfluidic systems where the Reynolds number indicates purely laminar flow, it is diffusion that allows mixing of fluids. Ficks first law is given by equation 2.5.

$$J = -D\nabla\phi \tag{2.5}$$

In this equation D is the diffusion coefficient measured in (m^2/s) which is a function of temperature, viscosity and particle size; given by the Einstein-Stokes relation (Einstein (1905), von Smoluchowski (1906)). ϕ is the substance concentration. The del operator (∇) is used when dealing with two or more dimensions. J is the diffusion flux measured in terms of the amount of substance moved over an area in a given time. For each dimension considered, J has the dimensions

$$\frac{mol}{m^2 s} \tag{2.6}$$

As the time taken for fluid to move through a chip is related to the channel length, for a given flux, a long channel will allow full mixing. Dimensional restraints may not make this possible so other approaches may be preferential. One approach is to increase the original concentration in order to create more flux; although this will not ensure full mixing is achieved quickly but rather that the initial concentration change is faster. The alternative, in order to achieve full mixing, is to increase the area over which the diffusion takes place. For a given volume of fluid this shortens the diffusive length and increases the area over which the diffusive boundary exists. In simple channel geometries this may mean splitting the fluid into multiple streams or twisting the fluid, as discussed in chapter 6. Using the smallest possible channels also reduces the total diffusive length, one of the benefits of microfluidics.

In systems which use sequential plugs of fluid the work by Taylor (1953) and Aris (1956) describes how the length of a plug will change as it moves through the system. Even in systems where the diffusion coefficient is low, axial diffusion can appear high due to the parabolic flow profile of the fluid causing plugs to lengthen. The seminal work by Taylor (1953) and Aris (1956) gives the dispersion coefficient (K) for a circular pipe as:

$$K = D_m(1 + \alpha Pe^2) = D_m\left[1 + \frac{1}{48}\left(\frac{Ua}{D_m}\right)^2\right] = D_m\left[1 + \frac{1}{192}\left(\frac{u_0 a}{D_m}\right)^2\right] \tag{2.7}$$

where Pe is the Peclet number, α is a constant, U is the mean flow velocity and u_o is the peak flow velocity, a is the pipe radius and D_m is the molecular diffusion constant. The constant $\alpha = 1/48$ (for pipes) is a function of the profile of flow; for piston flow (electro-osmotic flow), $\alpha = 0$ and $K = D_m$ (no dispersion, only molecular diffusion) (Aris (1956)). This model was modified for other channel cross-sections (Chatwin and Sullivan (1982), Dutta and Leighton (2001), Dutta et al. (2006)):

$$K = D_m \left[1 + \frac{1}{210} f\left(\frac{d}{W}\right) \left(\frac{Ud}{D_m}\right)^2 \right] \tag{2.8}$$

where the constant α is in two parts: the value 1/210 maintains unity with the parallel plate geometry, and *f(d/W)* is a function that depends on the exact geometry of the channel, with d the narrower cross-sectional dimension of the channel and W the greater of the two. Since dispersion scales with the square of channel dimensions, the dimensions should be as small as possible, but small channels create large pressure drops in flow through systems.

For Taylor-Aris dispersion theory to be applicable, the sample residence time in the channel must be long enough for the diffusing molecules to sample all the transverse streamlines before exiting the system (i.e. the cross-sectional diffusion time must be less than the longitudinal residence time) (Dorfman and Brenner (2001)). The system parameters must satisfy the following inequality (Ajdari et al. (2006)):

$$t_r \gg t_d \rightarrow \frac{L}{U} \gg \kappa \frac{a^2}{D_m} \tag{2.9}$$

where t_r is the residence time, t_d is the molecular diffusion time in the cross-section, L is the channel length and κ is a numerical prefactor that depends on channel geometry. The original work of Taylor considered a pipe with radius α and $\kappa = 1/96$ (Taylor (1953)). Dutta et al. (2006) determined $\kappa \approx 1/20$ for rectangular channels (a is replaced with W) and Ajdari et al. (2006) determined κ for shallow channels of varying geometries.

The dispersion profile for non-circular channels has been calculated by a number of authors (Dutta and Leighton (2001), Dutta et al. (2006), Kolev (1995)) and Chatwin and Sullivan (1982) provided a model for determining dispersivity in rectangular channels. For rectangular channels, Chatwin and Sullivan (1982) presented the exact solution for dispersion, below:

$$K = \frac{1}{4D_m} \left[2 \sum_{\substack{p \ even \\ \geq 2}} \left(\frac{a}{p\pi}\right)^2 W_{p0}^2 + 2 \sum_{\substack{q \ even \\ \geq 2}} \left(\frac{b}{q\pi}\right)^2 W_{0q}^2 + \sum_{\substack{p \ even \\ \geq 2}} \sum_{\substack{q \ even \\ \geq 2}} \frac{W_{pq}^2}{(p\pi/a)^2 + (q\pi/b)^2} \right] \tag{2.10}$$

$$\left.\begin{aligned} W_{p0} &= -\frac{32Gab^3}{\mu\pi^5}\sum_{n\ odd}\frac{tanh(n\pi a/2b)}{n^3(n^2a^2+p^2b^2}), \\ W_{0q} &= -\frac{2Gb^2}{\mu\pi^2q^2}\left\{1+\frac{8}{\pi^2}\sum_{n\ odd}\frac{q^2}{n^2(n^2-q^2)}\left[\frac{tanh(n\pi a/2b)}{n\pi a/2b}\right]\right\}, \\ W_{pq} &= -\frac{64Gab^3}{\mu\pi^5}\sum_{n\ odd}\frac{tanh(n\pi a/2b)}{n(n^2-q^2}\frac{1}{n^2a^2+p^2b^2}, \end{aligned}\right\}$$

Where a is the channel width, b is the channel height (where $a > b$), G is the pressure gradient and D_m is the molecular diffusion constant. From this, *f(d/W)* can be determined as the ratio of K/D_o0 where K is the exact dispersion for a rectangular geometry and D_0 is the dispersion for a parallel plate geometry, shown in Figure 2.2. For other channel cross-sections see Dutta and Leighton (2001) and Dutta et al. (2006) for *f(d/W)* and Bahrami et al. (2006) for pressure drop and velocity profiles. Dutta and Leighton (2001) also present an approximation to simply calculate the *f(d/W)* for rectangular channels, plotted in Figure 2.2.

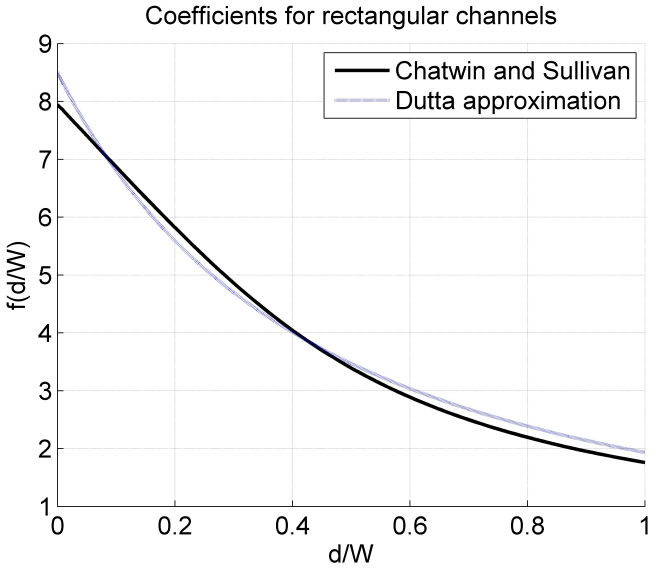

FIGURE 2.2: Coefficients for different channel geometries

To determine the final output plug profile from an arbitrary input plug profile, convolution of the dispersion impulse response function can be used. The concentration impulse function (one-dimensional along the axis of flow) is described by Socolofsky and Jirka (2002) as:

$$C(z,t) = \frac{M}{A\sqrt{4\pi Dt}}e^{\frac{-z^2}{4Dt}} \tag{2.11}$$

where t is time, z is the distance with respect to profile length (axially) , M is the total mass of a mixture, A is the cross sectional area ($M/A = 1$, unit area) and D is the diffusion coefficient (in this case the dispersivity coefficient)(Socolofsky and Jirka (2002)). In chapter 6 this is used to generate theoretical output profiles by performing convolution on the input pulse as:

$$Output(z,t) = Input(z) * C(z,t) \tag{2.12}$$

Chapter 3

Manufacturing Robust Microfluidic devices

This chapter is based upon the published manuscript in Appendix A.1. Figure 3.3 and Figure 3.5 were produced by Dr. Vincent Sieben for the manuscript and Figure 3.4 is based upon pictures provided by Robert Zmijan. They are included in this chapter thanks to the permission of these colleagues.

3.1 Introduction to microfluidic device manufacture

3.1.1 Material requirements for oceanographic sensor chip

The intention of this work is to produce a robust LOC solution for long term remote oceanographic chemical monitoring. Materials choices should allow production of the devices as cheaply and easily as possible. In order that these devices become commonplace and a large scope of data can be obtained they must be affordable.

Materials used in the microfluidic chip must be able to withstand chemicals with a wide range of pH values (Table 2.1). The reagents used to detect the species of interest range from acidic to alkaline. Ideally the chips will also be able to cope with a variety of solvents as these may be used for diluting solutions or cleaning purposes. The porosity of the substrates will be of interest in this area as swelling and uptake of sample are likely to degrade performance regarding detection limits. Consequently non-porous and non-swelling material combinations will be required for optimal performance.

Finally the materials choice must allow for mass production of robust devices. If these are to become widespread in use then time consuming processes which require expensive equipment and materials will increase price and reduce the likelihood of adoption. The

devices must be robust to withstand the environmental conditions to which they will be subjected as well as general handling and delivery.

This chapter concentrates on the production of a robust, rigid, optically transparent, microfluidic platform which allows the integration of external components and microfluidic channels. The further integration of membranes onto this platform is described in chapter 5.

3.1.2 Materials and manufacturing techniques

3.1.2.1 Historical manufacturing technologies

Traditionally microfluidic devices have grown up alongside microprocessor research and as such early devices were created using Silicon technology as the processes for manufacture were well defined (Esashi et al. (1989)). Simple channels and complex pump designs were developed (Esashi et al. (1989), Gerlach et al. (1995)). However Silicon is not ideal for rapid prototyping of devices as it is expensive to process small batch sizes (Zengerle et al. (1995)). It is also a fragile material so handling of devices must be performed carefully adding time to the manufacturing processes. The requirement for a clean room for anodic bonding of silicon (and glass) substrates quickly led to the development of other technologies.

Silicon continued to be used as a substrate but a liquid polymer layer was spun on top from which channels could be made. SU8 epoxy resins are often used as they can be easily exposed to UV light to cure them and developed using solvents (Lorenz et al. (1997)). These can be used to produce high aspect ratio features (e.g. >10:1 (MicroChem Corp.)) with good optical transmittance (absorbance <1.5 for 500 μm thick film for wavelengths above 400 nm (MicroChem Corp.)) and mechanical properties (Youngs Modulus = 2 GPa, Yield stress = 60 MPa (MicroChem Corp.)). These operations usually require a mask to ensure correct UV exposure. Features can be produced as small as 30 nm with a mask produced by vapour deposition and ion beam milling of metal patterned onto a glass substrate (Prober et al. (1980)). High resolution inkjet printing on acetate can be used for less accurate requirements where features are $\geq$20μm (Duffy et al. (1998)). For constantly changing designs it has been shown that an LCD display can be used as a mask if projection techniques are to be used, reducing cost and shortening development time (Itoga et al. (2008)). Other techniques that do not require a physical mask are reviewed in section 3.1.2.2. Where strength and toughness is required, metals can be used as a substrate as an alternative to silicon or even metal layers sputtered onto a silicon base (Svasek et al. (2004)). The adhesion of SU8 to both metal and silicon allows electrodes to be manufactured inside channels and adhesion to partially cured SU8 provides an easy way to bond enclosed channels. Other photoresists have been used which have

some advantages over SU8, such as 1002F which has reduced fluorescence. However, SU8 epoxies remain very popular (Pai et al. (2007)).

Lamination of a glass substrate and an Epoxy film allowed the development of a photolithographic process not dissimilar to those used with Silicon with the capability of bonding using just an oven. The laminate often used is Ordyl SY300/500 series (Elga Europe) which has good chemical resistance and is easy to work with (Vulto et al. (2005), Taberham (2008)). Other laminates have also been used such as AZ 4620 photoresist (Elga Europe) (Chen et al. (2007)). By utilising these materials simple devices can be realised in a semi-clean room environment and the development cost of devices is reduced. There are some difficulties present though. Designs cannot simply be transferred from Silicon to this new process due to the material limitations. Valves and pumps that previously used the etching of Silicon to produce thin stiff flaps and membranes cannot be transferred directly as the epoxy is not as robust as the silicon crystal substrate, limiting extreme changes in geometry at the required scales.

When softer lithography is needed to produce flexible structures the use of polydimethylsiloxane (PDMS) is widespread. Once again a photolithographic process is used but this time it is to produce a master from which the PDMS can be cast. Once cast the PDMS can be adhered to glass or similar substrates using oxygen plasma treatments, forming an optically clear channel through which fluid can be passed (Duffy et al. (1998)). Pumps and valves can be realised simply by creating a series of chambers which can be contracted and expanded, as discussed in later chapters. Flap valves made from PDMS provide good sealing of channels and it can also be used as a hinge and support for on chip structures (Loverich et al. (2006), Nguyen et al. (2008)).

3.1.2.2 Current manufacturing technologies

A number of groups are developing inexpensive microfluidic fabrication methods for polymer substrates that reduce dependence on a clean room. Techniques include hot embossing (Becker and Heim (2000), Kricka et al. (2002), Studer et al. (2002), Steigert et al. (2007), Becker and Gärtner (2000), Qi et al. (2002)), casting and injection moulding (Effenhauser et al. (1997)), direct write processes such as wax printer prototyping (Kaigala et al. (2007)) and stereolithography (Tse et al. (2003)), powder blasting, laser and mechanical micromachining (Friedrich and Vasile (1996), Heng et al. (2006), Bundgaard et al. (2004)), and dry film laminating (Vulto et al. (2005)). Techniques such as hot embossing, casting and injection moulding produce high quality devices with optical quality surfaces. However, these methods require masters (often made from SU8 or Si/Ni) that are fabricated in clean rooms. Injection moulding requires a precision metal master, which is expensive and unsuited to rapid-prototyping (Steigert et al. (2007)). Novel materials such as polystyrene (Shrinkydinks) have also been used to create microfluidic chips (Grimes et al. (2008)) although with poor dimensional accuracy caused

by shrinking of the substrates. Wax printing produces a poor surface finish and low aspect ratio devices (Kaigala et al. (2007)). Stereolithography has been used to produce microfluidic devices and microsensor packages (Tse et al. (2003)), where structures are created by curing a liquid resin with a laser; but surface roughness is often on the micron scale. Therefore, many of the current rapid prototyping techniques show promise for low-cost realisation of microfluidic designs, but they often compromise optical quality, are not cost-effective or retain some dependence on clean room facilities.

When building colourimetric nutrient sensors the optical clarity and stability of the substrate is important. The substrate must be transparent over a wide range of wavelengths (Table 2.1) and must not degrade significantly over time. An example of an unsuitable polymer is Polycarbonate which, although optically clear when fresh from the manufacturer, turns yellow after long term exposure to UV light (Ogonczyk et al. (2010)). Consequently PMMA and cyclic olefin copolymer (COC) were chosen for this work and are frequently used in microfluidic applications. They are low-cost and biocompatible thermopolymers with good optical properties transparent to light from UV to IR (Evonik Röhm Gmbh, TOPAS Advanced Polymers GmbH). PMMA and COC are also chemically robust and do not dissolve easily in organic solvents unlike other transparent plastics such as polystyrene.

Features are often created in these polymers by hot-embossing (Becker and Heim (2000), Kricka et al. (2002), Studer et al. (2002), Steigert et al. (2007), Becker and Gärtner (2000), Qi et al. (2002)) and injection moulding and yield high-quality surfaces, where the roughness can be of the order of 10 nm (Bundgaard et al. (2006)). Alternatively, micromilling is a relatively simple technique which is widely used to manufacture PCBs and can produce channel features down to 50 μm, sufficient for most microfluidic applications (Friedrich and Vasile (1996), Bundgaard et al. (2004), Yan et al. (2009)). The design to chip cycle is fast, typically a few hours, and the method has low running cost ($\sim$ £25/hr). As with most milling methods, it is able to produce 3D structures (often difficult with optical lithography techniques (Bertsch et al. (1999))), and a wide range of materials can be processed including most polymers and even stainless steel (Becker and Gärtner (2000)). Despite these advantages over typical microfabrication techniques, the surface roughness obtained by micromilling is generally quite poor (Steigert et al. (2007)) (hundreds of nanometres (Lee and Dornfeld (2004))) and is nowhere near optical grade, i.e. <10 nm (Kuo Yung et al. (2008)).

To improve the surface quality, a number of post-processing methods have been developed, including thermal cycling (Lian and Ling (2002)) and surface coating; both solid (static) (Tsao et al. (2007), Nakajima et al. (2001), Noh et al. (2004)) and liquid phase (dynamic) (Belder and Ludwig (2003)). Thermal cycling can be used to lower the surface roughness of PMMA; for example, heating the material from room temperature to 60 °C for 30 minutes (below the glass transition temperature) and cooling again reduces roughness without affecting features dimensions (Lian and Ling (2002)). Solid (static)

coatings (Tsao et al. (2007), Nakajima et al. (2001), Noh et al. (2004)) rely on complex protocols for coating channel walls, whilst liquid coatings (Belder and Ludwig (2003)) can be expensive or difficult to implement. Interestingly, exposure to a solvent vapour has been shown to modify the surface roughness of PMMA-PGMA copolymers by causing migration of the polymer chains separating each copolymer species (Prokhorova et al. (2003)). This effect reversed when the solvent migrated out of the surface and has only been shown with this specific co-polymer species. The smoothing is also only observed on already relatively smooth surfaces where the roughness changes from >70 nm to <10 nm. Surface smoothing techniques may also enable production of micro-systems including high-quality integrated optical elements (the vast majority) manufactured using technologies such as laser ablation; post ablation surface roughness >100 nm (Huang et al. (2010)). Currently the application of such treatments to microfluidics is still in its infancy .

After features have been created, various techniques are used to seal a lid onto the processed substrate to close the microchannels (Becker and Gärtner (2000)). Thermal bonding is typically used (Tsao and DeVoe (2009), Martynova et al. (1997)), but this produces a weak bond (<1 MPa). Surface treatment or adhesive may used (Sung et al. (2001), Lei et al. (2004), Chen et al. (2004)) to improve the bond strength; for example, dissimilar polymer layers can be used for bonding with microwave welding (Yussuf et al. (2005)), but such methods add extra processing steps and complexity. Solvent bonding provides an alternative method of sealing devices, giving high bond strengths and monolithic devices (ideal for chemical and biological compatibility).

TABLE 3.1: A summary of previous work utilising solvent bonding methods with PMMA

Author	Solvent	Exposure Method	Bonding Parameters	Bond Strength
Shah 2006	Acetone	80 μl injected through channel	1.1 MPa, 5 min	0.55 MPa (80 psi)
Klank 2002	Ethanol	10 min soak	90 min, 85 °C	–
Hsu 2007	Isopropanol	Dipped	24.5 kPa, 6 min, 80 °C	24 MPa (lap shear)
Sun 2007	Dimethyl sulfoxide	300 μl droplets	10 min	–
Brown 2006	47.5% dimethyl sulfoxide, 47.5% water, 5% methanol	Droplets applied to surface	3 kN, 30 min, 85 °C	5.5 MPa
Ng 2008	isopropanol	Soaked	155 kPa, 10 min, 70 °C	2.9 MPa (lap shear)
Lin 2007	20% ethylene dichloride, 80% ethanol	Droplets applied to surface	100 kPa, 5 min, 20 °C	3.8 MPa
Griebel 2004	isopentylacetate	Stamped	'tightly pressed' for 10 min	-
Kelly 2005	acetonitrile	400 μl droplets	14 kPa, 2 min	15.5 MPa (2250 psi)
Koesdjojo 2008	1-1-dichloroethane	300 μl droplets	21 kPa, 2 min	13.8 MPa (2000 psi)

In solvent bonding a thin (∼2 μm (Wallow et al. (2007))) surface layer is softened by exposure to solvent. Two halves are brought into contact and when the solvent evaporates the substrates are bonded. Application of a solvent in a controlled manner is key to producing a uniform and strong bond, and to ensure that no channel collapse occurs (Koesdjojo et al. (2008), Hsu and Chen (2007)). Solvent can be introduced

TABLE 3.2: A summary of previous work utilising solvent bonding methods with COC

Author	Solvent	Exposure Method	Bonding Parameters	Bond Strength
Wallow 2007	ethanol/decalin	15 min at 21 °C	1.2 MPa, 35 min, 60 °C	13.1 MPa (1900 psi)
Ro 2006	methylcyclohexane	3 min (vapour)	690 kPa, 10 min, 70 °C	-
Mair 2007	cyclohexane	90 s (vapour)	178 kPa, 3 min, followed by UV exposure	34.6 MPa
Chen 2008	cyclohexane	90 s (vapour)	-	9.3 MPa (1350 psi)
Liu 2007	methylcyclohexane	1 min (vapour)	1.4 MPa, 10 min, 40 °C	-

through capillary action (Shah et al. (2006)), soaked into the surface (Koesdjojo et al. (2008), Hsu and Chen (2007), Klank et al. (2002), Koesdjojo et al. (2009), Sun et al. (2007), Kelly et al. (2005), Griebel et al. (2004), Brown et al. (2006), Ng et al. (2008)) or applied through a vapour (Mair et al. (2007), Sauer-Budge et al. (2009), Ro et al. (2006), Liu et al. (2007)); the optimum process depends upon the actual polymer and solvent type. Channel collapse is a frequent problem (Koesdjojo et al. (2008), Lin et al. (2007)), but can be avoided in a number of ways including filling channels with ice (Koesdjojo et al. (2008)) or optimisation of solvent exposure time (Koesdjojo et al. (2009), Lin et al. (2007)). Channel collapse can be caused by overexposure to solvent, excessive heat during bonding, overpressure or non-uniformities in the applied pressure (Hsu and Chen (2007), Koesdjojo et al. (2009). The bond strength is improved with solvents which are less polar, or elevated temperature and pressure during bonding (Hsu and Chen (2007)). A summary of published solvent bonding techniques are shown in Tables 3.1 and 3.2.

3.1.3 Comparing microfluidic polymer substrates

TABLE 3.3: Comparison of COC and PMMA polymers

Property	COC	PMMA	Notes
Cost	$\sim$ £ 11 K /m^3	$\sim$ £ 3.5 K /m^3	based on purchase price
Colours available	1	> 10	-
Water Absorption	< 0.01 %	2 %	by mass after 24 hrs
Optical Transmittance	91 % (>350 nm)	92 % (>450 nm)	for transparent PMMA
Tensile Strength	46-63 MPa	72 MPa	-
Glass Transition Temp	75-170°C	103°C	-

The data in table 3.3 is based on literature from TOPAS Advanced Polymers GmbH and Evonik Röhm Gmbh (Plexiglas XT). This brief overview highlights the similarities in the mechanical properties of COC and PMMA materials. COC is relatively more expensive but is available in a variety of different grades with variable glass transition temperature and tensile strength. PMMA however is a popular commercial product which keeps the price lower and means multiple material colours are available. For systems where water absorption is of particular concern the very low absorption of COC may be advantageous.

3.2 Materials and Methods

3.2.1 Solvent vapour bonding and surface reduction technique

3.2.1.1 Preparation of substrates

PMMA sheets (thicknesses from 1.5 mm to 8 mm) obtained from Evonik Röhm Gmbh, and cyclic-olefin copolymer (COC) wafers (0.7 mm and 1.2 mm) from TOPAS Advanced Polymers GmbH (Grade 5013) were used to optimise the solvent vapour technique. Channels were fabricated by micromilling with an LPKF Protomat S100 micro-mill which was used to mill channels and cut out the substrates. Ports/threads for MINSTAC microfluidic connectors (The Lee Company USA) were also machined into the plastics prior to bonding. The design was created using Circuitcam software (LPKF Laser & Electronics AG), which calculates tool paths. This data was then imported into BoardMaster software (LPKF Laser & Electronics AG) which controls the micromill. The two halves were aligned using a custom made jig (Figure B.4 in Appendix B.3.5) prior to solvent bonding. Both structures were pushed into a corner and pressed together to secure them (Figure 3.1). This provided an alignment accuracy of typically 20μm, discussed in Appendix B.3.5.

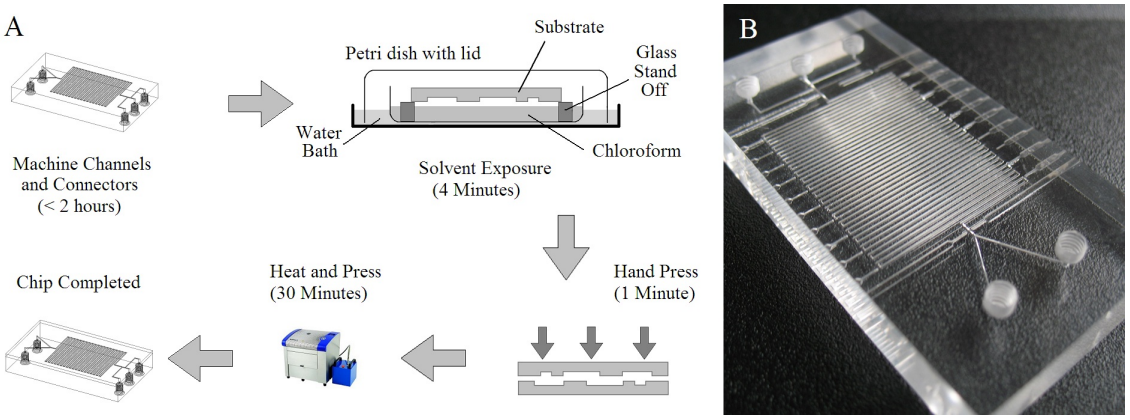

FIGURE 3.1: A. method for smoothing and bonding polymer substrates using solvent vapour, B. an example of a chip produced in PMMA

3.2.1.2 Solvent bonding method

Prior to solvent exposure the substrates need to be thoroughly cleaned with detergent, then rinsed in DI water in an ultrasonic bath. Substrates were subsequently rinsed in isopropanol followed by ethanol, and dried with nitrogen to ensure cleanliness and consequently uniform application of solvent vapour. Solvent vapour exposure was performed by suspending the substrates above a bath of solvent in a 100 mm diameter glass petri dish with lid. Four glass stand-offs 6 mm high were placed in the petri dish and approximately 30 ml of solvent (chloroform or cyclohexane) added to bring the level to

within 2 mm of the top of the standoffs. If glass stand offs are not available these can be substituted with stainless steel M10 nuts which does not appear to have any negative effect on the process.

Although chloroform and cyclohexane were used in this study based on availability, presumably other solvents described in reference (Hansen and Just (2001)) with similar Hildebrand total solubility parameters would suffice after optimisation. The substrates are placed on top of the stand offs and the lid placed over the whole assembly. The temperature of the assembly is controlled to 25 °C using a water bath which is essential if a number of devices are to be bonded in a batch process. If the temperature is not controlled the evaporation of the solvent causes cooling of the assembly reducing the density of the vapour atmosphere producing ineffective bonding. After 4 minutes of exposure the substrates are carefully removed. The parts are then aligned using a jig (such as Figure B.4 in Appendix B.3.5) and pressed together by hand to partially bond the substrates. They are then transferred to a hot press (LPKF Multipress) pre-heated to 65 °C where a pressure of 140 N/cm^2 is applied for 20 min. The press is then actively cooled to room temperature over 10 min. The chips are removed from the press and left to settle for 12 hours, improving bond strength by allowing excess solvent to migrate out of the substrates.

PMMA substrates are exposed to chloroform and COC to cyclohexane. This entire process is shown schematically in (Figure 3.1), together with a photograph of a finished microfluidic chip manufactured in PMMA.

After micromilling and solvent exposure, the micro-channels were examined using an Atomic Force Microscope and Scanning Electron Microscopy. The bond strength was characterised with an ASTM D1876 T-Peel test (ASTM (2008)) using an Instron 5569 tensile testing machine (Instron).

3.2.1.3 Surface roughness reduction method

If surface roughness reduction is required without bonding of substrates then the process is similar. Again the the substrates need to be thoroughly cleaned with detergent, then rinsed in DI water, isopropanol and ethanol before being dried with nitrogen. Solvent vapour exposure is performed as described in 3.2.1.2. After 4 minutes of exposure the substrates are carefully removed. The substrates are then left to settle for 12 hours allowing the solvent to migrate out of the surfaces. The substrates should be placed in a sealed chamber to ensure the surfaces remain clean.

3.3 Results and Discussion

3.3.1 Surface roughness measurements

Figure 3.2 shows an SEM of a microchannel milled in PMMA and COC immediately after machining, showing the typical quality obtained with a micro-mill. After milling the typical surface roughness was 100-200 nm R_t measured using AFM across the floor of the channel (Figure 3.3). Following vapour exposure the surface roughness was reduced substantially to typically less than 15 nm, close to the quality of the virgin wafers (<5 nm). When only a temperature cycle was performed (i.e. milling then a heat cycle with no solvent exposure), the surface roughness was reduced from 100-200 nm to 70 nm, suggesting that the smoothing was predominantly from exposure to the solvent vapour. Figure 3.2 (B and D) show SEMs of the treated surfaces and the AFM surface roughness data is summarised in Figure 3.3. The reduction in surface roughness is significant and returns the material surface close to the virgin quality. This simple solvent exposure technique is applicable to a range of different manufacturing methods such as laser ablation (Friedrich and Vasile (1996)).

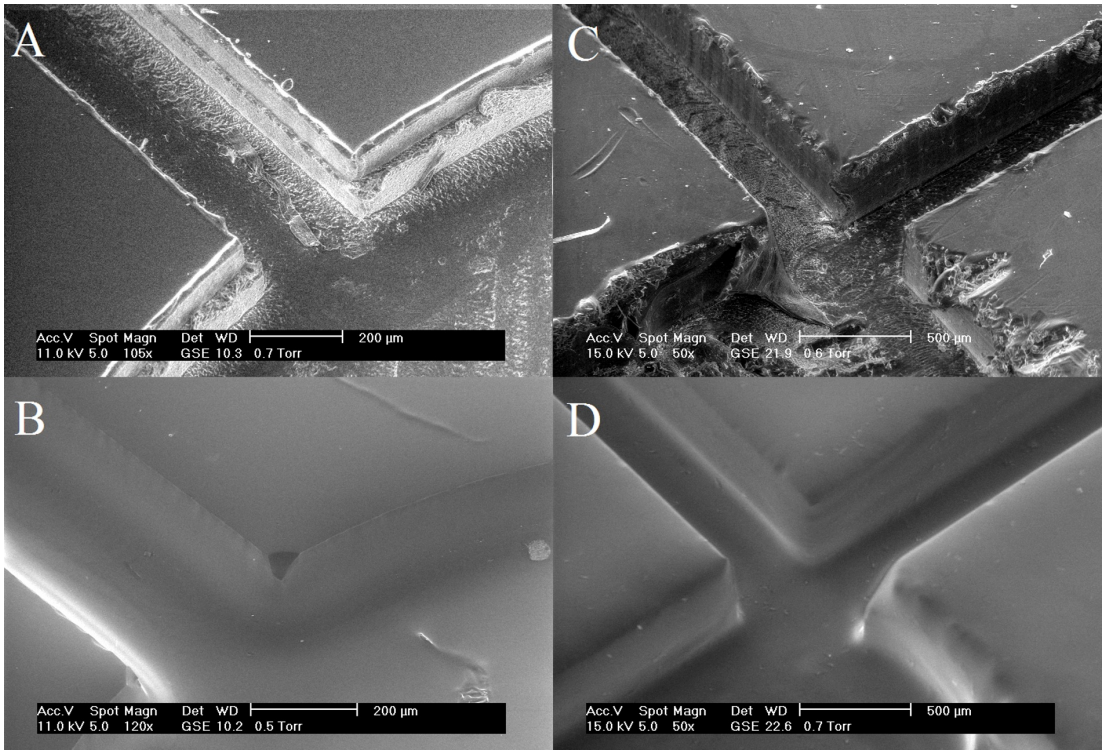

FIGURE 3.2: SEM images of microchannel (200 μm depth was achieved with two 100 μm cuts) demonstrating the smoothing effect of exposure to a solvent vapour;(A)PMMA post-milling;(B)PMMA after 4 min. chloroform solvent vapour and 30 min, 60 °C heat cycle; (C)COC post-milling (D)COC after 4 min. cyclohexane solvent vapour and 30 min, 60 °C heat cycle

Vapour exposure of the surface is much easier to control than exposure to a liquid solvent, particularly where the surface is topographically diverse (Wallow et al. (2007)).

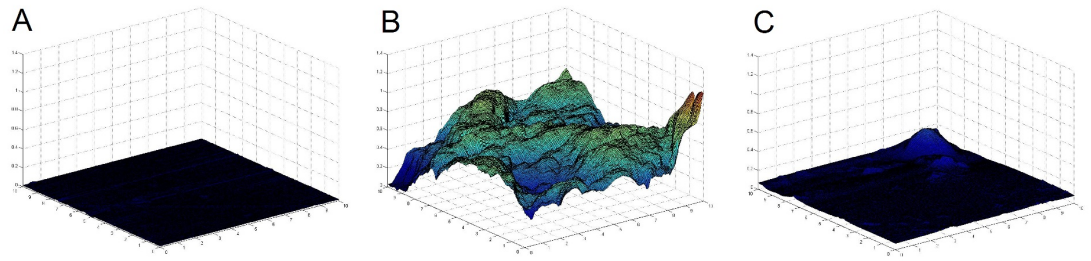

FIGURE 3.3: AFM scans for PMMA:(A) factory surface finish;(B) base of the milled channel;(C) base of the milled channel after 4 min chloroform solvent vapour exposure and 30 min, 60 °C heat cycle. Graph units are in microns.

The controlled delivery and uptake of solvent to the surface is achieved by exposure to a saturated vapour atmosphere. The thin solvent-saturated surface layer causes re-flow of the polymer and thereby smoothes out rough features; it also creates a gradient in the polymer viscosity in a shallow region at the surface. This profile enables mixing of the two polymer layers during bonding under pressure and temperature. Lin et al. (2007) characterised the impact of solvent treatment on surface roughness after bonding PMMA by exposure to a liquid solvent. The surface roughness of an embossed channel increased from 13.4 nm to 18 nm after coating the surface in solvent (20 % (by weight) 1,2-dichloroethane and 80 % ethanol) (Lin et al. (2007)). This liquid exposure method increased the surface roughness; whereas, the vapour exposure method presented here reduces the roughness on all the surfaces in the chip.

To further evaluate the surface smoothing effect, a planar cylindrical micro-lens (radius of 150 μm) was micro-milled, which collimates light across a microchannel. Figure 3.4 shows the chip implementation of the lens in PMMA. The light was launched into the microchip via a Thorlabs Ltd. (2010) HPSC 10 fibre (10 μm core, 0.11 N.A. silica fibre) coupled with a laser diode; 635 nm, 7 mW fibre output power (LDCU 12/9145, Power Technology Inc. (2010)). The channel dimensions were 250 μm deep by 250 μm wide. In order to raytrace the light, the channel was filled with DI water and 200 nm silica particles (PSi-0.2, G.Kisker) at a concentration of 0.5 mg ml^{-1} (100 fold dilution). Figure 3.4(A) shows the microchip after micro-milling and before solvent vapour treatment; the lens is ineffective as shown by the degree of light scattering at the interfaces and the degradation of the beam profile across the channel. Figure 3.4(B) shows the improvement of the lens performance after the solvent vapour treatment. Both Figure 3.4(A) and (B) were acquired with identical camera exposure times and settings.

3.3.2 Bond strength measurement

A major problem with solvent bonding techniques is channel collapse, e.g. Qi et al. (2002). The exposure time for solvent bonding was optimised and 4 minutes was found to be best; shorter exposures led to bond failure and non-uniformity over larger areas

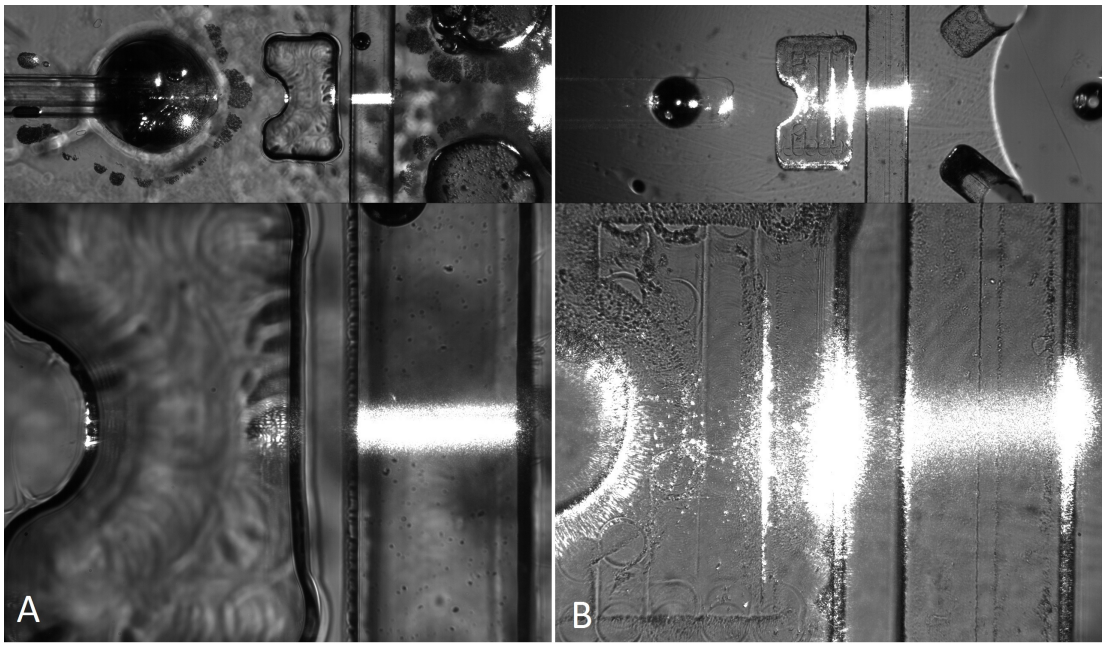

FIGURE 3.4: A planar cylindrical lens (radius of 150 μm) micro-milled in PMMA collimates light across a channel (A) The improvement in the lens performance after solvent vapour treatment. (B) For comparison this picture shows the chip after micromilling and before solvent vapour treatment; the lens is ineffective as shown by the degree of light scattering at the interfaces and the poor quality of the light beam across the channel

(most noticeable with exposure times less than 220 seconds), while longer exposures caused channel collapse (in excess of 255 seconds). The optimum bond pressure was also determined experimentally; higher pressures (greater than ~180 N/cm^2) led to channel deformation and eventual collapse. Figure 3.5 shows an example of the channel cross-section for a PMMA bonded chip. The channels are the same dimensions as in Figure 3.2, 250 μm wide and 200 μm deep. The final bonded structure shows little deformation and the bonded region is not visible to the naked eye; it is only visible when samples are broken and the cross section viewed under a microscope. The fractures that appear in this image are not from the bond, but from the process used to cross-section the wafer. The small lips on the inside corners of the channels on the right hand side occur because of small shifts in one half relative to the other during the bonding process. Channels that were assembled without use of the LPKF press did not show this deformation. The deformation also manifests as a misalignment if alignment pins are removed prior to placement of the substrates into the press. This is not observed with substrates bonded using clamps which retain their alignment if the pins are removed after the pre-pressing stage.

The bond strength was measured from the peak peel force required for delamination. Figure 3.6 shows a summary of the force as a function of time of exposure to solvent (at 140 N/cm^2) and pressure (for 4 minutes exposure) during bonding. For PMMA,

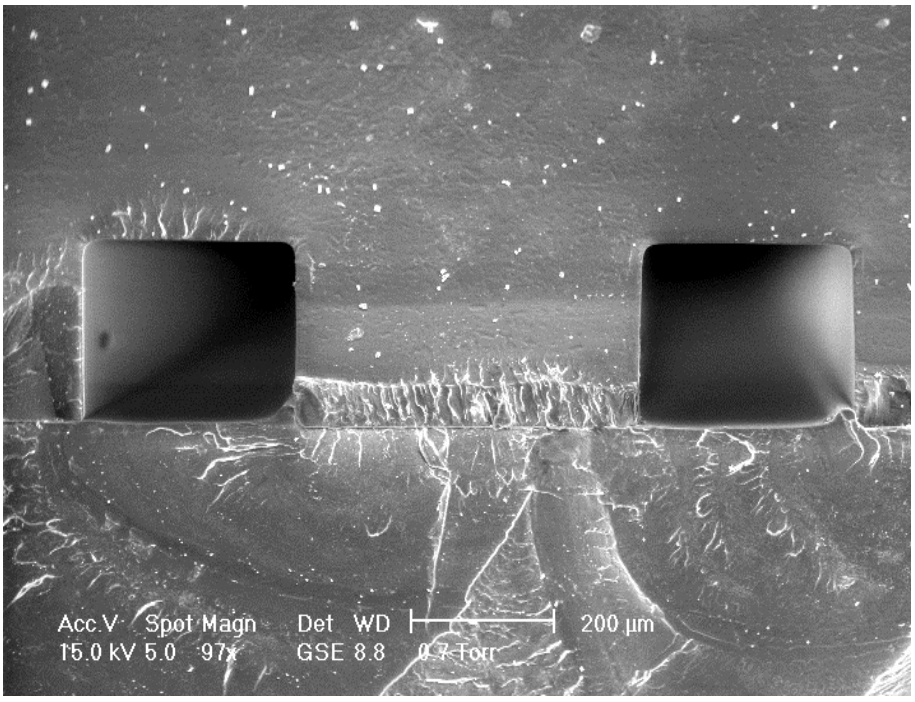

FIGURE 3.5: SEM image of microchannel cross section showing the smooth finish on the final channel walls and square cross section.

the data shows that the bond pressure has little influence on the bond strength; devices could be assembled by hand and cured in an oven. However, this method leaves some regions unbonded because residual stress in the material causes deformation in the plastic during the heating and cooling cycles. Therefore, some small pressure (greater than $\sim$100 N/cm^2) is recommended for optimum bond uniformity. Length of exposure to solvent has a large effect; doubling the exposure time doubles the bond strength. The reliability of this process is in excess of 95 %[1]even on larger designs where uniform bonds, without any inclusions, have been achieved on chip sizes that range from 15 mm by 70 mm to 80 mm by 100 mm.

For Topas 5013 COC the picture is rather different; reproducibility is such that only half of all samples bond well. The reasons for this are not clear, but may be due to variations in the quality of the Topas 5013 COC wafers or migration of the separate polymer species during solvent exposure, as discussed in Prokhorova et al. (2003) for PGMA-PMMA copolymers. This would produce substrates with surfaces of varying polymer composition. The data shown in Figure 3.6 is only for devices that had bonded. Variation of the solvent exposure time causes similar effects in COC to those observed in PMMA, but there is a clear advantage in using higher bond pressures. The data shows

[1]This figure is a conservative estimate based upon the feedback given by the group at CMM. The group has used this technique almost daily since mid 2009 and have bonded in excess of two hundred microfluidic chips, jigs and assemblies. Prior to late 2009 (when the cleaning process was refined to that included here) there were a number of failures, but none have been reported since then. An example of this was during a testing period in August 2010 where this author bonded 8 batches of 12 devices in which there were no failures.

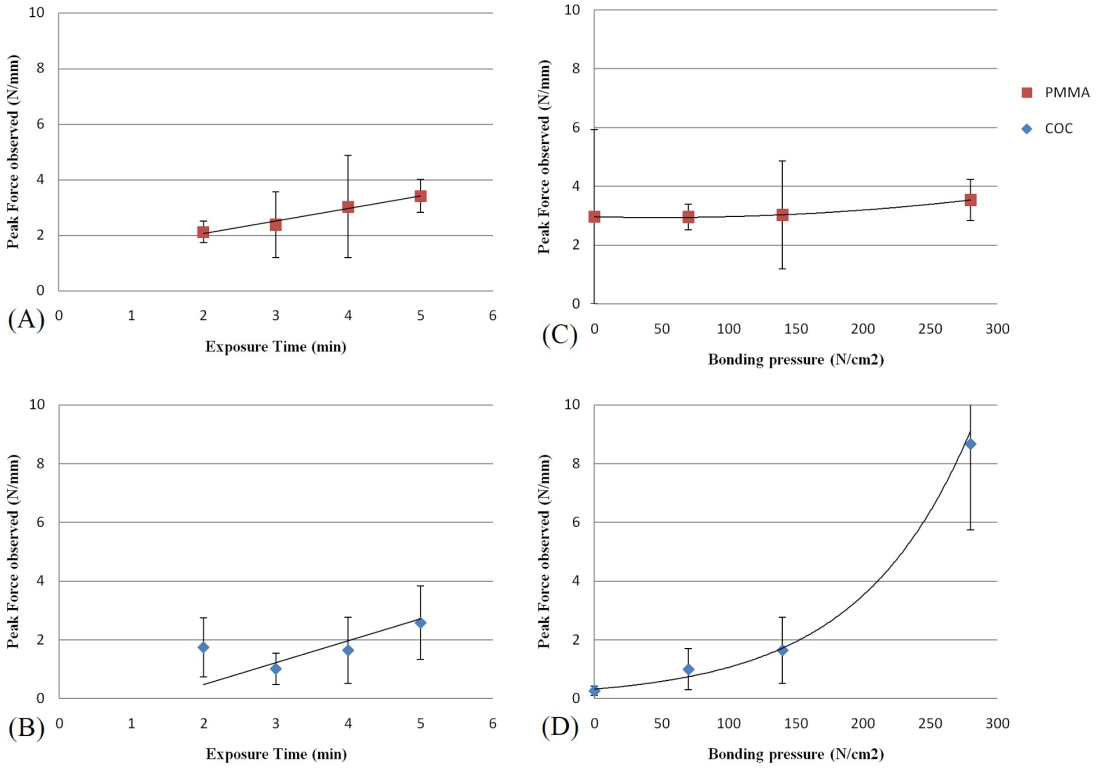

FIGURE 3.6: Effect of the exposure time on the peak peel force (A)PMMA; (B)COC; effect of bonding pressure on the peak peel force (C)PMMA; (D)COC

that a high pressure produces a stronger bond, but for the 250 μm channels used in this work, the optimum pressure without channel distortion was found to be 140 N/cm^2. In all cases the bond temperature must be set well below the glass transition temperature of the material to minimise the possibility of channel deformation, for example the Tg of PMMA is 115 °C (Becker and Gärtner (2000), Evonik Röhm Gmbh), and the bond temperature was set to 65 °C. Bonding of other grades of COC was attempted and it was found that the exposure time for lower Tg grades was considerably lower (for Topas 8007, Tg = 78 °C, the optimal vapour exposure was 35 seconds) and exposure time was higher for grades with higher Tg (for Topas 6015, Tg = 158 °C, the optimal vapour exposure was 5.5 min., Tg data is available from the TOPAS datasheets). It was difficult to obtain reliable bonds with the lower Tg grades as they are easily over exposed causing channel collapse, whilst the higher grades showed lower reproducibility of bond strengths.

In general, the mechanism responsible for the strong bonding is not well understood; however, in Ng et al. (2008) a simple mechanistic process is described. They postulated that the bond strength depends on the degree of polymer chain entanglement and the thickness of the diffuse interface. Solvent bonding creates a longer interaction length than thermal bonding (Ng et al. (2008)). They also attempted to link solubility to solvent strength and temperature without reaching any conclusions. The material production method may modify the uptake of solvent vapour, possibly due to different

cross-linking densities in the material, altering the total cohesive energy of the van der Waals forces. For example, extruded PMMA polymer had an optimum exposure time of 1.5 min, but cast PMMA required 4 min exposure. Each polymer/solvent combination requires optimisation of exposure times to minimise channel collapse and maximise surface smoothing and bond strength.

3.3.3 Lap shear testing

The bond strength of PMMA and COC samples was also tested using lap shear testing. This test involves bonding two substrates such that a portion of the substrate over laps the other. Clamps were applied to the unbonded substrate ends allowing them to be pulled apart. The samples tested were 1.5 mm thick, 30 mm wide and 70 mm long (per substrate). They were bonded such that the overlapping region was 10 mm ($\pm$ 0.5 mm) as this was the minimum that could be bonded within a useful tolerance (0.5 mm provides a 5 % error). Unfortunately this did not allow failure of the substrates in shear; instead they failed in tension across the 1.5 mm thick sections with cracks propagating from the edges. It is likely the failures started at saw marks along the edges. Without further investigation it is not possible to quantify the ultimate bond shear strength but it is possible to say it is in excess of 160 kPa. This estimated value is at least an order of magnitude smaller than those shown in tables 3.1 and 3.2 but the actual bond strength may prove comparable with further investigation.

3.4 Conclusions

This chapter demonstrates a rapid procedure for the manufacture of optical quality microfluidic devices in PMMA and COC. The channels were fabricated using micromilling using a 250 μm diameter milling cutter (20,000 rpm, 5 mm s^{-}1). It has been shown that exposure of the polymers to an appropriate solvent vapour (chloroform for PMMA, cyclohexane for COC) leads to significant reduction in surface roughness. The reflow of polymer when exposed to solvent vapour reduces the surface roughness from 200 nm to 15 nm. This reduction in roughness is comparable to that shown by Prokhorova et al. (2003) for PMMA-PGMA copolymer species but differs in that the effect is irreversible and uses PMMA and COC substrates. The technique given in this chapter is also simple to implement as it uses a vapour chamber constructed from a Petri dish rather than the pumped liquid cell used by Prokhorova et al. (2003). This novel surface treatment methodology may complement other rapid fabrication techniques for low-cost and high-quality microfluidic prototyping.

This method of bonding is independent of the manufacturing technique used to produce the structured substrates so can be applied to injection moulded devices as well as

micromilled chips. The advantage with utilising this technique for micromilled chips is the reduction in surface roughness which is due to the softening of the surface by the solvent vapour allowing the polymer to reflow. During solvent vapour exposure this effect can be observed as the post exposed surface visually appears to lose any roughness due to the micromilling, becoming once again transparent. This work was published in the Journal of Micromechanics and Microengineering (the published manuscript is included in Appendix A.1) and has since been adopted by four research groups known to this author.

Other bonding related observations made during this work are featured in Appendix B.7.

In the next chapter the design of an optical absorption cell is discussed. The chosen design can be integrated into devices manufactured with the methods detailed in this chapter.

Chapter 4

Integration of Absorbance Flow Cell

This chapter provides a discussion of possible methods to integrate optical flow cells into polymeric microfluidic devices and how this was refined into a practical technique. Working alongside Dr. Cedric Floquet the method described has been developed. While this author cannot claim full credit for the invention the development of the idea occurred during a brain storming session with Dr. Floquet and we agree there is a shared ownership. This discussion provided much of the following content and so here Dr. Floquet's contribution is acknowledged. These concepts were also used alongside contributions from colleagues at CMM to produce a manuscript published as a short communication in the journal Talanta. The published manuscript is included in Appendix A.2.

4.1 Introduction to absorbance flow cells

As the main focus of this work is on the manufacture of devices rather than characterisation and performance the following review is kept brief. A methodology for measuring very low open ocean concentrations of nutrients is required for implementation on microfluidic devices used in wet chemical sensors. Although methods measuring the fluorescence of a sample can be used, here absorbance methods are discussed as these are widely used for measuring the nutrients of concern.

4.1.1 Absorbance flow cells in literature

Colourimetric assays for determination of Nitrate / Nitrite (Griess (1879)), Phosphate (Atkins (1923)), Iron (Stookey (1970)) and Manganese (Chin et al. (1992)) are clearly defined in literature and have been used for a long time due to their ability to measure

a wide concentration range making them ideal for very low nutrient open ocean samples (Patey et al. (2008)). These methods have been used in both laboratories (Grasshoff et al. (1999)) as well as on ship (Armstrong et al. (1967)), and more recently as *in-situ* systems (Hanson (2000), Thouron et al. (2003), Adornato et al. (2005), Sieben et al. (2010)).

The fluidic and optical sub-systems in colourimetric analytical systems are both important in determining the system performance. Fluid is flowed through a fixed length optical cell, the length of which gives the absorbance length determining the concentration range over which useful measurements can be made. The idealised relationship between the measured optical power, absorbance and chemical concentration is described by the Bouguer-Beer-Lambert law (Bouguer (1729), Lambert (1760), Beer (1852)). A brief explanation of the mathematics of this law are given in Appendix B.5.

A number of different approaches to integration and miniaturisation of microfluidic absorption cells exist, many use thin and transparent materials to manufacture microchannel absorption cells (Hunt and Wilkinson (2008)). This approach is problematic because whilst these designs allow for low dead volumes in their opto-fluidic integration, the cells absorption length is typically short and stray light degrades performance. Masking of excitation source and detector in areas of the system where transmission of light is undesirable (i.e. using absorbing paints and opaque covers) can reduce these effects. However this approach does not necessarily reduce background environmental noise (although negligible in deployed under water systems) and also adds to the manufacturing cost of each device. Kuswandi et al. (2007) and Hunt and Wilkinson (2008) recently reviewed opto-fluidic integration highlighting recent advances, including absorption cell design.

The use of optical fibres for launching and collecting light can aid the rejection of stray light as the fibre can be positioned close to U-shaped (e.g. Liang et al. (1996)) or Z shaped channels (e.g Greenway et al. (1999)). It can be difficult to align the fibre and the opto-fluidic path to fully exclude stray light and optical power loss is present in coupling between fibres, sources and detectors. Coupling of out of plane sources and detectors to 10 mm long absorption cells using total internal reflection at an air interface in polymeric devices (Grumann et al. (2006)) can simplify this problem but stray light reduction still relies on collimation of the laser source used. For consideration in ocean going sensors air interfaces are not suitable as support structures will be required when systems are required to go to high ambient pressures at deep depths.

Lenses have been used to increase coupling efficiencies and can reduce stray light, but require fabrication of small highly accurate features and relatively short (500 μm) channels (Ro et al. (2005)). The manufacture of lenses is possible as shown in Figure 3.4 but again the use of optical fibres for robust systems is not ideal. Short path lengths are also not sufficient as resolution and limit of detection are proportional to length. Typical cell

lengths in macro systems are greater than 10 mm.

The use of liquid core waveguides (LCWs) enables both long path lengths and stray light rejection (Datta et al. (2003), Du et al. (2005), Duggan et al. (2003), Manor et al. (2003)). However LCWs require complex fabrication making integration into microfluidic chips difficult. Designs frequently rely on internal Teflon AF coatings that have poor long term performance which can be overcome with glass liners but this also adds further manufacturing complexity. Even with a glass coating surface changes (such as biofouling or microbubbles) have a large effect on the transmitted light as the guiding of the light in the waveguide results in multiple crossings of the fluid liner interface.

For a truly robust system ideally the substrate used to create the microfluidic chip is used for the opto-fluidic cell and with this in mind substrates doped with wavelength selective absorbent dyes (that enable spectral filtering) have been demonstrated in PDMS (Hofmann et al. (2006), Bliss et al. (2008), Hunt and Wilkinson (2008)). These have been used for optical filtering in fluorescence based systems but not used for colourimetric assays and the control of stray light. Furthermore PDMS is not an ideal material for long term use in wet chemical sensors (as discussed previously).

4.2 Materials and Methods

4.2.1 Discussion on flow cell integration

As discussed previously, detection of nutrients in seawater samples can be obtained by colourimetric assays: reacting the sample with a reagent to develop a dye. The intensity of the developed dye is proportional to the concentration of the reagent and sample according to the work of Beer (1852). In this example the dye concentration is directly proportional to the sample nutrient concentration. An absorbance method has been chosen for a number of reactions listed in table 2.1. Integration of these optical absorbance cells onto the microfluidic platform allows size reduction and so is of importance in this field.

The best solution developed to the problem of stray light is the use of tinted substrates, where the tint produces a high optical density within the monochromatic wavelength of the system. This technique is detailed below. However, it is also useful to highlight other options that we have investigated and these are discussed here.

First attempts to integrate a flow cell into a PMMA/SU8 based microfluidic chip are shown in Figure B.1 where optical fibres are used to deliver and collect the light. This enabled rejection of some stray light by locating the small collection area very close to the flow cell. However, fibres are difficult to align to the source and detector and to secure in position with sufficient accuracy to prevent optical drift (particularly with

changing pressure and temperature). This method is also very susceptible to signal interference from ambient light and in order to maintain a stable signal the system had to be placed in an opaque container. Light was also coupled from the source directly into the collection area by the surrounding substrate giving a non-linear response to concentration and a poor signal to noise ratio. As this is not a robust approach to the problem of stray light a different method was attempted.

Direct integration of the light emitter-collector pair (in this case an LED and a TSL257-LF TAOS light sensor, details given in Appendix B.4) was attempted with a clear monolithic PMMA device (Figure 4.2) manufactured using the method given in section 3.2.1. The performance of the transparent device was not adequate and investigation showed little change in the detected signal when even black dye was flowed through the cell. The conclusion drawn was that the light was being guided through the PMMA substrates to the detector making the background signal significantly higher than the signal through the detection path, as can be seen visually in Figure 4.2.

A possible method of isolatating the detection path from the bulk substrate is to use a pin hole arrangement, where light can only pass through the path of the flow cell and not around it. The pin hole effect can be produced in a number of ways but essentially the path in the line of the flow cell must be less opaque than the path around it. Figure 4.1 shows schematics for a number of possible methods of achieving this effect.

Each of the methods shown has advantages and disadvantages. The designs shown in Figure 4.1.1 and Figure 4.1.2 allow precise window thicknesses to be bonded at the end of the channel. However, these require precise machining of substrates and a bonding technique which can be performed out of plane. The design in Figure 4.1.3 allows the size of the pin hole to be precisely controlled, but any light that escapes into the bulk substrate may still be detected at the photodiode. These possibilities also present two difficulties: how to mount the light source and detector while providing precise alignment and also how to bond the different layers together out of plane of the bulk of the chip. It is possible to engineer around these difficulties; for example the inclusion of windows bonded out of plane could be achieved by machining a series of pockets and bonding or casting in small window sections. However, this adds complexity and makes it difficult to ensure uniform pressure is applied to all components during any bonding processes.

In terms of exclusion of stray light into and out of the detection path, it follows that the concepts shown in Figure 4.1.1 and Figure 4.1.2 appear to be offer better performance than the other concepts in Figure 4.1. However, this also brings forward a question: how dark must the dark polymer regions be? If the absorption of the light is such that stray light is excluded then it is possible that the substrate does not need to be completely opaque. Furthermore, how clear must the window be on each end? So long as the absorption of the window is negligible and consistent then it is possible it could be compensated for. Therefore it is possible that one material could suffice for both the

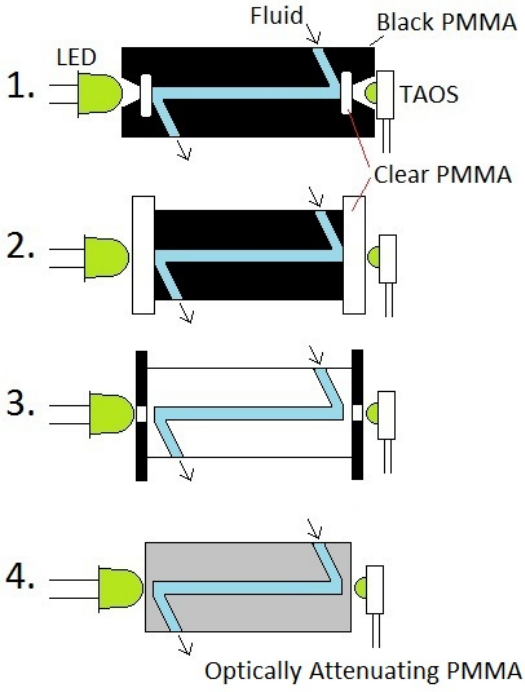

FIGURE 4.1: Four concepts which could be used to produce 'pin-hole' effects in polymer substrates. 1. Two transparent windows are bonded into machined grooves within a black substrate prior to sealing. Any colour can be substituted if it is opaque within the range of excitation and detection wavelengths, 2. Transparent windows are bonded onto the ends of a sealed channel within a black substrate, 3. A transparent substrate forms a sealed channel and 'pin-holes' are bonded to each end, 4. The channel is formed in a tinted material which absorbs light and provides a path with least absorbance along the channel with thin windows of tinted material at each end

window and the bulk substrate if the absorption of light at the window is low yet still large enough in the bulk substrate to reduce stray light enabling better linear response and improved signal to noise ratio. Utilising this concept a tinted substrate can be used to create the desired pin hole effect in the substrate, as shown in Figure 4.1.4.

4.2.2 Fabrication of absorbance flow cells

The production of chips is identical to chapter 3.2.1. Briefly, PMMA sheets (thicknesses from 3 mm and 5 mm, various grades as listed in Figure 4.3) were obtained from Evonik Röhm Gmbh and channels were fabricated by micromilling with an LPKF Protomat S100 micro-mill. Ports/threads for MINSTAC microfluidic connectors (The Lee Company USA) were also machined into the plastics prior to bonding. The design was created using Circuitcam software (LPKF Laser & Electronics AG), and then imported into BoardMaster software (LPKF Laser & Electronics AG) which controls the micromill. The two halves were aligned as discussed in B.3.5. The channel geometry was similar to that shown in Figure 4.1.4 with channels 500 μm wide and deep. Bonding was performed as discussed in 3.2.1.2. LEDs and Photodiodes are glued in place using Norland Products

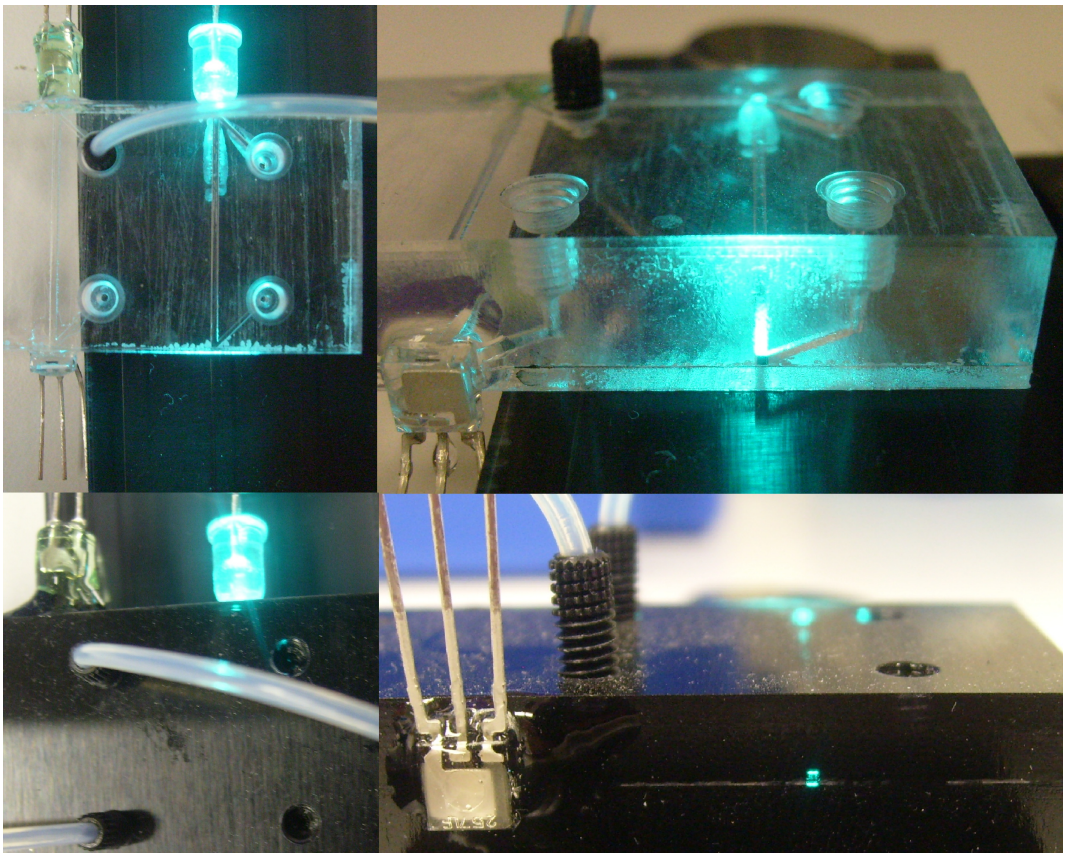

FIGURE 4.2: Top: Light is transmitted through the clear substrate hiding the flowcell effect, Bottom: Light is only transmitted through the thin windows of the flowcell and is absorbed by the tinted material surrounding it

Inc. 68 optical adhesive.

4.2.3 Measurement of absorbance spectra

Absorbance spectra for a range of commercially available samples were obtained using a Corporation U-28000 spectrometer. These are provided thanks to Ambra Milani who obtained the data shown in Figure 4.3.

4.3 Results and Discussion

Utilising the concept that a tinted substrate can be used to create the desired pin hole effect in the substrate, as shown in Figure 4.1.4, optical cells were manufactured. The channel structure, which incorporates the windows for excitation and detection, is machined into one substrate and a lid bonded on top. This lid need not be of the same material as the bulk substrate; it may be opaque as demonstrated in chapter 6. The pin hole effect is very clear when two identical cell geometries, one transparent and one tinted, are shown side by side as in Figure 4.2. When using LEDs as light sources and

photodiodes as the detectors in this type of arrangement it is very important to ensure alignment of the components along the axis of the flow cell. This can be achieved by manipulating the components while monitoring the output signal before gluing them in place with optical adhesive.

When designing flow cells for a specific chemistry it should be noted that the technique only works within the absorption spectrum shown for PMMA grades in Figure 4.3. The substrate must absorb strongly at the excitation/detection wavelength in order to absorb stray light from the emitter (i.e. assuming no external stray light sources). If a narrow-band detector is used with external light sources present this will also reduce their effect. If a wideband detector is used and external light sources are present the substrate absorbance must also be wideband so that only light passing through the thin end windows reaches the detector. Figure 4.3 shows that a wide variety of absorbance spectra are available with the varying PMMA grades with the coloured substrates giving good narrow band rejection while the grey tints provide wide band absorbance.

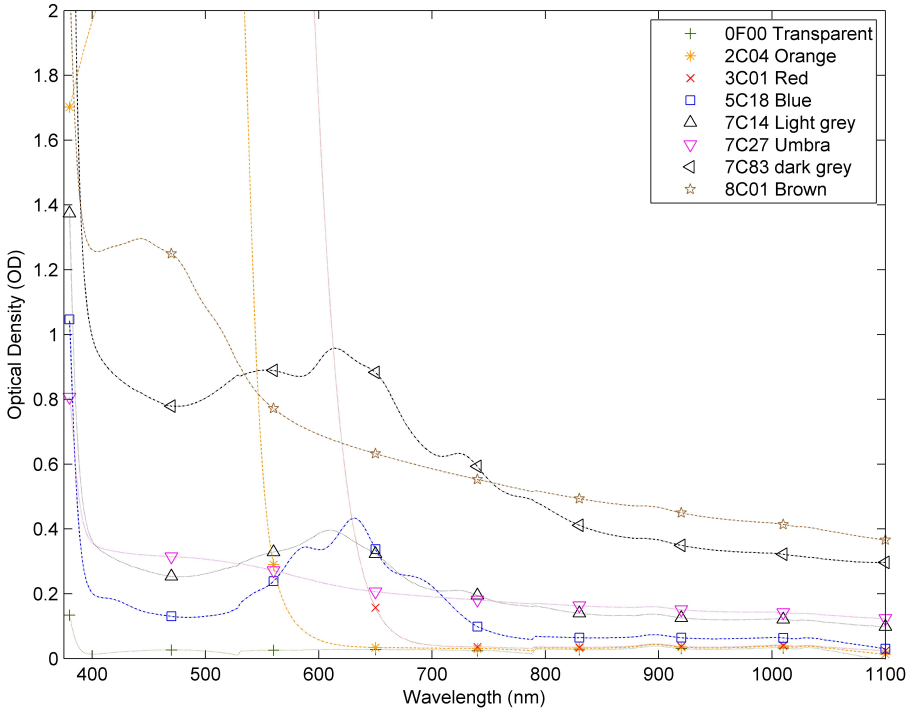

FIGURE 4.3: The absorbance spectrum of different grades of tinted PMMA. Optical density is given for a sample of 1 mm thickness

Choice of substrate for optimal optical design is limited by a number of factors. The lower limit of the substrate absorbance (total over the length of the cell) is given by the absorbance of the analyte/reagent at the maximum concentration of analyte. At this limit a signal due to concentration change will still be visible above the light source stray light baseline noise. The maximum substrate absorbance is limited by the minimum thickness to which the windows can be manufactured while still allowing light into the

cell. Limitations in the maximum light output of the emitter (and sensitivity of the detector) determine the maximum window thickness to give sufficient signal for a given substrate absorbance. Conversely if the minimum output power of the emitter is so high as to saturate the detector at low analyte concentrations the window thickness can be increased to provide attenuation. An explanation of the design process for an absorption cell is given in Appendix B.6.

It is also possible to use this method of making absorbance cells for use with optical fibres as shown in Figure 4.4. In this way light sources other than LEDs can be used as well as non-photodiode detectors. By allowing the optical cell component to be separated from the microfluidic platform it is also possible to use this technique in macro component based systems.

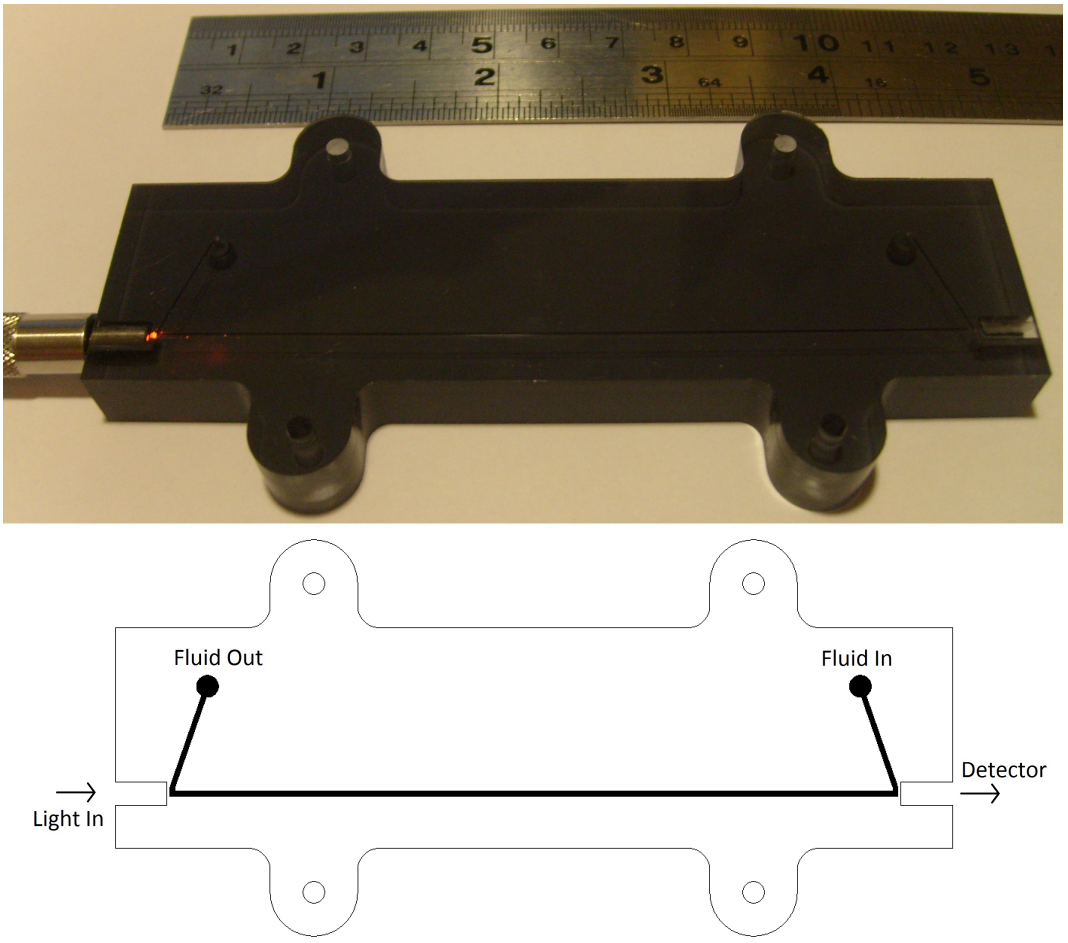

FIGURE 4.4: An absorbance cell designed for use with push in optical fibres allowing the use of various optical sources and detectors

4.4 Conclusions

The method presented within this chapter has allowed production of optical flow cells on chip along side other microfluidic channels in cheap readily available materials. The

chip shown in Figure 4.4 is manufactured from tinted 7F61 PMMA (Evonik Röhm Gmbh) which is comparable in price to opaque and transparent grades. Many products are currently manufactured in these materials through injection moulding and other techniques allowing the low cost mass production of these cells if required. This technique should translate to other materials although tinted grades of other polymers (such as COC) are currently commercially unavailable.

Performance of this design methodology has been assessed by Floquet et al. (2011) who states a factor of 6.4 improvement in the system sensitivity using a tinted PMMA substrate compared to transparent PMMA. This technique allows high performance absorbance spectrometry from mass producible designs. This is demonstrated by Sieben et al. (2010) who built a Nitrite detection system using the technique. A 14 nM limit of detection is demonstrated; an improvement of one order of magnitude over other systems in the literature. The optical cell has also been included in Phosphate detection systems detailed in Appendix A.4. By allowing integrated optical flow cells through a simple manufacturing technique this concept brings us one step closer to a robust fully integrated system.

In the next chapter the integration of membranes onto the microfluidic platform is discussed to allow robust systems with integral absorbance cells, valves and pumps.

Chapter 5

Integration of Membranes for Valves and Pumps

5.1 Introduction to microfluidic valves and pumps

This chapter contains a brief review of technologies which have been utilised to integrate valves and pumps onto microfluidic platforms. Following this are the details of a technique developed to integrate Viton ® membranes onto COC and PMMA microfluidic devices to create valves. This work was compiled into a manuscript published in the journal Lab on a Chip. The published manuscript is included in Appendix A.3.

5.1.1 Historical microfluidic valve and pump technologies

Check valves are operated by the direction of the fluid flow and are shut in one direction. They can simply consist of a flap of material which can be deflected away from an orifice. When fluid is flowing towards the orifice the flap covers it. In the opposite direction the fluid is able to flow past the flap. It is this principle that has been used for hundreds of years in bellows. In early MEMS publications flap valves were created using silicon (Esashi et al. (1989),Zengerle et al. (1995)) from which large arrays can easily be manufactured (Lee et al. (2007)). It is important in flap valves that the flap and valve seat are formed such that they touch to create a seal. This can be most easily achieved where either the flap or valve seat is formed from a conformal material; however, Silicon is stiff (Youngs Modulus = 190 Gpa (Tabeling (2006))) so is not suitable for all applications. In other work, using a similar principle, polymer check valves made from SU8 epoxy substrate and polymer films have been demonstrated (Böhm et al. (1999), Nguyen and Truong (2004), Mercanzini et al. (2005)). SU8 epoxy is more flexible than Silicon and able to withstand large strains without failure (Youngs Modulus = 2 GPa, Yield Stress = 60 MPa (MicroChem Corp.)). Polymer substrates, such as Mylar ®,

tolerate large strains before yielding allowing large valve deflections making possible the production of high flow rate pumps (upto 2 ml min^{-1} for water) (Figure 5.1) (Böhm et al. (1999)).

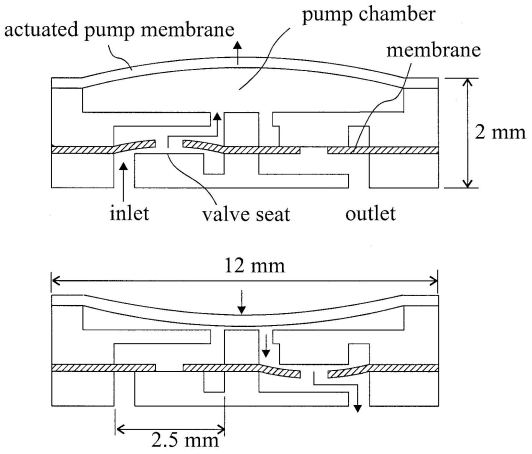

FIGURE 5.1: Schematic of a piezo driven polymeric pump. It utilises a piezo element to drive the pump membrane and flexible polymer membrane for the check valves (Böhm et al. (1999))

Flap valves can also be produced in hybrid rigid/elastomeric polymer structures. PDMS is easily bonded to glass and silicon allowing low leakage valves to be produced (Adams et al. (2005), Loverich et al. (2006)). The disadvantage of these materials is that the valves are also prone to adhering shut (Adams et al. (2005), Loverich et al. (2006)) although this can be reduced through roughening of the valve seat surface (Christabel et al. (2005)).

Nozzle-diffuser type one way valves have been demonstrated in silicon for valves and pumps (Figure 5.2.1)(Gerlach et al. (1995), Singhal et al. (2004)). These are designed such that the pressure drop when fluid is passed through them is significantly higher in one direction (around 10:1 or better) and usually optimised for the required flow conditions for Reynolds numbers up to 1000 (Singhal et al. (2004)). These designs do require the fluid to have some inertial energy and as such are unsuitable for systems where the Reynolds number is low and there is creeping flow. Tesla valves (Figure 5.2.2) also provide similar performance to nozzle-diffuser arrangements and agree closely with numerical models (Morris and Forster (2003)). Due to their 2 dimensional design they are easily incorporated into designs using lithographic processes for manufacture. The main disadvantage with the use of these devices as valves is the leakage flow and the ability of reagents and particulates to diffuse through the device. Where zero leakage in either direction is required these devices are not suitable; however when a pressure gradient is required they could be of some aid.

Ball valves can also be used to provide a check valve operation and have been demonstrated for microfluidics with glass substrates. The valve seat can be manufactured using powder blast erosion of glass (Yamahata et al. (2005)) or using a round tapering capillary (Pan et al. (2005)). These designs can also incorporate a 'spring' to aid closing of the valve, shown in Figure 5.3.1. Various designs have been analysed numerically indicating that they can withstand back pressures upto 3 kPa (0.03 bar) (Smistrup and Stone (2007)).

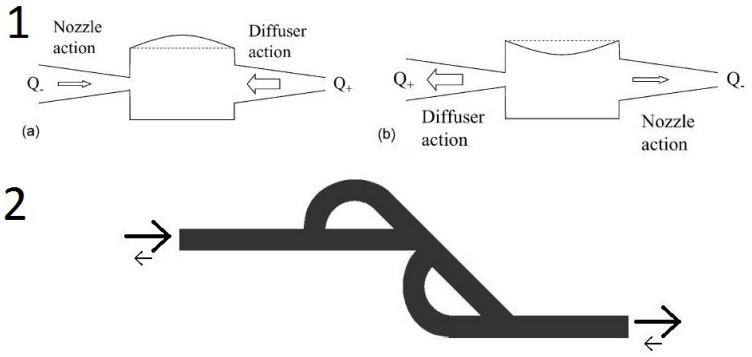

FIGURE 5.2: 1. Working principle of a nozzle/diffuser pump. a. Expansion/Intake stroke, b. Contraction/pump stroke (Singhal et al. (2004)) 2. Schematic of a Tesla 'check' valve. There is less pressure drop when fluid flows left to right than in the opposite direction meaning this valve partially rectifies the flow (Morris and Forster (2003))

Latching two-way valves can be realised by 'plugging' channel openings to remove fluidic paths or 'unplugging' them to enable fluid flow. With the small scale and tight manufacturing tolerances of microfluidic devices implementation of this concept becomes difficult. Often a moving membrane is used to cover or uncover an opening as this operation is scalable. For example early MEMS valves were demonstrated using silicon substrates and piezo elements for manipulation (Figure 5.3.2)(Esashi et al. (1989)). PDMS has been utilised as the soft polymer can be deformed mechanically using air pressure, vacuum or even electrorheological (ER) fluid. Mechanical actuators such as screws (Weibel et al. (2005)) and Braille displays (Gu et al. (2004)) have been demonstrated for actuation of PDMS membranes due to the ease of prototype manufacture (Liu et al. (2006)).

Displacement pumps use a change of geometry to cause elevated pressure in a chamber which drives fluid along connected open channels. These may or may not contain valves and are varied in their design. They are widely used for example as pumps for fuel injection systems (Cheng and Chien (2006)) or in nebulisers (Pan et al. (2007)).

Peristaltic pumps are a form of displacement pump and are widely available for macro systems from sources such as RS Components Ltd and Fisher Scientific UK Ltd.. These pumps have been available for many years and use the simple rotation of one or more cams to move a pinch point or seal that pushes fluid along a sealed compressible tube (Figure 5.4.1). They are flexible in design and can be used to push or pull the fluid through the system. This design has been shown to be reliable time and again and as such has been adapted for MEMS devices. Usually micro systems use planar pump designs where a number of chambers are placed in serial and compressed, or opened in sequences which cause fluid movement (Figure 5.4.2). Planar microfluidic pumps have been manufactured in silicon (Xie et al. (2004), Jang and Yu (2008)), PDMS (Goulpeau et al. (2005))and other polymers such as polyimide (Boden et al. (2006)). These systems

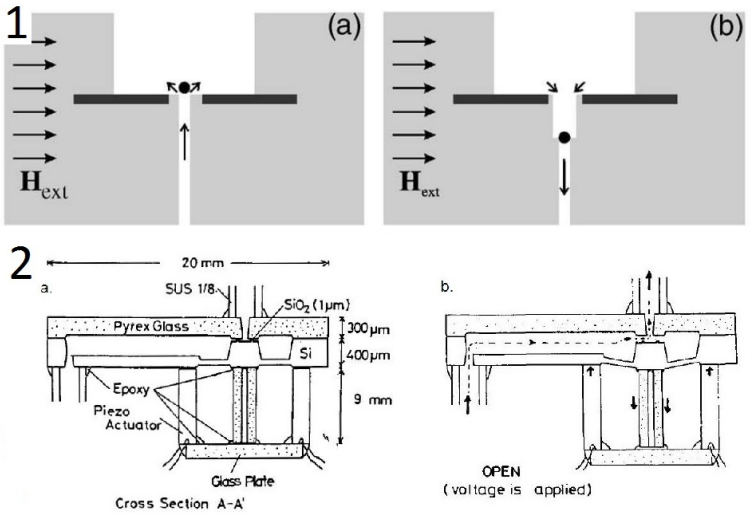

FIGURE 5.3: 1. Cross sections of a pair of proposed geometries for magnetically actuated ball valves. The dark gray plates are slabs of soft magnetic material, the lighter gray is the silicon or PMDS structure that defines the microfluidic network and the solid black circle is the magnetic bead or particle. The arrows indicate the expected direction of the fluid flow and the external magnetic field, H_{ext}. a. In this configuration the magnetic field is constantly on, and thus the magnetic bead blocks the outlet of a channel. b. An alternative configuration, where the magnetic field is initially off, but the fluid pressure holds the bead in the fluid inlet which is thus blocked. Turning on the magnetic field lifts the bead out of the inlet. (Smistrup and Stone (2007)) 2. Schematic of a Silicon valve. a. shows the closed position (no voltage), b. shows the open position (voltage applied) (Esashi et al. (1989))

are difficult to seal as the membrane must conform to the chamber geometry and valve seat. Membrane integration in a planar system is also complicated to manufacture while ensuring no leakage.

Other displacement pumps work with only a single actuated chamber and two passive check valves. There are a number of different actuation methods but these can be split into those using an electric/magnetic field effect to apply a force (electrokinetic) and those using a fluid pressure (hydrodynamic). Electrokinetic actuators include; electrostatics (Zengerle et al. (1995)), Xie et al. (2004), Kim et al. (2005b), Batra et al. (2007), Geipel et al. (2007), Geipel et al. (2008)), piezoelectric materials (Esashi et al. (1989), Jang and Yu (2008), Koch et al. (1998)), a Braille reader (piezo) (Gu et al. (2004)), magnets (Yin et al. (2007), Yamahata et al. (2005), Böhm et al. (1999), Pan et al. (2005)), Ferrofluids (Hartshorne et al. (2004)), Electro-osmosis (EO) (Yairi and Richter (2007), Hu and Chao (2007)), Electro-hydrodynamics (EHD) (Kano et al. (2007), Singhal and Garimella (2007), Stubbe et al. (2007)), Magnetohydrodynamics (MHD) (Lemoff and Lee (2000), Jang and Lee (2000), Homsy et al. (2005), Patel and Kassegne (2007)), shape memory alloys (Wilson et al. (2007), Ganor et al. (2007)), dielectric elastomer membranes (Loverich et al. (2006)) and ionic polymer-metal composites (IPMC) (Nguyen et al. (2008)). Hydrodynamic methods include; thermopneumatics (Song and Lichtenberg (2005), Boden et al. (2006), Cheng and Chien (2006), Boden et al. (2007), Jin Jeong

(2007)), compressed air/vacuum (Chun-Wei et al. (2006), Biao et al. (2006), Walker et al. (2007)), bubbles (Yin and Prosperetti (2005), Good et al. (2006)) and electrorheological (ER) fluid (Liu et al. (2006)).

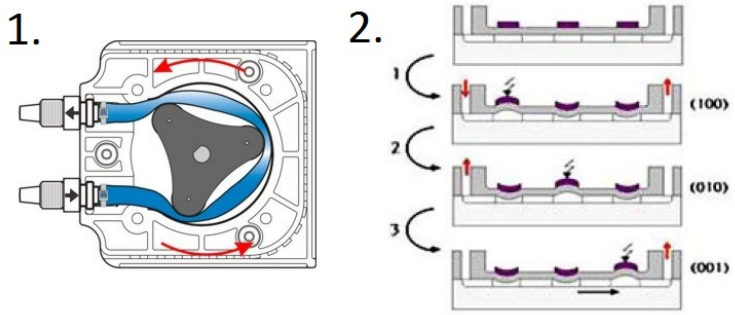

FIGURE 5.4: 1. Working principle of a typical Macro-Peristaltic Pump (Blue White Industries Ltd.), 2. Working principle of a Planar Peristaltic Pump utilising a 3-phase sequence(Jang and Yu (2008))

5.1.2 Current microfluidic valve and pump trends

The next generation of lab on chip devices require robust methods of on chip fluid control. There are two main methods of controlling fluid; electrokinetic and hydrodynamic (Quake and Scherer (2000)). Although electrokinetic is widely used, flow rate reliability and control can be difficult to achieve with real world environmental samples (Rainelli et al. (2003)). For hydrodynamic flow control micro-valve structures are essential for the manipulation of fluid (Oh and Ahn (2006)). To realise large scale integration (LSI) microfluidic devices standardised valve designs are required that need to be chemically robust, mass-producible and scalable (Thorsen et al. (2002)). Many hydrodynamic valves are pneumatically activated with off chip control; however, there is a need to develop compact low power on-chip actuation.

Poly(dimethylsiloxane) (PDMS) is often the material of choice for micro-valves. It has a low Youngs modulus (~750 kPa (Grover et al. (2008))), is gas permeable and is easy to bond and fabricate. A number of groups have realised normally-open (Thorsen et al. (2002), Unger et al. (2000)) and normally-closed (Mosadegh et al. (2011), Grover et al. (2003)) designs using PDMS membranes. A wide variety of valve schemes has been developed, from monolithic PDMS valves (initially demonstrated by the Quake group) (Thorsen et al. (2002), Unger et al. (2000)), to hybrid designs built from stacking glass, thermoplastic and elastomeric materials (Mosadegh et al. (2011), Grover et al. (2003), Lai and Folch (2011)). However, the porosity of PDMS (leading to cross-contamination or air-bubbles in microfluidic channels) and its inability to handle harsh solvents (typically the non-polar solvents, which lead to swelling and irreversible chemical alteration of the elastomer) are a concern (Thorsen et al. (2002), Grover et al. (2008), Prakash et al. (2006)).

Hybrid valves are generally built with a glass/PDMS/glass sandwich structure, due to the optical clarity of glass and the ease of manufacture (Grover et al. (2003)). Over the last decade, there has been a transition from glass to thermoplastics, such as poly(methyl methacrylate) (PMMA) and cyclic olefin copolymer (COC), which are suitable for mass-production, are cost-effective, and are easier to prototype (discussed in chapter 3). Zhang et al. (2009) demonstrated pneumatic microvalves with a PMMA/PDMS/PMMA stack structure. Their valves and pumps are fabricated by sandwiching a PDMS membrane treated by a UV ozone cleaner, similar to the method used with glass/PDMS bonding. The PMMA-PDMS bonds formed were reversible, but sufficient enough to survive the range of vacuum and pressures applied to the device (fluid pressure of 60 kPa). Recently Gu et al. (2010) reported a method for bonding COC to PDMS using surface activation by corona discharge, surface modification using 3-(trimethoxysilyl) propyl methacrylate (TMSPMA), and thermal annealing. Valves were fabricated with a COC/PDMS/COC stack, but the method was also applicable to PMMA. The bond was much stronger and the device withstood ∼689 kPa without delaminating. Similarly, Lee and Chung (2009) have established a "chemical gluing" method of bonding PDMS surfaces by using an aminosilane and epoxysilane. The terminal amine of the (3-Aminopropyl)triethoxysilane (APTES) interacts to ring open the epoxy group of the (3-glycidoxypropyl)trimethoxysilane (GPTMS), which creates a strong covalent bond between the two surfaces (Lee and Chung (2009)). This technique is established in the literature (Tennico et al. (2010), Kim et al. (2010), Tang and Lee (2010), Lee and Ram (2009), Vlachopoulou et al. (2009)) as a method of creating strong bonds between material surfaces but has previously not been shown with Viton® or other fluorinated polymers.

Alternative robust elastomeric membrane materials have been used to make microvalves, such as polytetrafluorethylene (PTFE) Teflon (Willis et al. (2007)), fluorinated ethylene-propylene (FEP) Teflon (Grover et al. (2008)) and Fluorocur™ perfluoropolyether (PFPE) (Willis et al. (2008)). The bonding of fluoropolymers is difficult and requires aggressive surface treatment (Taberham et al. (2008)) or functionalisation. Grover et al. (2008) demonstrated glass/Teflon/glass valves that were formed by a thermal bond between the commercially available treated FEP film ("cementable") and glass. The bonding relied on the cementable FEP film, which had a degraded surface that enabled bonding. The device Grover et al. (2008) demonstrated was capable of delivering piranha solution (concentrated sulfuric acid with hydrogen peroxide) and the bond strength was sufficient to withstand 48 kPa fluid pressure on a closed valve (pneumatic valve closing pressure of 50 kPa). The first commercial fluoroelastomer was Viton® and although it has excellent chemical resistance and thermal stability to temperatures as high as 316 °C (Wang and Legare (2003)), it has not been used for micro-fabricated valves.

Viton® is compatible with most organic solvents, swelling only in ketones, esters, amines, organic acids and strong bases. It is suitable for high temperature service

(>200 °C) as well as low temperature dynamic applications (<-20 °C). Similarly COC is compatible with most solvents, acids and bases although it dissolves in non-polar solvents such as toluene and cyclohexane, as discussed in chapter 3. It is also suitable for high temperature applications with grades available with glass transition temperatures ranging from 75 °C to 170 °C. PMMA is less resistant to a typical panel of chemicals and solvents. It swells and dissolves in most organic solvents. It is however low-cost and optically transparent making it a popular choice for rapid prototyping of devices where only water, ionic solvents and dilute solvents are required (Sieben et al. (2010)).

5.1.3 Commercial microfluidic valves and pumps

Pumps are available for micro and macro fluidic applications where the need for full integration is not required; the disadvantages encountered when these are used in microfluidic systems are discussed in the next chapter. Systems have been built based on these devices utilising a manifold to integrate the microfluidic channels and larger external fluid control components (Sieben et al. (2010), Cleary et al. (2008)). In the section that follows some examples are discussed in order to highlight current technologies used in microfluidic systems which may be suitable for deployable nutrient sensors.

thinXXS Microtechnology AG produce microfluidic chips for many different systems from glass and polymers as well as a range of microfluidic pumps. These pumps are made from polymers with elastomeric membrane check valves and piezo actuators as shown in Figure 5.5.a. The output flow rate of these pumps is dependent on fluid viscosity, temperature, and differential pressure which results in ill defined flow rates in unattended systems (our target application). In addition the performance of the check valves used (see Figure 5.5.a) will be affected by particles, and the actuator requires an air / gas backing to enable resonance which is not possible in deeply submerged systems.

The use of pumps with a fixed volume per stroke (hereafter called “dosing pumps”) allows precise control of sample volumes and consequently solenoid driven dosing pumps from The Lee Company USA were used in initial systems developed at CMM. The Lee Company USA produce models which pump 20 μl and 50 μl doses per actuation (Figure 5.5.b). These pumps work well and have been proven to operate down to depths of 3000 m (Abi Kaed Bey (2011)) but as the chip designs at CMM have become smaller the internal chip volume is now similar to that of each pump dose. This makes creating sample/reagent mixing ratios of anything other than 1:1 very difficult. Even unity ratios are difficult to achieve as the pumps must be synchronised in order that segmented flows are not produced. Similar solenoid driven pumps made by the UK company Dolomite have the same problems. Both of the companies also produce solenoid driven microfluidic valves which are similar in design. Those produced by The Lee Company USA have lower power consumption, lower internal dead volume and better tolerance to pressure than those by Dolomite so have been favoured at CMM. These valves feature in the current

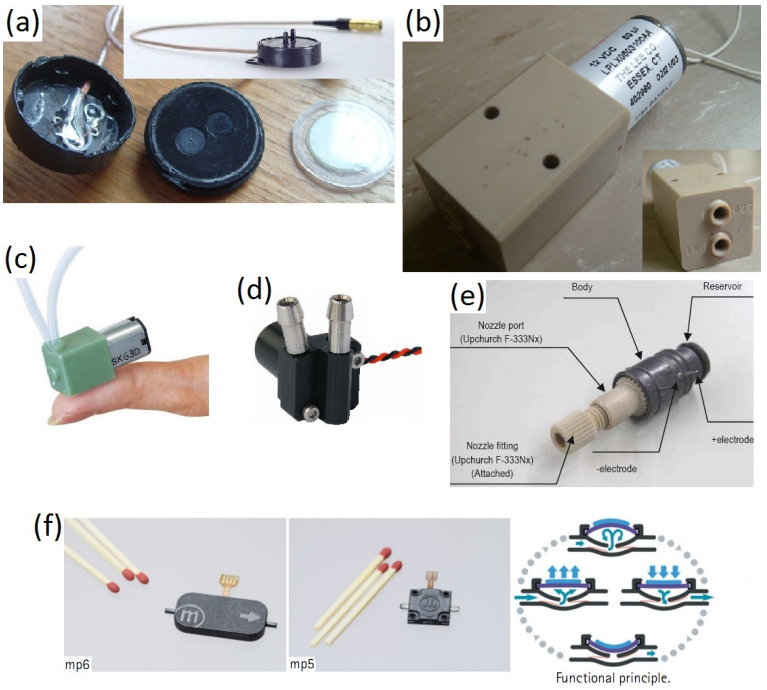

FIGURE 5.5: (a) Piezo driven pump from thinXXS Microtechnology AG, flow rates up 9 ml min^{-1} and back pressures upto 50 kPa for water with $\approx$ 250 mW power consumption, (b)Solenoid pump from The Lee Company USA, pumps 50 μl per actuation, maximum 2 actuations per second, (c) Miniature peristaltic pump from Dolomite, flow rate 450 μl min^{-1} and max pressure 50 kPa at 120 mW power consumption, (d) Centrifugal pump from RS Components Ltd, specification says maximum flow rate 650 ml min^{-1} and maximum head 1.9 m, (e) Electro Osmotic pump from Microfluidica, upto 190 μl min^{-1} and 110 kPa back pressure, (f) Piezo driven pumps from Bartels Mikrotechnik GmbH, flow rates up 6 ml min^{-1} and back pressures upto 500 mbar with $<$ 200 mW power consumption

system iteration as external bolt-on components (Beaton et al. (2011)). Dolomite have also recently started to produce a miniature peristaltic pump shown in Figure 5.5.c.

Other commercial pumps that this author has utilised include a range of centrifugal macro pumps sold by RS Components Ltd. Shown in Figure 5.5.d, the literature provided with these pumps indicates that they can pump fluid at 2 l/min and to a 3.5 m head. However whilst testing these pumps this author was unable to pass fluid through a 1 m long serpentine (300 μm high and wide, equivalent to $\sim$0.1 bar drop at 120 μl/min with Re=8.5) at any flow rate.[1]

Other companies with which the author has no experience of the devices are Bartels Mikrotechnik GmbH who produce piezo micropumps (Figure 5.5.e), check valves and microfilters. Microfluidica also produces a range of Electro osmotic pumps (Figure 5.5.f which as discussed in section 5.1.2 are unlikely to be suitable for wet chemical sensors.

[1] A batch of ten pumps were purchased for use in a filter test rig. Characterisation was attempted using a serpentine channel on a microfluidic chip as described. Not one of the batch was able to pump fluid through the device as the specification would suggest they could. This author assumes that either this was a faulty batch or the specifications given contain errors. Further testing was not performed due to time restraints other options being available.

5.1.4 Conclusions from Valve and Pump Review

Many valve designs are presented in the literature but only those of a bolt-on nature have been proven suitable for oceanographic nutrient sensors (Sieben et al. (2010)). These valves use a moving membrane which is formed from a compliant FKM elastomer. Each of these commercial valves has an internal volume of 13 μl (The Lee Company USA) however other integrated valve designs present in the literature (Unger et al. (2000), Thorsen et al. (2002), Grover et al. (2003)) do not have this problem. As such the focus of this work was upon a method to integrate chemically robust elastomeric membranes onto the microfluidic platform to create valves similar in design to those of the Mathies group (Grover et al. (2003)).

5.1.5 Development of robust integrated microvalves using the fluoroelastomer Viton ®

To address the need for robust integrated micro-valves and pumps, proof of principle pneumatically operated devices were fabricated in PMMA and Viton® and characterised. Viton® is a robust fluoroelastomer widely used in macro valves and pumps, but has previously not been used for microvalves as it is difficult to bond to polymers. To overcome this a novel, reliable and robust technique for the irreversible bonding of chemically-inert Viton® membranes to PMMA and COC substrates was developed. A schematic of this process is shown in Figure 5.6(a)-(e), which relies on the formation of a covalent amine epoxy bond between the two silanes. Commercially available 250 μm Viton® membrane material was used to build a normally-closed valve made in micro-milled substrates from PMMA or COC.

The valve architecture is based on a tri-layer structure of PMMA/Viton®/PMMA or COC/Viton®/COC, as shown in Figure 5.6. The top substrate incorporates fluidic channels, the middle layer is a deformable elastomeric membrane, and the bottom substrate contains the pneumatic control channels. A valve consists of two fluidic channels separated by a barrier, below which is a displacement chamber in the pneumatic control layer. Opening and closing the valve is achieved by controlling the pressure in the displacement chamber using a commercial solenoid valve (similar to Sieben et al. (2007)). To close the valve, a pneumatic pressure is applied (135 kPa) forcing the Viton® membrane against the barrier. To open the valve, vacuum is applied to the displacement chamber (-70 kPa) pulling the Viton® membrane away from the barrier and opening a fluidic pathway.

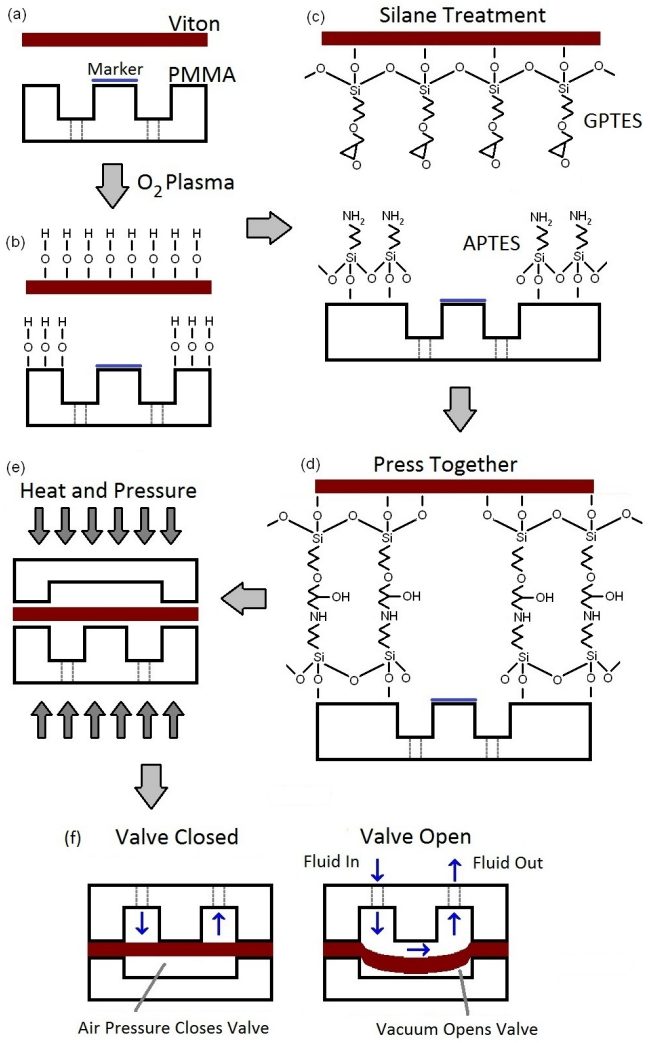

FIGURE 5.6: Schematic showing the bonding process for bonding two rigid polymer substrates to a Viton® Membrane. First the valve barriers are masked with a permanent marker pen (a) before the polymers are treated with an oxygen plasma (b). This provides surface functionalisation which reacts with silane molecules when the polymers are placed into silane solutions (c). Bonding of the substrates is performed under pressure to increase conformal contact and with heat to aid the chemical process (d, e). A normally closed valve is produced which is controlled by changing the air pressure on the pneumatic control layer (f).

5.2 Materials and Methods

5.2.1 Novel integration method for commercial Viton® membranes

PMMA sheets (1.5 mm thick) were obtained from Evonik Röhm Gmbh, Cyclic-Olefin Copolymer (COC) wafers (0.7 mm and 1.2 mm thick) from TOPAS Advanced Polymers GmbH (Grade 5013) and Viton® sheet (250 μm thick grade A, black 75 shore) from J-Flex Rubber Products. Channels and features were made in the polymer substrates using micromilling as described in chapter 3. All channels were 160 μm wide x 160 μm

deep. Standard 76 mm x 26 mm borosilicate glass slides were obtained from Fisher Scientific UK Ltd..

The bonding process was also applied to substrates that were prepared using hot embossing. COC samples were prepared with channels 30 μm deep and 300 μm wide by a colleague, Dr. Sam Birtwell, at the University of Southampton. These samples were embossed using a PDMS master at 138 ^{o}C and 200 N mm^{-2} for 10 min and then cooled to room temperature over 30 min.

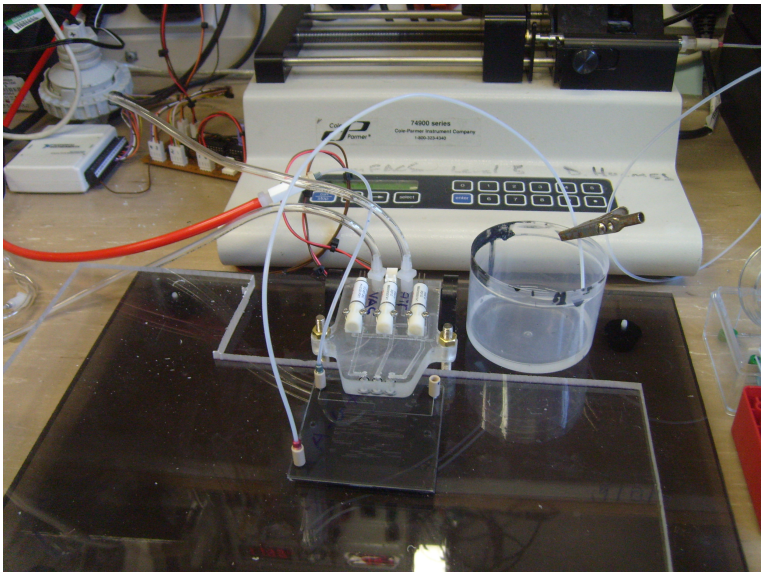

FIGURE 5.7: In this setup the syringe is used to push fluid through a serpentine where pressurised air is applied to the back of a bus valve. When the valve is actuated a bubble is created in the serpentine fluid. Periodic actuation of the valve can be used to produce a train of bubbles.

For bonding, the substrates were thoroughly cleaned and then treated with oxygen plasma (Femto RF, Henniker Scientific Ltd.) prior to immersion in a silane solution. Specifically PMMA, COC and glass surfaces were plasma treated for 30 seconds and Viton® substrates for 60 seconds, both at 50 Watts power and 45 sccm. A common problem with assembling these valves is bonding across the valve seats. To prevent this, the PMMA/COC surfaces were shielded from oxygen plasma using a permanent marker pen. This can be removed from the finished device by flushing with 50% Methanol/Water solution if required. For smaller structures, a similar effect could be obtained using metal masking or a recessed valve seat (Lai and Folch (2011)). After plasma surface modification, PMMA, COC and glass substrates were immersed in a 5% v/v solution of APTES (3-Aminopropyl)triethoxysilane) solution (50% DI water and 50% ethanol). Viton® substrates were immersed in 5% v/v GPTES (3-Glycidyloxypropyl)triethoxysilane) solution. Both solutions were freshly made prior to use. The temperature of the solvent was set at 50°C and controlled using a water bath. After 30 minutes immersion the substrates were removed, rinsed with ethanol and dried with nitrogen. The different parts were aligned using precision milled holes and pins (described in Appendix B.3)

and pressed carefully together by hand to avoid air inclusions. They were then clamped using a custom made jig consisting of sprung clamps and brass plates (shown in Appendix B.3) to achieve a uniform pressure of ~800 kPa and transferred to an oven pre-heated to 80°C. FKM sheet 0.5 mm thick (Goodfellow Cambridge Ltd.) was used as a packing material between the brass plates and rigid substrates to ensure even pressure distribution. After 12 hours at this temperature and pressure the chips were removed from the oven and were ready for use.

Optimisation of the oxygen plasma exposure time was performed and the lowest contact angles for each of the materials used. Contact angle measurements for the PMMA and COC are given in Appendix B.7. These exposure times were 30 seconds for PMMA and glass, 60 seconds for Viton® and 12 seconds for COC. A temperature of 80°C was chosen for annealing which is below the glass transition temperatures of the materials and reduces polymer reflow; therefore, maintaining channel topography. The technique is also successful at room temperature but requires longer contact time (several days).

Valve testing was performed with the chip design shown in Figure 5.8. The chip was coupled to pneumatic solenoid valves using a manifold clamped to the top of the chip. Seals are made with O-ring gaskets. Pressure regulated air was provided by a compressor and vacuum with a vacuum pump connected to the manifold via push fit connections (Figure 5.7). Control of the manifold valves is performed using custom electronics driven by a Labview interface (NI USB-6009, National Instruments Corp.).

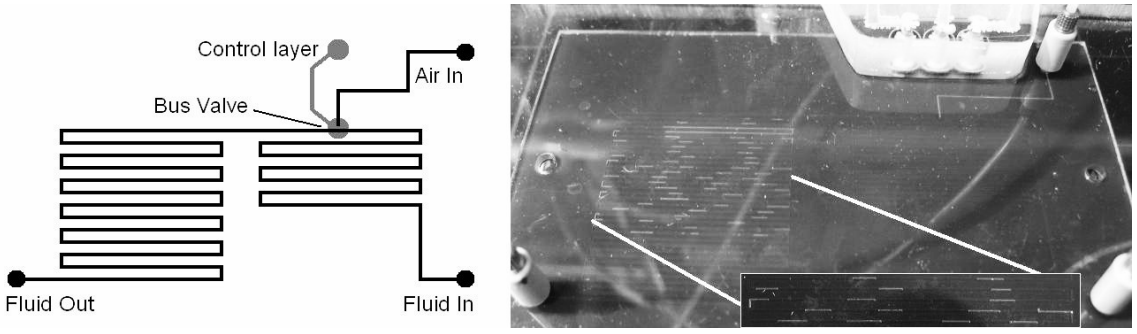

FIGURE 5.8: Chip layout for testing of valve leakage rate (left). The chip is comprised of two serpentines and a bus valve controlled by a pneumatic manifold. A photograph of the system is shown on the right along with a bubble train, which demonstrates opening and closing of the valve. Also highlighted is a zoomed photograph of the opened and closed states of the valve.

5.3 Results and Discussion

When bonding to COC the Viton® was bonded as described without any apparent channel collapse. Embossing can cause a lack of flatness in the surface(s) to be bonded (Toh et al. (2008)). This technique is tolerant to such topography because of the use of a relatively thick and compliant elastomer. This demonstrates the flexibility of this

procedure for preparation of devices requiring an integrated elastomeric membrane.

The adhesion of the Viton® to the substrates was tested by pressurising the fluid behind a valve that had been permanently sealed (bonded without masking the barrier during ozone treatment) until the Viton® membrane delaminated. The pneumatic seat area was approximately 1 mm^2. A fluid pressure of 400 kPa (PMMA/Viton®) or 310 kPa (COC/Viton®) could be applied before leakage or burst failure, a pressure sufficient for most microfluidic applications. This test represents the worst case as the membrane is allowed to deform into the valve seat in the control layer. A higher leakage pressure will be obtained when the elastomer is more restricted with the backing of the control layer, such as in a channel.

The bond strength of Viton® to glass was not tested as extensively; however, the Viton® could not be removed from the glass without tearing. Although bonding Viton® to glass is useful for many applications, the aim of this work is to produce valves using rapid-prototyping techniques based on thermoplastics. Glass/Viton®/Glass valves could be investigated in future work if required however the current trend at CMM (and the microfluidics community generally) is towards all polymer devices and as such further investigation is not warranted at this time.

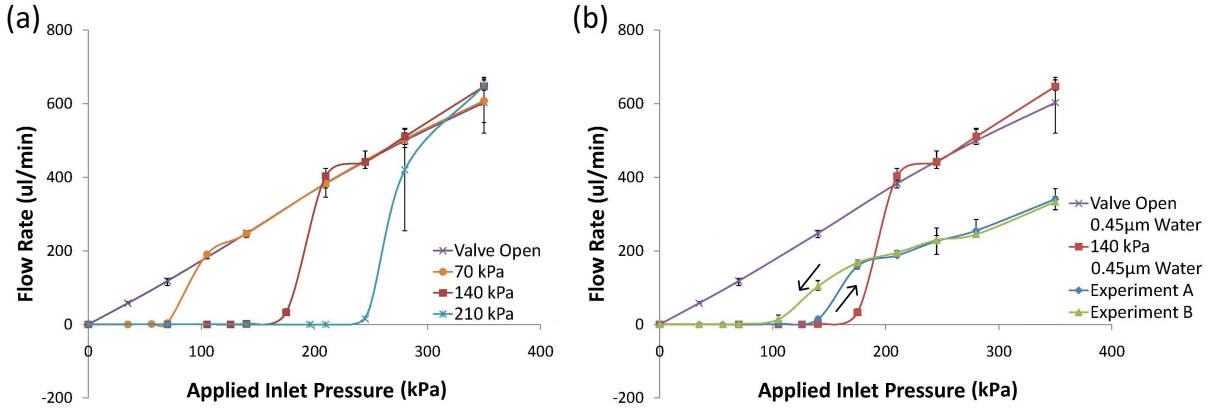

FIGURE 5.9: (a) Leakage flow rate versus applied fluid pressure for an open valve and for three pneumatic sealing pressures applied to the control layer (70, 140, 210 kPa) flowing 0.45 μm filtered water. The valve leakage rate dramatically increases when the applied fluid pressure is comparable to the pneumatic sealing pressure; (b) Leakage flow rates for 60 μm filtered seawater. Experiment A: seawater is flowed through an open valve with 20 kPa applied fluid pressure. The valve is then closed (140 kPa), an increasing fluid pressure is applied and the flow rate recorded. Experiment B: Following experiment A, seawater is flowed through the leaking closed valve with 345 kPa applied fluid pressure while 140 kPa pneumatic closing pressure is applied to the control layer. Fluid pressure is gradually reduced to zero and the flow rate recorded. Between repeats 1 ml of seawater was flowed across the open valve to clear any particles collected in the valve. The difference in flow rate observed between A and B is due to the increased viscosity of the seawater.

Valve leakage was tested using the chip shown in Figure 5.8, which comprised two serpentine channels together with a valve. A bubble train was created by alternately opening and closing the valve with pressurised air supplied to the valved inlet, shown

in both Figure 5.8 and Figure 5.10. The performance of PMMA/Viton®/PMMA valve was tested by measuring the flow rate of water (0.45 μm filtered) at different pressures (0-345 kPa water pressure applied to the valve inlet) for two states: valve-open or valve-closed (Zhang et al. (2009)). Figure 5.9(a) shows leakage flow rate versus fluid inlet pressure at different pneumatic pressures (70, 140, 210 kPa) on the control layer. This works as the valve sealing pressure. The flow rate was measured by recording the time taken for a bubble to travel a predetermined distance along a tube connected to the outlet. Closed valves have no detectable leakage; the bubble did not move over a one hour period. When the fluid inlet pressure equals the applied pneumatic control pressure, the valve leakage is a few nanolitres per second (less than < 25 nl s^{-1}), which is comparable to previous work (< 100 nl s^{-1}) (Grover et al. (2008)). This increases dramatically as the inlet pressure is increased (at fluid pressures in excess of sealing pressure), and the valve behaves like an open valve.

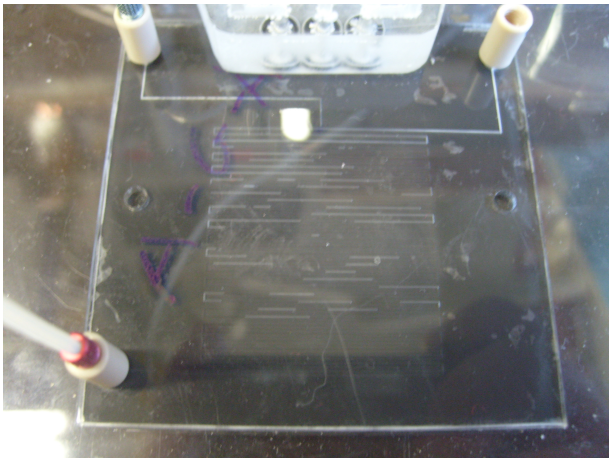

FIGURE 5.10: Picture shows a bubble train on a microfluidic chip used as shown in Figure 5.7. Push in PEEK connectors are used to adapt the Lee company MinStac tubing to the chip and the pneumatic connection is made by a compression fit manifold.

To test the behaviour of the valve with typical environmental samples, the leakage flow rates were measured when the DI water was replaced with seawater filtered through a 60 μm filter. The seawater flowed through the channels with 20 kPa applied pressure when the valve was open. The valve was then closed (135 kPa air pressure), and the fluid pressure was varied from 0 to 345 kPa whilst recording the valve leakage. This data is shown in Figure 5.9(b) and indicates that the valve leaking pressure was lower than that for DI water, presumably due to particulates in the valve seat. The fluid pressure was then reduced to zero, and the valve closed which revealed an opening and closing hysteresis that was repeatable. After flowing 400 ml of seawater through the valve, the valve continued to function. This demonstrates that the valve is robust enough for use in oceanographic sensors and other applications requiring robustness to harsh fluids.

Although the valves are externally actuated using pneumatic controls as described in the literature (Sieben et al. (2007)), the bonding of the Viton® to the substrate is robust enough so that other actuation methods could be used. These include hydraulics (Gu

et al. (2007)), magnetics (Chen et al. (2011)), screws or solenoid valves (Hulme et al. (2009)) or phase change polymers (Kaigala et al. (2008)).

The use of Viton® membranes, which are opaque, necessitates care in design of on chip optical systems. This may require alteration of designs developed using transparent polymers such as PDMS. The opaque membrane is an advantage in designs which use side illumination and detection as it reduces light coupling from external sources along one channel wall. An example of this is long path length absorbance cells as discussed in chapter 4. In fluorescence systems which allow for side illumination, three transparent channels walls are available for imaging and the black Viton® background again reduces stray light coupling. For systems requiring bright field illumination the Viton® can be removed (i.e. cut away, milled, punched) at the detection chamber prior to bonding to allow light through all substrates. Although to some it may seem problematic at first, the use of an opaque membrane offers a number of advantages for on chip optical and microfluidics system design.

5.4 Conclusions

In this chapter a method for permanent bonding of chemically-inert elastomeric fluropolymer membranes has been demonstrated, in particular Viton®, to PMMA and COC. Microvalves were made from this material and characterised. Whilst these initial demonstrations used COC- or PMMA-Viton® structures, enhanced chemical robustness can be achieved by using fluoropolymers or glass as the rigid substrate. Bonding to borofloat glass surfaces using the same silane chemistry has been achieved. This bonding approach complements other microfabrication methods and enables the integration of chemically robust Viton® valves in a wide range microfluidic devices.

The work from this chapter was published in Lab on a Chip titled *Chemically resistant microfluidic valves from Viton® membranes bonded to COC and PMMA*. The manuscript is included in Appendix A.3. In the following chapter this method of integrating membranes is used to create a microfluidic system with on chip valves and pumps.

Chapter 6

Designing Nutrient Sensor Systems

The design and production of the push-pull system featured in this chapter was completed in collaboration with Dr. Vincent Sieben. The collection of data for both systems was also performed in collaboration on a common platform in order to reduce time spent duplicating experimental setups.

Design and production of the Multiplexed Stop-Flow system featured was entirely my own work. The published manuscript is included in Appendix A.4.

6.1 Introduction to nutrient sensor design

6.1.1 The process of nutrient sensor system design

When designing systems the series of operations which make up the system process must be considered. In colourimetric nutrient sensors this involves taking a sample, mixing it with a reagent and measuring the optical properties of the product. If using an absorption cell then the length must be determined and the method of manufacture considered as discussed in chapter 4. The performance of the system will be limited firstly by the design and performance of this sub-system as well as the sample consistency (mixing ratio, contamination, pressure variations) determined by the fluidics of the system.

Within the fluid handling components of the system multiple steps are required to process a sample. The minimum sample volume is determined by one of two methods. The flushing volume required to clear the previous sample first determines the minimum sample volume which ensures a fresh uncontaminated sample. Alternatively, if the flushing volume is smaller than the detection chamber volume (which is not usually the case) then it is the detection chamber volume which determines the minimum sample volume.

In order that the sample and reagent are fully mixed they may need to remain resident within the system prior to the detection chamber to allow diffusion of the multiple streams into each other. Next the mixed sample may require a post-mixing residence time for the chemical reaction to take place and any colour to fully develop. At this point the sample is ready for the measurement chamber and, depending upon the method of detection chosen, it may require a further hold time within the detection cell for measurement stability. Further delays may be required to prepare the system for following samples such as processing of blanks and standards for the calibration of the optical cell. In a continuous flow system these delays can be designed in through the addition of longer fluid path lengths.

Although the addition of delays are not in themselves an issue for data logging systems, the additional residence time aids Taylor dispersion within continuous flow systems. Equation 2.11 (in section 2.2.3.2) shows that as time becomes $t \gg 0$ the concentration axially away from $z = 0$ becomes non-zero. As this time, t, is increased so the axial growth of the plug increases. Minimising this dispersive growth allows smaller distinct sample volumes to be resolved.

The system manufacturing approach is dependent upon the components chosen to build it. The substrate, valve type and pump choices create their own set of considerations. Most options are not perfect so reduce performance of the system. An example of this may be the introduction of additional dead volumes and/or path lengths due to a planar or laminar manufacturing method.

Optimal temporal performance and system accuracy (and resolution) are mutually exclusive. For a given optical performance the temporal performance is affected by a number of factors, discussed in the following sections. The system designer considers this trade off when designing a system for a required performance.

6.1.1.1 Definition: Temporal Response

The temporal response of a system, t_r is the system performance measure which defines the *quantity* of samples which can be measured. It is defined as the time taken for the system to respond to a change of sample and provide the correct output (within the system measurement capability).

Consequently it determines the number of samples which can be measured within a given time period. Reduction of the temporal response is desirable. It allows discrete measurements to be made quickly so that datasets with fine temporal and (in the case of moving vehicles) spatial resolution are possible.

6.1.1.2 Definition: Accuracy, Resolution and Limit of Detection (LD)

These factors define the performance of the system in terms of the *quality* of the measurements which are made.

"Accuracy refers to the correctness of data ... it is related to the deviation of the determined value from the true value." Grasshoff et al. (1999). This may be affected by the stability of the optical system (detector and emitter pair) as well as stability of reagents for dye production (although this can be calibrated out to some extent with blanks/standards).

The resolution of the system is the minimal change in sample concentration required before a difference is measured in the output signal.

"The limit of detection (LD)... is commonly defined as the lowest concentration level that is statistically different from a blank at a specified level of confidence" Grasshoff et al. (1999). This is often the lowest sample concentration which can be measured above the system noise. Grasshoff et al. (1999) also states that signals must be at least the blank value plus three standard deviations of the blank or should be reported as 'not detected'.

Each of these parameters requires system stability for best performance. Variations in the fluid flow, the optical emitter/detector pair, mixing ratio, mixing efficiency and other factors cause variance in the output signal and degraded performance.

6.1.2 Performance limitations in microfluidic colourimetric sensors

Dead volumes, areas in channels where there is little or no flow, require additional flushing between samples. These may be present due to design restraints, such as commercial valve internal volumes which are only flushed during operation, or the system assembly method such as laminar construction which does not allow for round corners. Any dead volume not flushed between samples dilutes the sample (decreases or increases concentration depending upon chemistry) affecting the measurement. These may be as large as the detection volume for certain designs: the LFNA1250125H (The Lee Company USA) valves have a 13 μl internal volume. Reduction of system and detection volume allows for smaller channels to be used, reducing possible dead volumes and delays created due to flushing. Regular calibration with blanks and standards maintains confidence in measurements (Grasshoff et al. (1999)) but also adds delays between each sample and increases reagent consumption. Using the smallest system volume reduces the impact of these operations upon total reagent consumption but the delays remain present. Although these delays are not a problem for logging systems the additional flushing requirements do increase the Taylor dispersion and hence decrease the temporal response, reducing the maximum valid data rate for the system.

As described in section 2.2.3.2 Taylor-Aris dispersivity is the longitudinal dispersion between samples as they pass through microfluidic channels. This causes plugs of fluid to 'smear' into each other as they pass through the system, the extent of which is given by the equations given previously. This phenomena limits the number of discrete samples which can be made as it causes unknown regions between each sample where the contents are a mixture of the distinct samples either side. System characteristics which cause large Taylor dispersion reduce the temporal response in this way directly.

Using the mathematics discussed in section 2.2.3.2 we can assess whether the system can be modelled with the Taylor-Aris dispersion theory. The diffusion coefficient depends on the exact chemistry used; for example phosphate is measured using molybdo-vanado-phosphoric acid giving a yellow complex (Sequeira et al. (2002)) with a diffusion constant of between (5.51 - 9.48) x 10^{-10} m^2 sec^{-1} in water (Tsigdinos and Hallada (1970)). For our devices (κ= 1/20, W = 300 μm), the characteristic molecular diffusion time ranges from 4 to 8 seconds. Since the residence times for most colourimetric chemistries are in minutes, equation 2.9 holds true and the system can be modelled this way.

6.1.3 System design schemes

There are a number different ways of arranging pumps and valves within a system in order to allow it to perform certain tasks. Each of these has advantages and disadvantages which are discussed here.

6.1.3.1 Push-push

This is perhaps the simplest method of employing a multiple flow stream system, Figure 6.1. Separate pumps inject fluid into each inlet of the chip, whilst the outlet is free flowing. If the optical sub-system can tolerate pulsed flow peristaltic pumps may be used: otherwise pulseless flow pumps are essential. Assuming syringe pumps are used, each is filled with its respective sample or reagent. When pumped into the system the fluids are layered along side each other and form multiple layered streams. Each of the syringes requires an inlet and outlet valve to ensure flow only in one direction.

6.1.3.2 Pull on waste

In this arrangement a negative pressure (relative to the rest of the system) is created at the outlet of the system, Figure 6.2. Syringe or peristaltic pumps may be used depending upon the required operation. Without additional component requirements low dead volumes are possible at the sample inlet and, due to the laminar fluid behaviour in microfluidic systems where the back pressure is proportional to the fluid path length,

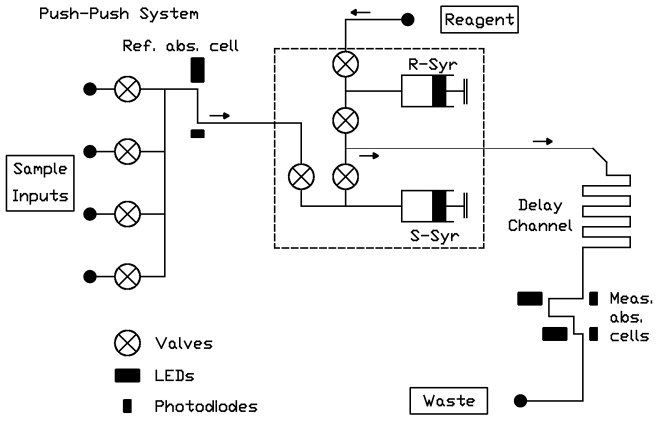

FIGURE 6.1: Diagram shows a system using a push-push pumping scheme

facilitates flow control/metering by careful design of channel length. In theory this allows for consistent system dosing.

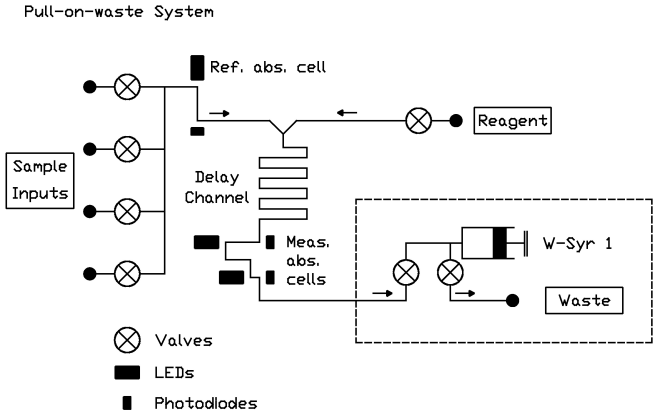

FIGURE 6.2: Diagram shows a system using a pull on waste scheme

6.1.3.3 Push-pull

This arrangement uses multiple pumps to inject fluid into all but one inlet of the chip and another pump to draw fluid from the outlet. It is a compromise between the 'push-push' and 'pull on waste' concepts, Figure 6.3. The ratio of the pump rates at the inlet and outlet provides a consistent dosing arrangement, similar to a 'push-push' system. The benefit is that the measurement stream (sample, standard or blank) may be switched without flushing of the pumps. Delays in emptying/filling of syringes may be minimised by increasing syringe size and/or using parallel pumps (i.e. one fills while the other empties). The system remains flow rate (rather than pressure) controlled and is hence immune to variations in the pressure of the reagent, blanks or standard reservoirs.

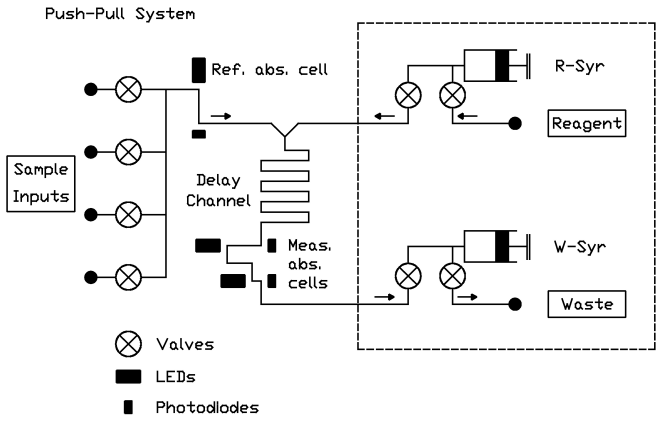

FIGURE 6.3: Diagram shows a system using a push-pull pumping scheme

6.1.3.4 In-line on-chip pumping

There are a number of system designs possible if in-line on-chip pumps are utilised, Figure 6.4. The reduction in dead volume and small actuation volume allow very small samples to be pumped and multiple pumps to be included. Combined with on-chip valves, with little or no dead volume, very complicated and/or high performance systems can be achieved. The disadvantage is that actuation of multiple valves/pumps is complicated as described in the previous chapter.

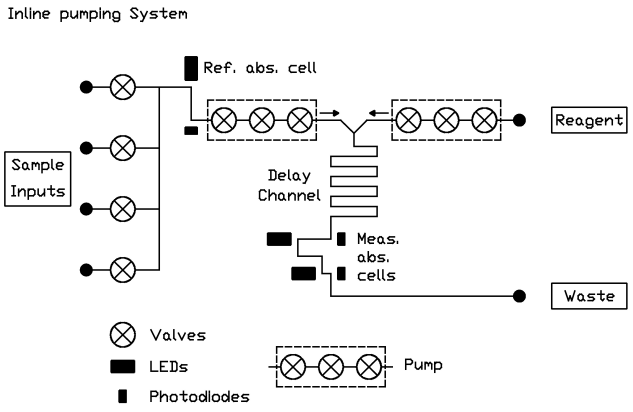

FIGURE 6.4: Diagram shows a system using an in-line on chip pumping scheme

6.1.3.5 Discrete and continuous pumping

The push-push scheme is a good example of a system which inherently makes discrete measurements: each fill of a syringe is essentially a single sample. Syringe pumps may be adapted for continuous operation (Figure 6.5) in systems such as the push-pull scheme. The addition of an extra pair of valves allows measurements to be made one after the other without creating discrete samples. This is demonstrated in section 6.2.1.1.

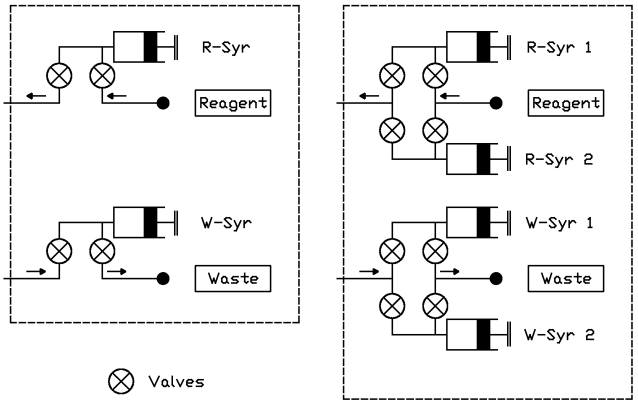

FIGURE 6.5: (left) Diagrams show syringes arranged for dosed operation. (right) Using a pair of syringes and a pair of valves on each it is possible to produce continuous flow operation by withdrawing one syringe while pushing the other

6.1.3.6 Detection systems

In systems where the mixing and reaction time are short, flow through detection chambers may be suitable. But where the reaction time is slow it may be advantageous to hold the sample in the detection chamber to allow for full colour development. Figure 6.6 shows the difference between two detection systems which still allow for continuous operation. Figure 6.6.a is a standard flow through cell for continuous measurement. Figure 6.6.b shows a series of cells multiplexed and separated with valves to allow discrete samples to be held while measurements are made. Multiplexing in this way reduces smearing and contamination between samples (while maintaining constant throughput) as movement of fluid within the system is minimised and samples are separated by valves. Unfortunately this multiplexed scheme requires multiple valves which further adds complexity.

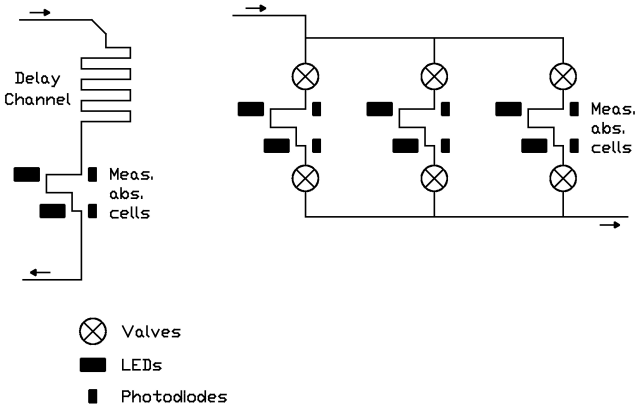

FIGURE 6.6: (left) Detection system arranged for continuous flow operation (right) Schematic of a multiplexed detection system

6.1.4 Mixing requirements in microfluidic colourimetric sensors

In certain system designs a mixer may be required to aid the mixing of the sample and reagent streams. This is determined by the diffusion time of the chemical species and the ratio of mixing time to reaction time. The system designer will often attempt to minimise the total sample residence time within the system (t_r) prior to the measurement being taken as discussed in 6.1.2. As such when using chemicals with slow diffusion rates and fast colour development a mixer may be desirable. When the diffusive mixing time is short (a few seconds) and the colour development time is considerably slower (an order of magnitude) then the impact of diffusive mixing is less significant. In these cases a mixer will provide little benefit and, in some cases, may reduce performance by increasing channel length and internal system volume. The following subsection features a brief overview of mixers which appear in scientific literature and may be suitable for those systems discussed.

6.1.4.1 Microfluidic mixers in literature

In wet chemical systems the perfect mixer causes full mixing of sample and reagent instantaneously without causing axial dispersion of the sample; however the driving mechanism in microfluidic mixers is diffusion making instantaneous mixing unlikely. However the mixing time should be minimised.

Turbulence can be used to mix sample and reagent at the macro-scale, for example by moving a stirrer through a beaker. This method speeds up the diffusion of molecules and reduces reaction completion times. In this case mixing of two chemicals in a beaker is trivial. However mixing two chemical species within a laminar flow regime, as occurs in a microfluidic chip, relies on diffusion. At this scale inertial effects are small in comparison to viscous effects. In order to speed up the process the diffusive boundary may be manipulated. This is the purpose of on chip mixing components. It has led to much interest in the field of microfluidic mixer design and a number of recent reviews on the subject (Hessel et al. (2005), Nam-Trung and Zhigang (2005), Green et al. (2007)).

Mixers come in active (requiring external power input) and passive varieties (where the energy is extracted from the fluid flow). The flow requirements through the chip, the channel dimensions and the system operating environment determine the suitability of a design. For reference, using a flow rate of 100 μl min^{-1} against a back-pressure of 1 bar the pumping power requirement is 164 mW.

Active mixers in microfluidic chips work using the same principle as macro-fluidic mixers. They encourage fluid movement which would not exist in the normal flow through some powered means. The means by which the movement is introduced is usually a physical action such as moving a stirrer (Lu et al. (2002)), causing bubbles to form and collapse

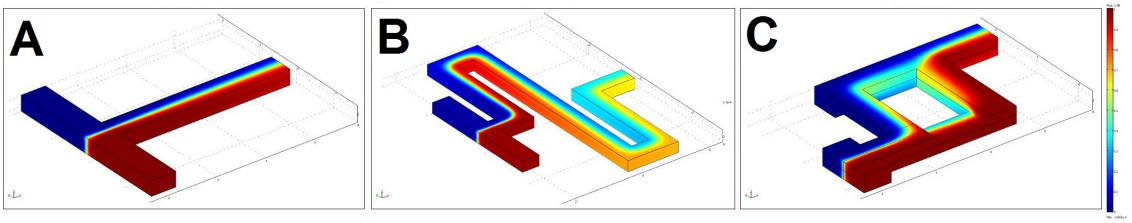

FIGURE 6.7: A. Simulation of the mixing of two fluids in a T-mixer, B. Simulation of the mixing of two fluids in a chicane mixer, C. Simulation of the mixing of two fluids in an F-mixer (Payne (2008))

(Tsai and Lin (2002)) or simply passing the fluid over a moving membrane (Yang et al. (2001)). Movement can also be transmitted into the device by these methods to drive pump actuators, discussed in section 5.1. It is also possible to use magnetohydrodynamic and electrohydrodynamic forces (Fu and Chien (2005)). Active mixers can be switched off to allow un-mixed fluid plugs to be passed if required, but this functionality is at the cost of added system complexity and power requirement.

Passive mixers manipulate the flow in order to increase the area over which diffusion can take place by changing the geometry of the fluid channel. The energy used to manipulate the fluid is taken from the fluid itself. This increases channel resistance and pressure drop through the system. No additional external components are required making these mixers reliable and suited for small *in-situ* systems. Simple designs include T (Figure 6.7.A) and Y channel shapes along with chicane mixers. These are simply long channels bent such that sections lay alongside each other increasing the residence time and diffusive length, Figure 6.7.B. Other planar mixing elements include Tesla type geometries (also used as valves)(Hong et al. (2004)) and recirculating geometries (Hung et al. (2005)).

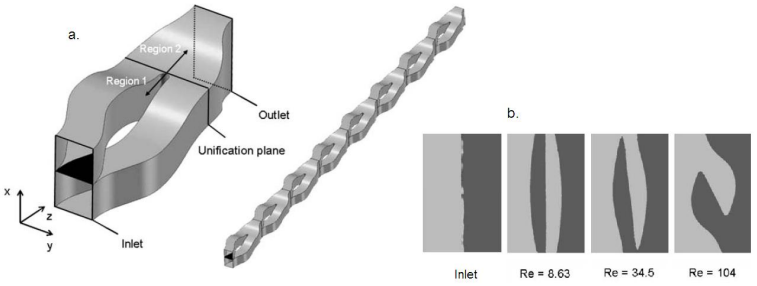

FIGURE 6.8: a. A design for a split and recombine mixer, b. A series of flow profiles at intervals through this mixer design (Hardt et al. (2006))

Increasing the diffusive area aids mixing and can be achieved by combining multiple inlet streams so as to laminate multiple layers of fluid alongside each other. The same affect is achieved when split and re-combine (SAR) designs are used (Figure 6.8). Some of these designs use large channels with obstructions to achieve the required fluid manipulation (Lee et al. (2006)). Others use multiple channels (Hardt et al. (2006)). Twisting the fluid during the manipulation also aids these designs, such as in F-mixers (Figure 6.7.C)

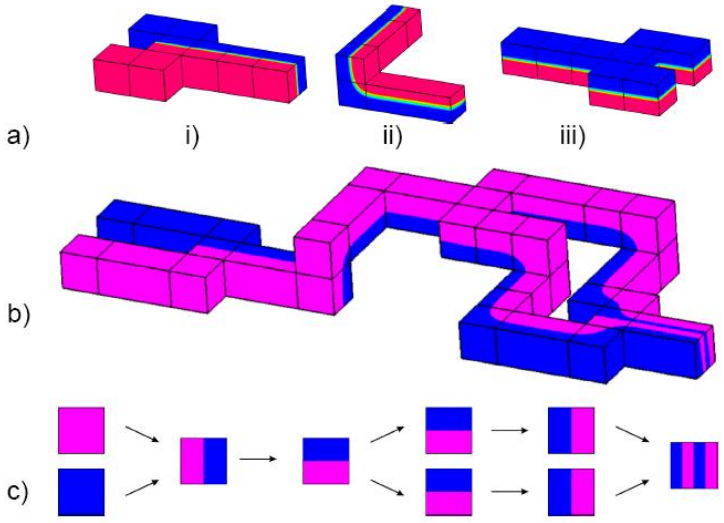

FIGURE 6.9: a. Modular components of the S&R mixer i) combine, ii) twist and iii) split structure. b. CFD-simulation of the S&R mixer. c. Schematic working principle of the mixer. (Cupelli et al. (2005))

as it further increases the diffusive boundary: beneficial at low Reynolds numbers (Chen and Meiners (2004)). Certain channel manipulations provide predictable flow changes. This allows them to be split into modular pieces making modular design possible, shown in Figure 6.9 (Cupelli et al. (2005)).

Chaotic advection can be used to mix fluid within microfluidic channels. Changes in the channel geometry such as obstructions (Bhagat et al. (2007)) or cutaways in the walls can be used to create local pressure nodes and circulation of fluid. Herringbone structures cut into the channel walls cause circulation of fluid from the outside of the channel into the channel centre (Williams et al. (2008)). Diagonal grooves introduced into the top and bottom of the channel can be used to similar effect also (Howell et al. (2005)).

6.1.4.2 Development of a mixer for wet chemical nutrient sensors

Using Comsol and Solidworks software a mixer suitable for in-line mixing of sample and reagent was developed. The final design, Figure 6.10, is similar to that presented by Hardt et al. (2006) but reconfigured to allow for laminar 2.5D construction. The design operates on the principle of splitting the fluid horizontally Figure 6.11.a, moving the top and bottom sections laterally away from each other Figure 6.11.b, bringing both streams onto the same plane Figure 6.11.c and then recombining them side by side Figure 6.11.d. The inlets introduce the fluids alongside each other giving a side-by-side lamination into the first element. A 4-layer lamination of the two fluids is created after the first element. When this is then fed into another element an 8-layer laminate is formed at the output. The introduction of 2 laminates into n mixing elements will cause the output to contain

2^n laminates. After each mixing element the width of each laminate is reduced to half of its previous geometry. In this way two input streams are combined into multiple much thinner streams over which the time to fully diffuse is much smaller.

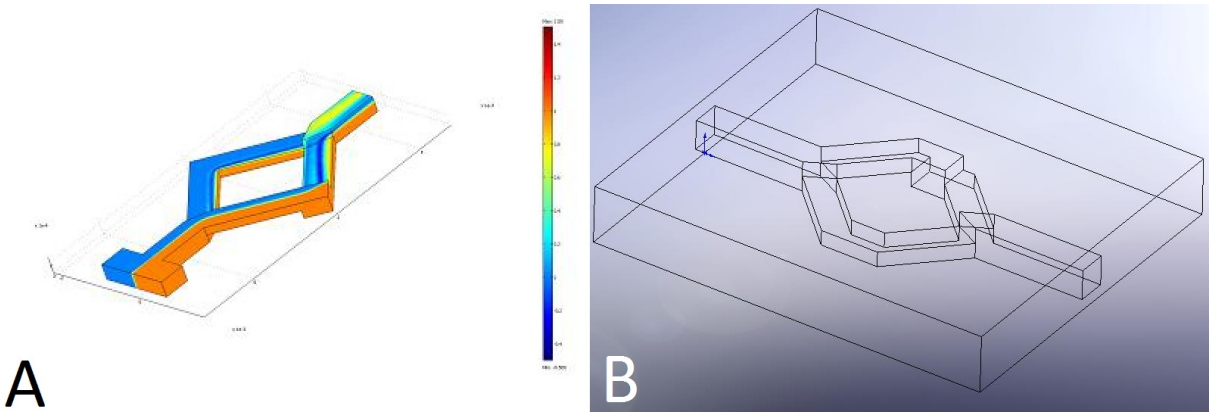

FIGURE 6.10: A. a novel mixer design modelled in comsol. Designed by this author and modelled by David Payne (2008) while on placement at CMM, B. a mixer design adapted from A (designed and drawn by this author) using a similar principle to Hardt et al. (2006) but designed for sub-millimetre laminar manufacturing methods

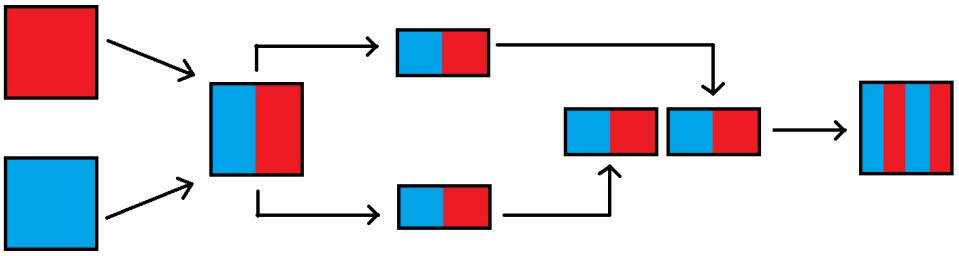

FIGURE 6.11: Operating principle of mixer design shown in Figure 6.10.B

6.1.4.3 Bench testing of mixer

The mixing elements are designed so that dead volumes are minimised when manufactured in a laminar way. Further reduction is possible with full 3D micromilling to smooth the corners which create the dead volume regions, though this has not been attempted yet. Exclusion of dead volumes should provide constant flow velocities in each of the legs of the mixer elements. This is also a design feature; if a bubble is formed in one leg the increase in the pressure drop across the mixing element will encourage the bubble to move through. This is due to the changing depths as shown in Figure 6.11, where the depth of the channel in each of the mixer legs is half of the channel before and after the mixer. If one of these legs is blocked the fluid will experience a velocity increase through the other leg in order to maintain its volumetric flow rate. According

to the Darcy-Weisbach equation (shown in chapter 2) this will cause an increase in the pressure drop in this region. The increased pressure gradient across the mixing element encourages the movement of the bubble if it is large enough to overcome the surface energy of the blockage.

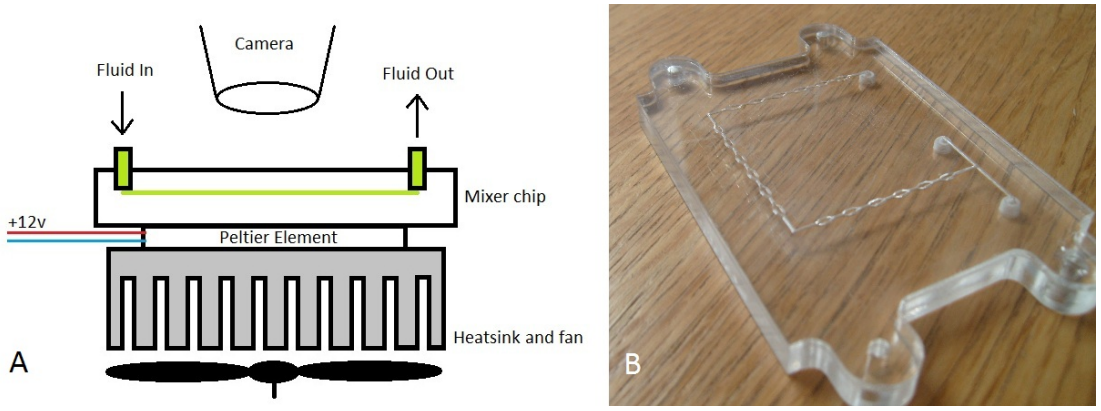

FIGURE 6.12: A. Schematic of mixer testing. Peltier is used to cool the chip in order to slow the diffusion of the food dye, B. Example mixer test chip including pin-alignment holes at each corner

This function of this mixer was investigated using food dye, which enables visualisation of stream lines, and hence the production of laminated flows. The food dye rapidly diffuses in water at room temperature so the system was cooled using a peltier element. A schematic of the setup is shown in Figure 6.12. An image showing dye based streamline and laminated flow visualisation is shown in Figure 6.13. Prior to the first element there are 2 fluid streams and afterwards this becomes 4 fluid streams, demonstrating the principle of the mixer.

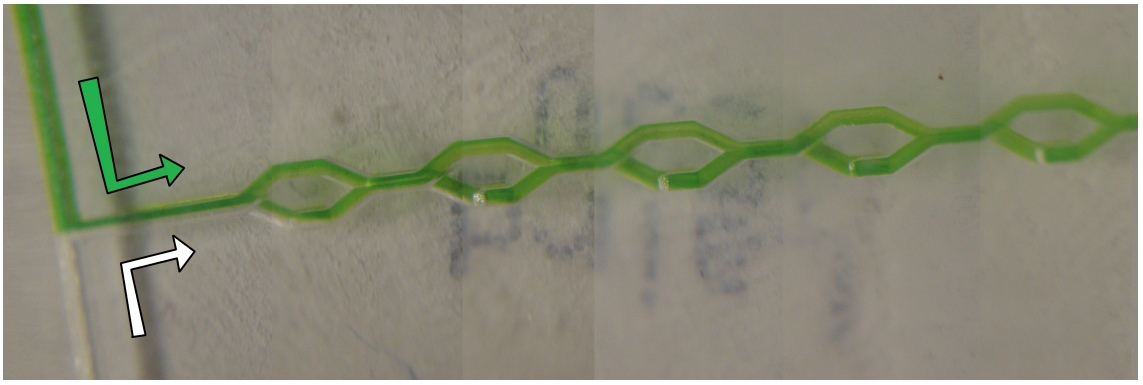

FIGURE 6.13: Operation of original SAR mixer with green food dye and water on a cooled peltier assembly to slow diffusion and aid visualisation

6.1.5 Nutrient sensors in literature

Accurate and robust long-term monitoring of nutrients, dissolved gases and trace metals is an important area of research (Moore et al. (2009)); and detection methods include

electrochemical, capillary/column, biosensing and spectrophotometry (Dutt and Davis (2002), Finch et al. (1998), Hanson (2005), He et al. (2007), Moorcroft et al. (2001)). Spectrophotometric or colourimetric approaches are stable and reliable. They can be calibrated using standard samples and have good detection limits (sub-nanomolar). Along with this their dynamic range makes them a viable, accurate and economical option for implementation in low-cost miniaturised sensors suitable for mass deployment (He et al. (2007), Patey et al. (2008), Sieben et al. (2010)). Commercial colourimetric systems that measure nutrient concentrations have limited deployment capabilities, often due to their large physical size (e.g. 44cm long and 13cm dia.)(Johnson and Coletti (2002)), high power consumption (typically 10-150 W)(Hanson (2000)), and excessive reagent usage (mL per sample)(Hanson (2005), Johnson and Coletti (2002)). Microfluidic systems are able to overcome many of these problems; however the sampling speed of these systems (both macro and micro) need to be considerably improved to allow accurate measurement of steep chemical gradients or small scale phenomena.

The most common methods of fluid handling include: stop-flow (Bowden et al. (2002b), Slater et al. (2010), McGraw et al. (2007), Greenway et al. (1999)), continuous flow (Jannasch et al. (1994)), flow-injection analysis (FIA) (Carlsson et al. (1997)), segmented flow analysis (SFA) (Gardner and Malczyk (1983)) and sequential injection analysis (SIA) (Wu and Ruzicka (2001), Ruzicka and Marshall (1990)). Typical miniaturised stop-flow systems have sampling rates that range from 5-20 samples per hour (Bowden et al. (2002b), Slater et al. (2010), McGraw et al. (2007), Cleary et al. (2010), Bowden et al. (2002a), Bowden and Diamond (2003), Sequeira et al. (2002)), limited by the time required for full colour development, which can be minutes. Continuous flow systems achieve higher sampling rates by constantly flowing both sample and reagent streams through a delay loop until detection is carried out. For example, the SubChemPak Analyser can sample at 900 $h^{-}1$ (Hanson (2000)), albeit with a large reagent and sample volume consumption (1 mL/min of reagent, 20 mL/min sample). These systems compromise on sensitivity by not achieving full colour development since they are seldom designed to allow reaction times of 5 min or more (Carlsson et al. (1997)). In continuous flow systems the performance is limited by dispersion of the sample, so in practical terms sample smearing leads to substantially lower sample rates. Flow injection analysis is a common variant on continuous flow, where a fixed sample volume is injected into a carrier stream containing the reagent. This method can process 20-180 samples per hour (Carlsson et al. (1997), Yaqoob et al. (2004)) but reagent consumption is excessive. Segmented flow systems limit dispersion by separating sample plugs with air bubbles injected into the sample/reagent stream, and achieve throughputs of 15-30 samples per hour (Patey et al. (2008)). Sequential injection systems lower reagent consumption by stacking discrete volumes of sample and reagent in a holding coil, which is then propelled to a reaction coil for sufficient time to allow for colour development (Ruzicka and Marshall (1990)). A throughput of 20-70 samples per hour was demonstrated for SIA systems, and is dependent on the reaction kinetics (Wu and Ruzicka (2001)).

6.1.6 Summary of introduction to nutrient sensor systems

In this chapter two microfluidic architectures are presented (continuous flow, and multiplexed stop flow) for miniaturised colourimetric nutrient sensors. These systems are compared with respect to the temporal response for optimisation of sampling rate and reduction of reagent consumption. The continuous-flow system is capable of a sampling rate of 60 h^{-1}, which is limited by the Taylor dispersion. The novel multiplexed stop-flow (MSF) microsystem is not limited by dispersion. A demonstration MSF system consisting of two stop-flow channels is presented. This requires 12.6 s to load each sample into a measurement channel and when scaled to include 43 detection chambers would be capable of a throughput of 285 h^{-1} (with full color development). The MSF architecture is manufactured in PMMA/Viton®/PMMA, utilizes on-chip valves, and is scalable, thereby permitting sampling at much faster rates (subsecond). Either system is capable of remote deployment and continuous measurement of nutrient concentrations. The MSF architecture is particularly suited for applications requiring high temporal or spatial resolution; such as from moving vehicles. The architecture of the two different microfluidic systems are shown in schematic form in Figure 6.14 and Figure 6.15. The temporal performance of the two different designs is compared by measuring phosphate in water using the well known Molybdo-vanado-phosphoric acid or "Yellow method" (McGraw et al. (2007)).

6.2 Materials and Methods

6.2.1 Theory and design considerations

6.2.1.1 Continuous flow systems

In continuous flow analysis systems, the temporal resolution is limited by reaction kinetics and broadening of the sample plug as it travels to the detector. In pressure-driven microfluidic systems, the dispersion of solutes is caused by the parabolic flow profile and this Taylor-Aris dispersion can have a greater effect on plug broadening than molecular diffusion (Dutta and Leighton (2001)). Electroosmotic pumping overcomes this problem, but is unsuitable for remote *in-situ* nutrient sensor systems that operate with variable unknown sample streams.

To determine the optimal temporal response a few simple design constraints need to be considered. The 25 mm long absorption cell is a 300 μm wide and deep channel and has a 2.25 μL volume. The most demanding use of chemical sensors is on a profiling float such as the Argo, which ascends at approximately 10 cm/s (Gould et al. (2004)). A temporal response of 10 s would yield a spatial resolution of 1 m. To achieve this the flow velocity would be >2.5 mm/s, with a volumetric flow rate >13.5 μL/min. Each input sample

also requires a residence time prior to measurement for full colour development. This time is set by the reaction kinetics which for the chemistries used in typical nutrient analysis (Griess method for nitrite and nitrate, and the yellow method for phosphate (Bowden et al. (2002b))), ranges from 1 to 10 minutes.

Using the model in 2.2.3.2 the dispersion for the continuous flow microfluidic setup shown in Figure 6.14 can be estimated. It has rectangular channels (L = 1.65 m and U = 17 mm/s) giving an axial residence time, $t_r = 95$ seconds. A model of this geometry was created in Matlab and a number of injection lengths inputted. The results are shown in Figure 6.16.A.

6.2.1.2 Multiplexed stop flow systems

Stop flow systems do not suffer from sample dispersion; however, the temporal response of these systems is limited by the time taken for colour development. This can be improved by incorporating multiple sample holding chambers that are loaded sequentially using multiple valves (and/or pumps), which necessitates on-chip microvalves. In such a time-multiplexed system, pump actuation time can become rate limiting.

6.2.2 Chemistry preparation for Phosphate detection

Phosphate standards were made from a stock solution of 3 mM prepared by dissolving 0.408 g of potassium dihydrogen phosphate, KH_2PO_4, in 1 L of MilliQ water. This 3 mM stock solution was then diluted with MilliQ water to create the various concentrations used in this study. The Molybdovanadophosphoric acid method or "Yellow method" reagent was prepared with 7.2 g ammonium molybdate (A-7302, Sigma-Aldrich Company Ltd., CAS Number: 12054-85-2) and 0.36 g ammonium metavanadate (20555-9, Sigma-Aldrich Company Ltd., CAS Number: 7803-55-6) dissolved in 95 mL HCl 37 wt. %. and filled up to 1 L with MilliQ water (McGraw et al. (2007)). When the reagent is mixed with a sample containing phosphate ions, a yellow-coloured complex is produced that has an optical absorption proportional to the concentration of phosphate (strongly absorbing below 400 nm) (Bowden et al. (2002b), McGraw et al. (2007), Quinlan and DeSesa (1955), Michelsen (1957), Misson (1908)).

6.2.3 Fabrication of systems

6.2.3.1 Continuous flow microchip system fabrication

A schematic diagram of the continuous flow system is shown in Figure 6.14. It was fabricated by micro-machining from a block of poly(methyl methacrylate) (PMMA).

Figure 6.14.A shows the architecture of the chip. A series of commercial valves were mounted onto the chip, and used for sample selection (either ultra pure water blank, two phosphate standards, or a sample), followed by a reference absorbance cell (2.5 cm path length), a Y-junction (for addition of reagent), a serpentine delay loop to allow colour formation (1650 mm long) and two measurement absorbance cells (2.5 cm and 0.5 cm path lengths). Details of the optical absorbance cell can be found in chapter 4. The chip was machined in 5.0 mm thick tinted-PMMA (Plexiglas GS 7F60, Evonik Röhm Gmbh) by micro-milling (Protomat S100 micromill, LPKF Laser & Electronics AG). A solvent vapour bonding procedure was used to polish the channel surfaces and to bond the two halves as described in chapter 3. All channels were 160 μm wide and 300 μm deep, except the optical absorption cells which were 300 μm wide and 300 μm deep. Fluid connectors, optical alignment grooves and valve mounts were all milled into the lid or chip. Fluid handling was performed using twelve micro-inert valves (LFNA1250125H, The Lee Company USA) and a push/pull syringe pump (PHD Ultra 70-3009, Harvard Apparatus) simultaneously driving two reagent and two waste syringes. For 1:1 (v/v reagent:sample) studies, 250 μL (Hamilton Company 1725CX) and 500 μL (Hamilton Company 1750CX) syringes were used for reagent and waste, respectively. For 1:4 (v/v reagent:sample) studies, 500 μL (Hamilton Company 1750CX) and 2.5 mL (Kloehn Inc. 17598) syringes were used for reagent and waste, respectively. The total fluid flow rate was 50 μL min^{-1} for continuous flow experiments. High powered UV-LEDs were used (XRL-375-5E, 375 nm, 19-26 mW, Roithner Lasertechnik GmbH) as light sources and photodiodes for detection (TSL257-LF, TAOS); both bonded to the chip with Norland Products Inc. optical adhesive 63.

The system was controlled using custom made electronics with a National Instruments Corp. Digital Acquisition Device PCI 6289 card installed in a ruggedised PC running Labview 2009. A Labview state machine performed automated sampling and syringe pump control. To achieve continuous flow with syringe pumps, two reagent and two waste syringes were used, such that when one pair of syringes was manipulating fluid in the chip (waste syringe withdrawing fluid from the chip with reagent syringe injecting), the other pair of syringes were preparing for the next run (waste syringe emptying into the waste outlet and reagent syringe loading). This push/pull scheme requires eight valves and is shown in Figure 6.14.A (dashed-box). To analyse a sample from any one of the four inlets, the appropriate valve was opened and the sample was drawn into the device using the waste syringe. The size of the injected sample plug was controlled by the open time of the sample inlet valve. The sample plug passed through the reference absorption cell and reagent was added at the Y-junction.

6.2.3.2 Multiplexed stop flow system fabrication

The stop-flow colourimetric measurement system is shown in Figure 6.15. It has two absorption cells and multiple on-chip valves to control fluid input and for pumping.

These microvalves were made from a PMMA/Viton®/PMMA stack, as described in chapter 5. Briefly, substrates were treated with oxygen plasma (Femto RF, Henniker Scientific Ltd.) and soaked in a silane solution. PMMA substrates were soaked in a 5% v/v (3-Aminopropyl)triethoxysilane (APTES) solution and Viton® substrates in a 5% v/v (3-Glycidyloxypropyl)triethoxysilane (GPTES) solution. Viton® sheet (250 μm thick grade A, J-Flex Rubber Products) was bonded between the two PMMA blocks using mild pressure and temperature as described in chapter 5.

The valve architecture is similar to that used by the Mathies group (Grover et al. (2003)) and is based on a tri-layer structure of PMMA/Viton®/PMMA (Figure 6.15.B). The bottom substrate incorporates fluidic channels, the middle layer is the elastomeric membrane (Viton®) and the top substrate contains the pneumatic control channels. All channels are 160 μm wide x 300 μm deep, except absorption cells which are 300 μm wide. A valve consists of two fluidic channels separated by a barrier, above which is a displacement chamber in the pneumatic control layer. Opening and closing of valves is achieved by controlling the pressure in the displacement chamber using commercial solenoid valves (LHLX0500200BB, The Lee Company USA) on a manifold that is actuated with custom electronics driven by a Labview interface (NI USB-6009, National Instruments Corp.) Figure 6.15.C.

The chip schematic shown in Figure 6.15.A includes: a sample bus with 4 valved inlets, a reagent input, two on-chip peristaltic pumps operating in parallel (P1 for reagent and P2 for multiple samples) and two hold chamber units (entry and exit bus valves and an absorption cell) that are on a common bus. The system operates by sequentially loading the hold chamber absorption cells, with sample and reagent, waiting an appropriate length of time for near full colour development followed by an absorbance measurement.

6.3 Results and Discussion

6.3.1 Continuous flow microchip performance analysis

Taylor-Aris dispersion profiles were calculated for 4 different input sample lengths (15, 30, 60 and 120 sec. injections, equivalent to sample lengths of 240, 480, 960 and 1920 mm, respectively), shown in Figure 6.16.A by the square inputs. The figure shows how the profile of the sample changes as it travels from input to output through the 1650 mm serpentine at various times (0, 0.25 t_r, 0.5 t_r, 0.75 t_r, and t_r, where t_r is the residence time). For the 120 second (1.92 m long) injection the plateau or peak height barely changes and would give a clear resolvable signal. The 60 second injection becomes more disperse, but the peak amplitude is constant. This sample length is the temporal response limit. The 15 and 30 second injections reduce in amplitude, smear and overlap with adjacent plugs of similar size making them difficult to resolve.

This observation is also seen experimentally. The "reagent" was replaced with MilliQ and four different samples were analysed consisting of MilliQ, 0.025%, 0.05% and 0.1% (v/v) yellow food dye. Figure 6.16.B shows the photodiode voltage when 0.1% (v/v) plugs of food dye were injected with MilliQ plugs on either side. Figure 6.16.C shows the same data in terms of absorbance. The initial sample plug length was 1.92 m and was changed to 0.96 m at 500 seconds. The reference cell (grey, Figure 6.16.B) shows the plug entering the serpentine approximately square (rise/fall times were 30 seconds, due to valve dead volume). The final sample plugs (black, Figure 6.16.B) have half the absorption value of the initial plug (due to a 1:1 dilution with MilliQ) and the width of the samples have broadened, as expected from dispersion. Both the 120 second and 60 second plug profiles are in qualitative agreement with Figure 6.16.A. For a 30 second long sample plug the amplitude reduced, similar to Figure 6.16A.

Aris (1960) found that periodic flow, as generated by a syringe pump, is usually not a significant contribution to dispersion. It contributes less than 1% to the total dispersion, unless the amplitude of the fluctuations in the pressure gradient are larger than the mean. However, Ng (2006) notes that slow pulsations (oscillation period comparable to the advection time-scale) can lead to much higher contributions to the dispersion. In this work, the average flow rate was 50 μL/min, provided by the syringes in discrete volumes of 3.42 nL/step (14,640 steps/min), so that pulsations can be ignored and are unlikely to contribute to dispersion.

Successive dye plugs were injected at increasing concentrations (Blank, 0.025%, 0.05% and 0.1%, sequentially), and the results are shown in Figure 6.17.A. Identical data is used in Figure 6.17.B but this graph is in terms of absorbance. The plug sizes were 480, 720, 960 and 1920 mm (as labelled by the 30, 45, 60 and 120 sec. injections, respectively). For each of the plug lengths the reference cell (grey, Figure 6.17.A) shows the input profiles of 4 laddered plugs entering the serpentine with sharp edge transitions. The final output profiles (black, Figure 6.17.A) have 50% of the absorption value of the initial plug due to the 1:1 dilution, MQ:Dye. The slopes have decreased, as expected from dispersion. The 45, 60 and 120 second injections yield output profiles that have distinguishable plateaus; however the 45 second injections do not recover to the blank level on the MilliQ water plug (plug transition from 0.1% to MQ). The 30 second injections showed overlapping of the samples, such that the original input profile had smeared to a gradient of dye concentration.

To measure phosphate using the "Yellow method" the chip was configured as in Figure 6.14. Successive phosphate plugs were injected at the 120 s optimal injection time for increasing concentrations (MilliQ, 20, 30 and 40 μM, cycled) and the results are shown in Figure 6.17.C. Identical data is used in Figure 6.17.D with the graph in terms of absorbance. The reference channel measures the sample before addition of reagent where there is no colour development. After the sample is mixed with reagent (1:4, reagent:sample) and travels through the serpentine, the output profile is measured in

the absorption cell. The dispersion is similar to that observed for the food-dye. The transients seen on some of the plateaus occurred when valves were switched; these fluctuations were not visible in the dye experiments. Similarly, when the pump changed directions (switching syringes) with the yellow method, fluctuations were seen in the measurement data. This is presumably caused by variations in refractive index due to loss of synchronised flow when mixing reagent with the standards. This does not occur when using dyes. When sampling continuously (valves not switched), transients are not observed because there are no pressure perturbations.

6.3.2 Multiplexed stop flow system performance analysis

The demonstration multicell microchip was evaluated with both dye (to investigate sample loading and dispersion) and with the phosphate "Yellow method" to investigate the effects of reaction kinetics within this system. In dye experiments, coloured samples of increasing concentration (blank, 0.05%, and 0.1%; cycled) were successively injected and the results are shown in Figure 6.18.A. Again identical data is used in Figure 6.18.B with the graph in absorbance. Samples were diluted with Milli-Q water connected to the reagent input (1:1 (v/v) dilution by use of the parallel peristaltic pumps). Each pump cycle delivered 8 μL, governed by the valve seat cross-sectional area and depth. To evaluate the stability of the optical cell in this pumping configuration, sample plugs were injected in 10 pump cycles (80 μL, 42 seconds) followed by a hold time of 90 s. Figure 6.18.A shows that it takes 2-3 pump strokes to change over a sample, for example 0.1% dye to MilliQ. This is notable by the steep gradient or transition between samples. The perturbation that occurs during a pump cycle is seen by the small change during a rising or falling edge, circled in grey in Figure 6.18.A (similar in position on each repeat). The inset box shows that pump strokes 4-10 (before the wait time) have little effect on the absorption signal. As each pump cycle takes 4.2 s (6 x 700 ms per actuation), the device can swap samples in the absorption cell every 12.6 s.

The temporal performance of the implementation presented is limited by the time taken for the sample within a hold chamber to be changed. The system is designed such that mixing and reaction times affect only the number of chambers required to achieve the maximum temporal performance. The maximum temporal performance is in turn limited by the pump actuation time; that is, the speed at which the valve membrane changes state (from closed to open) multiplied by the number of steps in a peristaltic pump sequence. The pneumatic solenoid actuators used to open and close the on-chip valves have a minimum actuation time of 35 ms; however it was determined experimentally that accurate and repeatable pump volumes require more than 500 ms per actuation. Actuation speed (technology-dependent, here pneumatic) will be the limiting factor that determines pump speed and thus sensor temporal performance with the MSF architecture.

To demonstrate the combined effects of quick diffusion (short mixing time) along with slow reaction kinetics, the system was used to measure phosphate by the "Yellow method", which has a typical color development time of 9 min. Reagent and phosphate standards were successively injected at increasing concentrations (blank, 20 μM, and 40 μM; cycled), and results are shown in Figure 6.18.C. The data shown in Figure 6.18.D is identical with the graph in absorbance. 10 pump cycles (80 μL) were used but the hold time was increased to allow nearly full color development (9 min). Comparison of Figure 6.18 panels A and C (or B and D) shows that transients from pumping are more apparent when the phosphate chemistry is used. The transients are larger with the stop-flow setup than the continuous-flow setup since peristaltic pumping used in the stop-flow system produces sudden changes in flow velocity and profile. However these transients do not interfere with the final measurements which are taken during a 5 s window at the end of each hold time (Sieben et al. (2010)). Even when reagent assays have fast reaction kinetics, slow mixing times may become the limiting factor for colour development. For example the determination of Iron concentration with the Ferrozine method (Stookey (1970)) where the mixing time is in the order of hundreds of seconds for these channel sizes. In this case the total hold time would be the combination of the diffusion time and the reaction time; which is typically greater than the pump actuation time. It is this total hold time divided by the time taken to fill each chamber that defines the number of chambers required to achieve maximum temporal performance.

The performance of the current two-channel system is close to that required for continuous measurement of phosphate (every 10.8 s) onboard an Argo float deployment. The system can move a new sample into each chamber every 12.6 s, which can provide a 1.17 m resolution. This assumes that the system will have enough chambers to allow for colour development and measurement. With a hold time of 9 min (full colour development), 45 hold chamber units would be required to achieve a 12.6 s temporal resolution. However shorter hold times could be used (3 min for phosphate chemistry (Bowden et al. (2002b))) but at the expense of reduced sensitivity. A 3 min hold time requires 15 hold chamber units.

6.4 Conclusions

In this chapter possible valve and pump architectures for microfluidic colourimetric sensor systems have been discussed and a brief overview of mixers included. The use of components within the system affects the system performance and some functions may not be required (such as mixers) when certain architectures or system operational modes are chosen. Continuous flow systems often require an in-line mixer and a SAR design suitable for these types of system has been demonstrated.

In order to study the temporal response of microfluidic colourimetric sensors two sys-

tems have been demonstrated utilising continuous-flow and stop-flow architectures. The continuous flow system is capable of sampling every 60-120 s (30-60 samples·h^{-1}) and is limited by the Taylor dispersion. By decreasing channel size, dispersion could be reduced and the sampling rate improved. Alternatively, a novel multiplexed stop-flow (MSF) microsystem was demonstrated requiring 12.6 s per sample (up to 285 samples·h^{-1}). The MSF architecture utilizes on-chip valving, is scalable, requires no mixer, and would permit sampling at much faster rates (i.e. subsecond). Furthermore, the platform would be capable of handling multiple chemistries to sample a wide range of nutrients on a small-footprint device. With further work to reduce the size of the valve actuation mechanism the system could be deployed remotely to continuously measure nutrient concentrations in the environment.

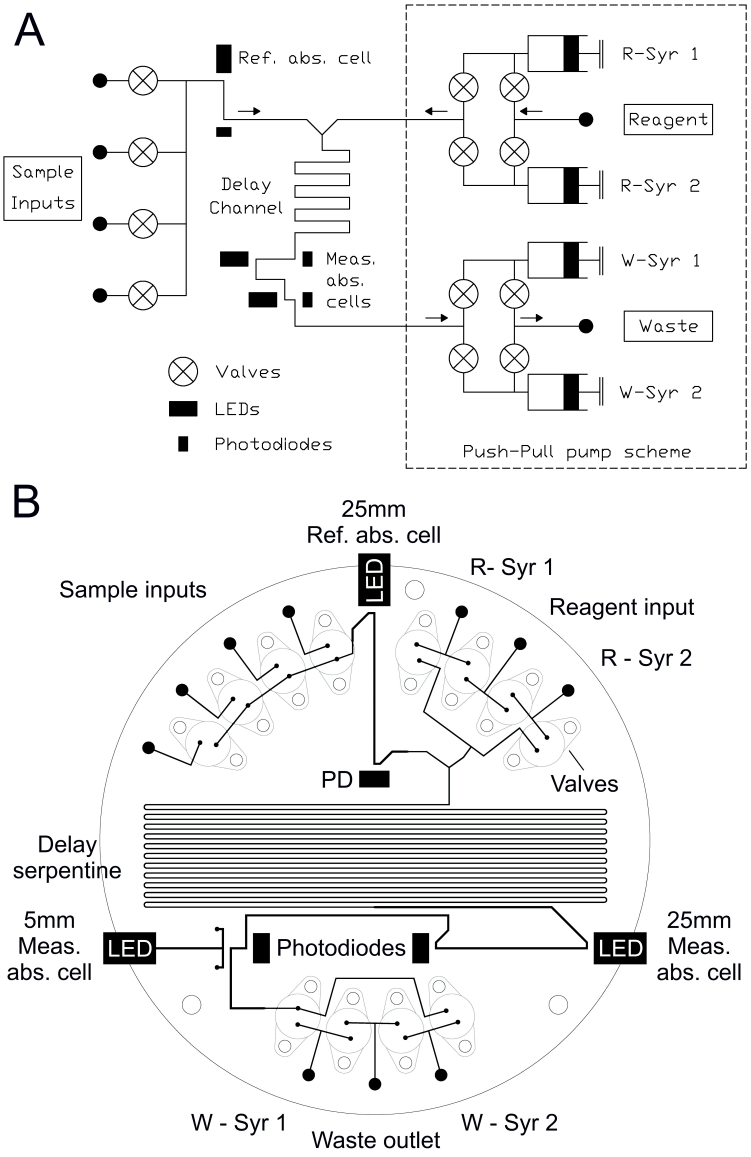

FIGURE 6.14: (A) Continuous flow system diagram. The system is based on a push/pull scheme, where eight valves, two waste and two reagent syringes enable non-stop operation. To analyse one of the samples, the appropriate valve was opened and the sample was pulled into the chip by the waste syringe (pulling syringe). The sample is passed through the reference absorption cell and reagent was added at the Y-junction (pushing syringe). The long serpentine was then used to create a time delay allowing the formation of colour, which was finally recorded with two dog legged measurement absorption cells. (B) The continuous flow microfluidic chip schematic (diameter of 90 mm). A series of commercial valves were mounted onto the chip and permit sample selection, followed by a reference absorbance cell (2.5 cm path length), a Y-junction, a 1650 mm long serpentine and two measurement absorbance cells (2.5 cm and 0.5 cm path lengths).

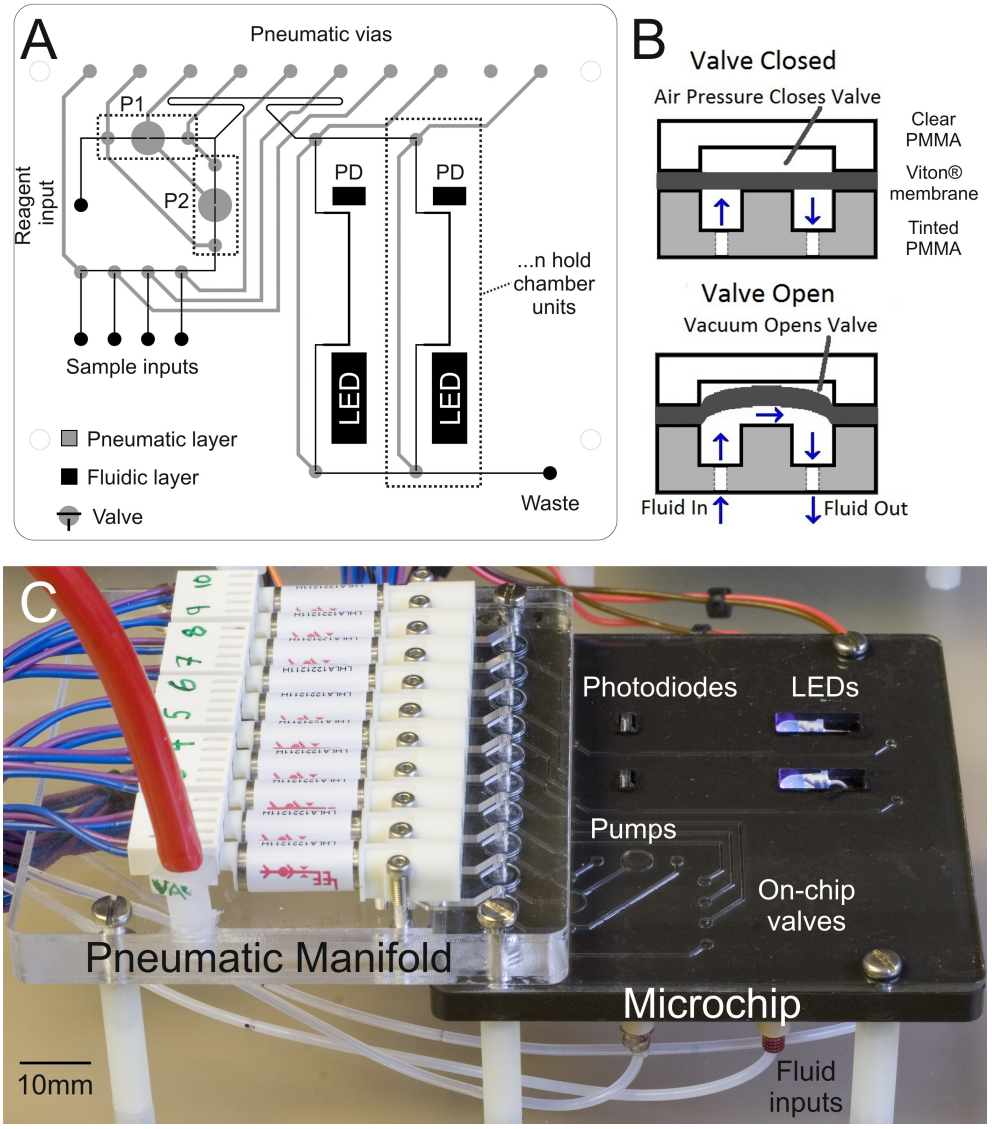

FIGURE 6.15: (A) The multiplexed stop-flow (MSF) chip schematic with multiple absorption cells; a sample bus with 4 valved inlets, a reagent input, two peristaltic pumps that operate in parallel (P1 for reagent and P2 for sample), and two hold chamber units (entry and exit bus valves and an absorption cell) that are on a common bus. The system operates by sequentially loading the hold chambers and allowing colour development. The system is scalable and allows 'n' number of hold chambers. (B) The valve architecture implemented, based on a tri-layer structure of PMMA/Viton/tinted-PMMA. The bottom substrate incorporates fluidic channels, the middle layer is a deformable elastomeric membrane, and the top substrate contains the pneumatic control channels. Opening and closing of valves is achieved by controlling the pressure in the displacement chamber. (C) Photograph of the multiplexed stop-flow system.

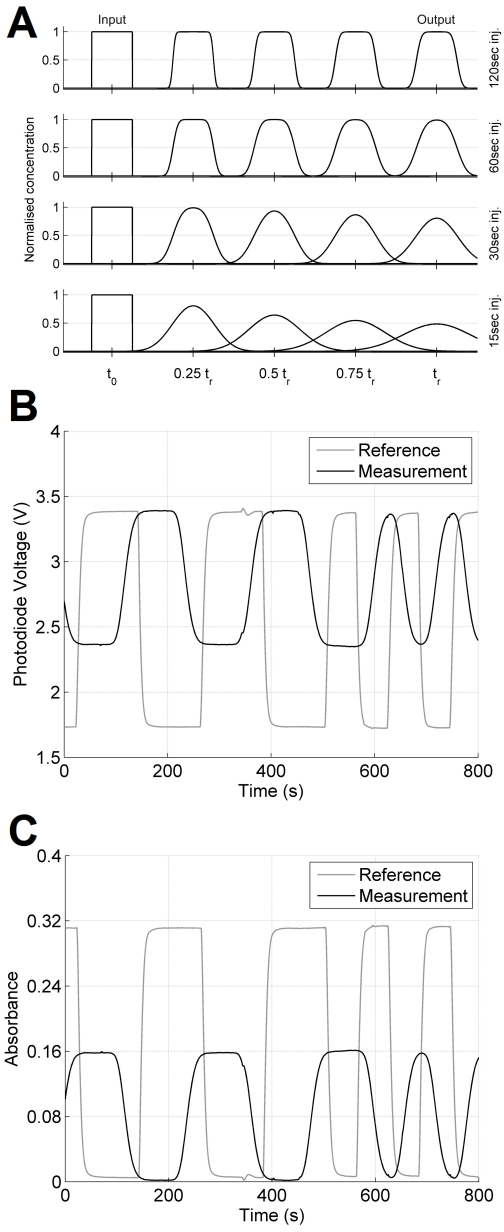

FIGURE 6.16: (A) Theoretical Taylor-Aris dispersion calculated for 4 input plug sizes. The plug profile is shown as it travels to the detection cell (output) at various times (where t_r is the total residence time). (B) Taylor-Aris dispersion using the continuous-flow microfluidic devices with yellow food dye. 0.1% dye plugs were injected with MilliQ plugs on either side (plug sizes were 1.92 m and were changed to 0.96 m at 500 seconds). The reference cell (grey) shows the plug entering the serpentine approximately square. The final plugs (black) have half the absorption value of the initial plug (1:1 dilution with MilliQ) and the slopes have decreased. Qualitatively, the 120 second and 60 second plug profiles agree with the profiles calculated in (A).

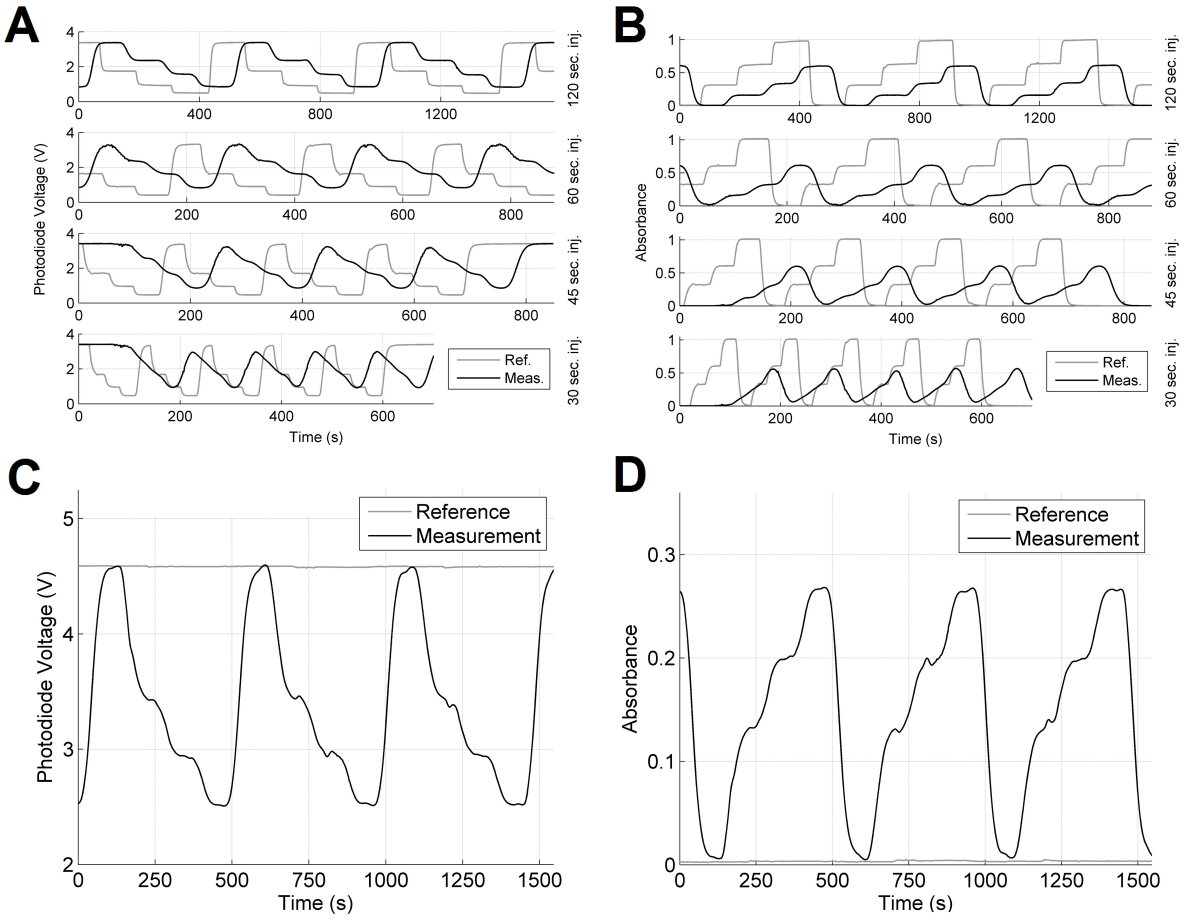

FIGURE 6.17: Continuous flow chip: (A) Successive food-dye plugs were injected with increasing concentration (Blank, 0.025%, 0.05% and 0.1%, and repeated). Four plug sizes were used and the reference cell (grey) shows the input profiles entering the serpentine. The final output profiles (black) show Taylor dispersion and have 80% of the absorption value of the initial plug (1:4 dilution, MQ:Dye). (B) Shows the data in A as absorbance values. (C) Successive phosphate plugs were injected (120 sec. injections) with increasing concentration (MilliQ, 20, 30 and 40 μM, and repeated) and mixed with reagent. The reference channel (grey) shows the samples before the addition of reagent, and thus does not show the input profile as there is no colour development. The measurement channel (black) shows the dispersion is similar to the food-dye experiments and the plateaus are discernible. (D) Also shows the data in C as absorbance values.

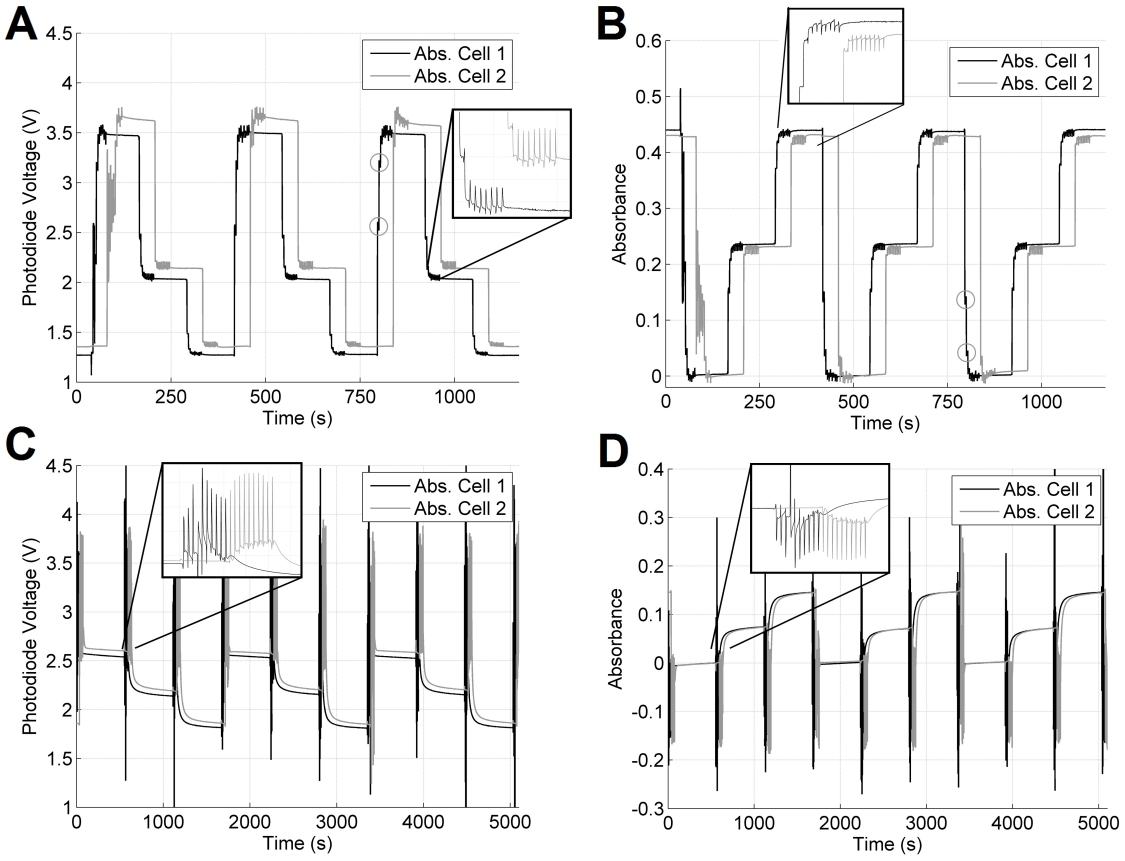

FIGURE 6.18: Multiplexed stop-flow (MSF) microchip: (A) Successive dye samples with increasing concentration (Blank, 0.05% and 0.1%; cycled) were mixed on chip with MilliQ (1:1 v/v) and injected into absorbance cells 1 and 2. The sample plugs are injected using 10 pump cycles (80 μL), before a hold-time (90 seconds). It takes 2-3 pump strokes to change a sample, observed by the rapid transition between samples. The pump cycles can also be seen on the slope during a transition, circled in grey (similar position on each repeat). The inset box shows the remainder of the pump strokes before the wait time. (B) Shows the data in A as absorbance values. (C) Phosphate standards successively injected with increasing concentration (Blank, 20 and 40 μM; cycled) and mixed with reagent. The hold-time for colour development is 9 minutes. The box (inset) shows the 10 pump strokes for each channel before the wait time. (D) Also shows the data in C as absorbance values.

Chapter 7

Conclusions

7.1 Thesis Summary

Here I have summarised the evolution of this thesis work which resulted in the development of a microfluidic platform for wet chemical nutrient sensors. The purpose of this work was to produce components for *in-situ* oceanographic nutrient sensor systems from robust low cost materials. The outcome is a microfluidic chip with integrated valves and pumps produced in PMMA with a robust, chemically resistant Viton® membrane.

In chapter 3 a solvent vapour based bonding process was introduced for COC and PMMA polymers. This procedure allows physically robust, optical quality microfluidic devices to be realised in micromilled substrates. SEM pictures and AFM scans were taken of treated and untreated surfaces. These show that exposure of the polymers to an appropriate solvent vapour (chloroform for PMMA, cyclohexane for COC) led to significant reduction in surface roughness. This reduction is due to the softening of the surface by the solvent vapour, allowing the polymer to reflow. The polymer reflow reduced the surface roughness from 200 nm to 15 nm. The bonding and surface roughness reduction method shown can also be used with other fabrication techniques for low-cost and high-quality microfluidic prototyping. Since publication of this work in the Journal of Micromechanics and Microengineering the method has been adopted by a number of microfluidics research groups.

Chapter 4 includes a discussion on possible methods to integrate optical absorbance cells onto the microfluidic platform. The method presented within this chapter was possible due to the bonding and surface reduction method presented in the previous chapter. A demonstration chip manufactured from tinted 7F61 PMMA (Evonik Röhm Gmbh) was presented. This is a low cost commercially available polymer which can be injection moulded for mass production of low cost devices. The absorbance spectra for this material and other grades of PMMA was presented. A demonstration device suitable for use with optical fibres was also shown. Performance of this design methodology has been

assessed by Floquet et al. (2011) who states a factor of 6.4 improvement in the system sensitivity using a tinted PMMA substrate compared to transparent PMMA. This technique allows high performance absorbance spectrometry from mass producible designs. This was demonstrated by Sieben et al. (2010) who built a Nitrite detection system using the technique. A 14 nM limit of detection was demonstrated; an improvement of one order of magnitude improvement over other systems in the literature. The optical cell design was also used in chapter 6 as part of the two demonstration systems.

Control of fluids upon the microfluidic system platform is important and, while bolt-on commercial valves allow these functions to be performed, the cost and fluidic disadvantages limit system architecture possibilities. In chapter 5 a method for permanent bonding of chemically-inert Viton® membranes to PMMA and COC was demonstrated. Low dead volume microvalves were made from these materials and characterised using pneumatic actuation. MilliQ water and seawater were passed through the valve and the leakage pressure, with different actuation pressures, observed. The repeatable hysteresis due to seawater fouling of the valve was presented. A bubble train demonstrating repeatable actuation of the valve was also included. The bonding approach described complements the microfabrication methods in chapter 3 and enables the integration of chemically robust Viton® valves in a wide range microfluidic devices. This work was published in Lab on a Chip journal titled *Chemically resistant microfluidic valves from Viton® membranes bonded to COC and PMMA*.

In chapter 6 the effect of different system architectures and the requirement for certain components within microfluidic colourimetric sensor systems was discussed. This included a brief overview of mixers and a discussion on their requirement. A split and recombine mixer design developed by this author, suitable for continuous flow systems, was shown operating with food dyes.

Two demonstration systems were built to study the temporal response of microfluidic colourimetric sensor systems using continuous-flow and stop-flow architectures. The continuous flow system can sample every 60-120 s (30-60 samples h^1) and was limited by the Taylor dispersion. A novel multiplexed stop-flow (MSF) microsystem was demonstrated requiring 12.6 s per sample which if scaled to have more measurement channels (>43) would be capable of up to 285 samples h^{-1}. The MSF architecture utilises on-chip valves allowing for small sample volumes. Operational data for food dyes and the phosphate yellow method was given for both systems. The MSF system demonstrates the advantages of microfluidic systems in nutrient sensor technology. With small sample volumes and high temporal response this system demonstrates what is possible in this field.

The next step in this work is to take a MSF architecture high temporal response system such as that demonstrated and package it for a real world deployment. Further suggestions on how this work could be continued are included in the next section.

7.2 Future Directions

There are a number of directions in which this research could be taken. These are described in the following sections.

7.2.1 Materials

The method described in chapter 5 was optimised for bonding Viton® to PMMA and COC, but for certain chemistries these may not be the optimal materials. Optimisation of this process for bonding of Viton® and other robust elastomers to fluoropolymers such as Teflon® would allow for a wider range of solvents especially to be used within the systems.

7.2.2 Valve Actuation

Although the pneumatic actuation featured in chapter 5 was suitable for proving the valve principle and for demonstration of a system in chapter 6 it is not an ideal actuation method for *in-situ* deployment. For remote deployments an actuator is required for valves and pumps within the system without the external pneumatic infrastructure. This is an area of interest to a number of microfluidic groups so the impact of success in this area would be far reaching.

7.2.3 Mixers

I have touched upon this subject within this thesis in chapter 6 but mixer design was not the core objective of this work. To take the mixer work forward involves improving the qualitative results which may be achieved by visualisation utilising an alkali and indicator as used in work by Kim et al. (2005a). By using sodium hydroxide solution and phenolphthalein indicator solution the boundary between the two fluids is seen as a pink line. The diffusion of the large phenolphthalein molecule is slow meaning the effect of the mixing elements should be more obvious optically than the food dye used in this work. It will give a good indication of the effectiveness of the mixer to mix rather than show the diffusion of the two fluids.

In order to assess the effect on the cross-sectional profile a confocal microscope could also be used to view the through channel profile while water and fluoroscein are used as the two fluids. This should allow a sequence of pictures similar to Figure 6.11 to be obtained confirming the operation of the elements.

Finally there is a need to run real life chemical reactions through the mixers so that the effectiveness of mixing fluids with different viscosities and at different mixing ratios can

be assessed. The Iron/Manganese reagents could be used for these assessments as there is a desire to reduce the overall volume of the reagents used in these systems and the high viscosity of the reagent makes it an ideal candidate. The mixers should reduce reagent consumption if mixing speed is increased but any increase in dead volumes (compared to the currently used chicane mixers) will increase the flushing time and required volume of flushing solution. The mixing efficiency could be assessed using an optical flow cell with known concentrations of sample comparing premixed and on-chip mixed results. The dead volume effects could be assessed using the same experimental setup but by flowing sample and reagents followed by flushing and measuring the cross over between signals.

7.2.4 Further Miniaturisation

In order to turn the demonstration system featured in chapter 6 into a usable *in-situ* system it needs to be packaged to create a self-contained device. This work should be performed alongside any valve actuation developments so that these advances can be taken into account within the design. With correct design I would foresee that the finished device could be <0.25 dm^3 without reagent storage which would vary in capacity dependant upon the required deployment duration.

7.3 Impact of the thesis research

The measurement of nutrient concentrations is going to further understanding of ocean systems and improve modelling. Currently cost and physical size of devices are boundaries in wide scale deployment of sensors. In this work I have demonstrated a scalable microfluidics platform which has the potential for mass production allowing cost per measurement to decrease. The final system is capable of hundreds of discrete measurements per hour providing an order of magnitude improvement upon existing systems.

Future work would include building systems for all nutrient chemistries upon the platform, as well as further development into mixers for chemistries requiring fast mixing along with short reaction times. With these developments low-cost, physically small systems are obtainable and mass sampling of the ocean will be possible. This work goes a long way to realising these targets and has enabled system deployments which have been published in literature (Sieben et al. (2010), Beaton et al. (2011)).

7.4 Postgraduate Research and Training

7.4.1 Modules

Lab-on-a-chip - ELEC6100
Microsystems Technology - ELEC6079

7.4.2 Presentations

Table 7.1 gives a list of presentations given during this doctural study.

TABLE 7.1: Presentations given during doctoral study

Topic	Audience
Novel Fabrication of Microfluidic Devices	BioMEMS Group
Microfluidics for Oceanographic Sensors	N.S.I Group
Novel rapid prototyping methods for microfluidic devices suitable for in-situ chemical sensors	RMST Programme Review Group
Various (weekly/fortnightly)	CMM

7.4.3 Conference Attendance

Ocean Sensors 08 - Germany
MicroTAS 2010 - Groningen, Netherlands

Appendix A

Publications

The full published texts have been omitted from this E-Thesis due to copyright. However in this appendix the links to, and the reference for, each of the publications is included for the readers convenience.

A.1 Publication: Reduction of Surface roughness for optical quality microfluidic devices in PMMA and COC

Iain R. G. Ogilvie, Vincent J. Sieben, Cedric F. A. Floquet, Robert Zmijan, Matthew C. Mowlem, and Hywel Morgan. Reduction of Surface roughness for optical quality microfluidic devices in PMMA and COC, *Journal of Micromechanics and Microengineering*, 20, 065016, 2010. DOI: 10.1088/0960-1317/20/6/065016.

The full text may be found at www.iopscience.iop.org/0960-1317/20/6/065016

A.2 Publication: Nanomolar detection with high sensitivity microfluidic absorption cells manufactured in tinted PMMA for chemical analysis

Cedric F. A. Floquet, Vincent J. Sieben, Ambra Milani, Etienne P. Joly, **Iain R. G. Ogilvie**, Hywel Morgan, and Matthew C. Mowlem. Nanomolar detection with high sensitivity microfluidic absorption cells manufactured in tinted pmma for chemical analysis. *Talanta*, 84(1):235-239, 2011. DOI: 10.1016/j.talanta.2010.12.026.

The full text may be found at www.sciencedirect.com/science/article/pii/S0039914010010167

A.3 Publication: Chemically resistant microfluidic valves from Viton® membranes bonded to COC and PMMA

Iain R. G. Ogilvie, Vincent J. Sieben, Barbara Cortese, Matthew C. Mowlem, and Hywel Morgan. Chemically resistant microfluidic valves from viton® membranes bonded to coc and pmma. *Lab on a Chip*, 11(14):2455-2459, 2011. DOI: 10.1039/C1LC20069K

The full text may be found at pubs.rsc.org/en/Content/ArticleLanding/2011/LC/C1LC20069K

A.4 Publication: Temporal Optimization of Microfluidic Colorimetric Sensors by Use of Multiplexed Stop-Flow Architecture

Iain R. G. Ogilvie, Vincent J. Sieben, Matthew C. Mowlem, and Hywel Morgan. Temporal optimization of microfluidic colorimetric sensors by use of multiplexed stop-flow architecture. *Analytical Chemistry*, 83(12):4814-4821, 2011. DOI: 10.1021/ac200463y

The full text may be found at pubs.acs.org/doi/abs/10.1021/ac200463y

A.5 Publication: An automated microfluidic colourimetric sensor applied in situ to determine nitrite concentration

Alexander D. Beaton, Vincent J. Sieben, Cedric F. A. Floquet, Edward M. Waugh, Samer Abi Kaed Bey, **Iain R. G. Ogilvie**, Matthew C. Mowlem, and Hywel Morgan. An automated microfluidic colourimetric sensor applied in situ to determine nitrite concentration. *Sensors and Actuators B: Chemical*, 156(2):1009-1014, 2011. DOI: 10.1016/j.snb.2011.02.042

The full text may be found at www.sciencedirect.com/science/article/pii/S0925400511001535

A.6 Publication: Microfluidic colourimetric chemical analysis system: Application to nitrite detection

Vincent J. Sieben, Cedric F. A. Floquet, **Iain R. G. Ogilvie**, Matthew C. Mowlem, and Hywel Morgan. Microfluidic colourimetric chemical analysis system: Application to nitrite detection. *Analytical Methods*, 2:484491, 2010. DOI: 10.1039/c002672g.

The full text may be found at pubs.rsc.org/en/Content/ArticleLanding/2010/AY/c002672g

A.7 Publication: Solvent procession of PMMA and COC chips for bonding devices with optical quality surfaces

Iain R. G. Ogilvie, Vincent J. Sieben, Cedric F. A. Floquet, Robert Zmijan, Matthew C. Mowlem, and Hywel Morgan. Solvent processing of pmma and coc chips for bonding devices with optical quality surfaces, *Proceedings of MicroTAS 2010*, Groningen (The Netherlands), 3-7 October 2010, pp. 1244-1246.

The full text may be found at www.rsc.org/binaries/LOC/2010/PDFs/Papers/425_0849.pdf

A.8 Publication: Autonomous microfluidic sensors for nutrient detection: applied to Nitrite, Nitrate, Phosphate, Manganese and Iron

Vincent J. Sieben, Alexander D. Beaton, Cedric F. A. Floquet, Samer Abi Kaed Bey, **Iain R. G. Ogilvie**, Edward M. Waugh, Matthew C. Mowlem, and Hywel Morgan. Autonomous microfluidic sensors for nutrient detection: Applied to nitrite, nitrate, phosphate, manganese and iron, *Proceedings of MicroTAS 2010*, Groningen (The Netherlands), 3-7 October 2010, pp. 1016-1018.

The full text may be found at www.rsc.org/binaries/LOC/2010/PDFs/Papers/348_0722.pdf

Appendix B

Further Notes

B.1 Example of laminar flow in a microfluidic channel with a high Peclet number

Using Phosphate ions in water (at 20°C) as the diffusing species, the diffusion coefficient is $D = 5.51\text{-}9.48\ e^{-10} m^2 s^{-1}$. The other constants used are given below.

$$L = 300\ \mu m \tag{B.1}$$
$$\mu = 1\ e^{-3} Pa.s \tag{B.2}$$
$$\rho = 1000\ kgm^{-3} \tag{B.3}$$
$$Re = 10 \tag{B.4}$$
$$\tag{B.5}$$

Rearranging equation 2.1 for velocity and inputting the above constants gives

$$v = 0.033\ ms^{-1} \tag{B.6}$$

Using equation 2.4 gives

$$Pe = 10548 \tag{B.7}$$

In this case the Reynolds number indicates laminar flow conditions and the Peclet number indicates convection driven diffusion.

B.2 The development of previous devices at CMM

The development of a simple manufacturing method for chemically and physically robust microfluidic devices has been an important focus in this work. CMM have previously used a lamination method to produce microfluidic devices by laminating an epoxy sheet onto glass microscope slides, exposing to UV light to cure the polymer and then development of the fludic structure in a solvent. The structure is then thermally bonded to a glass slide to form a lid or a dual layer device. The methodology of this technique is similar to that presented by Vulto et al. (2005) discussed in chapter 3.

Although this method can be used to produce devices with features down to 50 μm, the finished devices are both brittle (uses glass substrates) and awkward to connect to external systems. Interconnects must be created by drilling vias in the glass substrates and external tubes or connectors must be glued in place. A close fit of components must be maintained to ensure seals are created and reduce any possible addition of dead volumes. The integration of elastomeric materials into this type of device is trivial (Duffy et al. (1998)) but PDMS is unsuitable for a number of applications due to its porosity and hydrophilic nature.

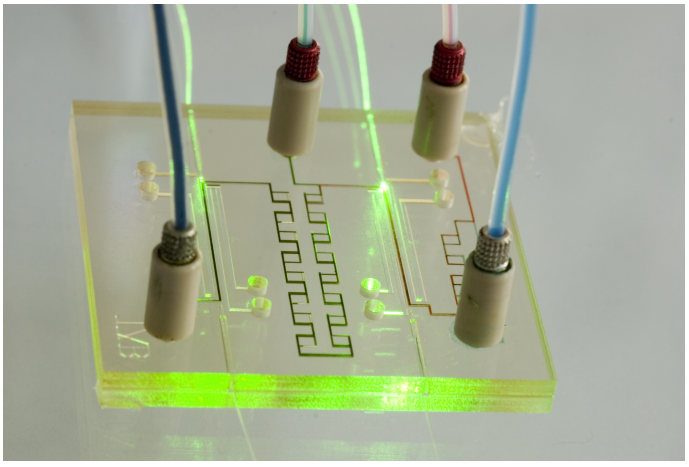

FIGURE B.1: An example chip manufactured for CMM by external contractor made with PMMA substrates, patterned with SU8 features (Taberham (2008))

Although the lamination technique works well with glass it requires high temperatures (~180 °C) to cure the laminate making it unsuitable for many thermopolymers. There are suppliers whom can supply microfluidic chips with polymer substrates and Epoxy features such as shown in Figure B.1. This device is manufactured with Poly (methyl methacrylate) (PMMA) outer substrates and has features patterned in SU8 photoresist. A batch of these chips takes around 6 weeks for the supplier to turnaround making rapid development difficult. The mis-alignment of the upper and lower layers on dual layer designs is also large (>20 μm) which causes problems in mixer designs encouraging bubbles to be trapped in the added dead volumes.

B.3 Notes on bonding robust microfluidic devices

B.3.1 Bonding Tips

If using an LPKF multipress be aware that the internal surfaces stay hot even after the cooling process so it is wise to wear heat proof gloves and be very careful. Also note that after time the internal pressure plates of the press appear to warp so it is recommended that a Viton® sheet is used between the substrates and stainless steel of the press. The inclusion of thin PET sheets (laminating pouches over a cardboard sheet work well) will reduce adhesion of the Viton® to the substrates also. The Viton® sheet conforms to the shape of the surface ensuring even pressure distribution while the laminated mats provide flat clear non-stick surfaces ensuring the outer chip surfaces remain optically clear.

B.3.2 Bonding tinted PMMA substrates

A variety of PMMA substrates are available manufactured in one of two ways. Commonly thin sheets (<3 mm) are made by extruding the bulk polymer to the desired thickness; all Evonik Röhm Gmbh grades labelled XT are of this type. Alternatively thicker sheets are manufactured by casting. Coloured grades are also available (typically cast) and the addition of the colouring material increases the solvent vapour exposure time of the substrates. For tinted PMMA (Plexiglass GS 7F61) the exposure time is increased to 4 min 15 s. These substrates are often less flat than the transparent substrates so it is beneficial to fly-cut the bonding surfaces prior to micromilling of features.

It is also beneficial to increase the pressure, temperature and time the substrates are in the press. For tinted PMMA (Plexiglass GS 7F61) these factors become 180 N cm^{-2}, 80 °C and 120 min.

B.3.3 Fabrication using Thermopolymers: Attempts to repeat processes

Development of a rapid prototyping method for robust materials motivated this investigation into possible suitable substrates. Poly(methyl methacrylate) (PMMA) and Cyclic Olefin Copolymer (COC) were chosen as possible alternatives to the glass substrates already used. As mentioned previously these materials are popular choices for microfluidic devices and their low cost makes them attractive for prototyping situations. By micromachining these substrates with an LPKF S100 micromill (LPKF Laser & Electronics AG) designs can be realised in a matter of hours. Bonding of the micromachined substrates was investigated and a number of the procedures (and extrapolated versions of) in Tables 3.1 and 3.2 were attempted with PMMA (Evonik Röhm Gmbh) and COC

(Grades 8007 (Tg 78 °C) and 5013 (Tg 134 °C), TOPAS Advanced Polymers GmbH) substrates. A summary of the results is shown in Table B.1.

The details of the experiments in Table B.1 have been omitted as multiple methods based on these materials were attempted. The temperature, pressure and bonding time were kept at 65 °C, 140 N/cm^2 and 20 min. Strength of bonds was assessed by peeling two substrates apart by hand. Those that were easily peeled apart were deemed too weak whereas those that were very difficult (usually resulting in one of the substrates snapping) were deemed strong enough for a robust device. The exposure of the substrates to their respective solvents was varied and multiple drying methods attempted in order reduce exposure with the soaking/dipping processes.

TABLE B.1: A summary of attempted bonding methods

Materials	Method Attempted	Author	Result
PMMA & Acetone	Injected through channel	Shah 2006	Channel collapse
PMMA & Acetone	Soak one substrate	-	Channel collapse
PMMA & Ethanol	Soak for 10 min	Klank 2002	Weak bonding
PMMA & Isopropanol	Dip one substrate	Hsu 2007	Clouding of substrate, weak bonding
PMMA & Isopropanol	Soak one substrate	Ng 2008	Clouding of substrate, weak bonding
PMMA & Chloroform	Soak one substrate 1.5 min	Koesdjojo 2009	Clouding of substrate, channel collapse, strong bond
COC & Cyclohexane	90 s vapour exposure	Mair 2007	very weak bond
COC & Cyclohexane	Soak one substrate 30 s	-	strong bond, channel collapse
COC & low Tg COC	Spin & laminate	Steigert 2007	strong bond

The outcome of the experiments was of limited use as no definitive method was found for bonding both PMMA and COC substrates, however two important lessons were learnt. The method presented by Steigert et al. (2007) for COC polymers proved to be usable for bonding strong chips, an example of which is shown in Figure B.2 (built according to Figure B.4 in order to observe alignment of multiple substrates). This methodology was not able to be transferred across to PMMA as different grades with wide ranging glass transition temperatures (Tg) are not available from suppliers. Also micromilling of the lower glass transition temperature COC proved difficult due to the heat produced during the cutting causing the adhesive layer to melt and damage the cutting tool. This method is useful for producing simple devices when milling with large (>1 mm) cutting tools which do not heat up quickly and may be practical with micromills which use wet cutting and coolant. It is less practical when the heating of the cutting tool melts the low Tg adhesive layer clogging the tool. As the desired outcome of this work is microfluidic devices with very small channels (<200 μm) a more practical method of bonding smaller channels is needed.

The second important outcome was that chloroform and cyclohexane were able to be used to produce strong bonds with PMMA and COC respectively. These solvents soften and dissolve the polymers very readily. This was shown when a PMMA lid was placed over a container of chloroform as a temporary lid and it collapsed showing that even in vapour form they are effective. Controlling this vapour softening effect can be used

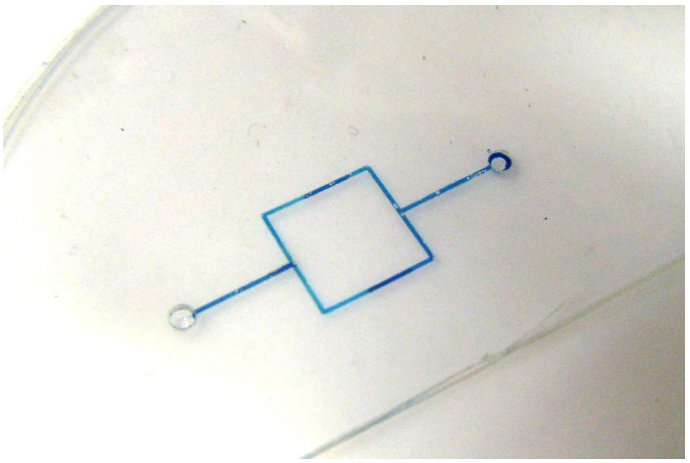

FIGURE B.2: A two layer chip manufactured in COC, features were micromilled using a 400μm diameter bit 200 μm deep after adhesive layer was spun onto substrates. The substrates were then bonded according to the method by Steigert et al. (2007). The overlapping layers can be seen where the dye is darkest showing aligned features can be produced using this method

to soften a very thin layer of the polymer substrates which causes them to bond when pressure is applied between them. In this way the bonding method discussed in section 3.2.1 was obtained.

B.3.4 Low cost bonding equipment

For widespread acceptance of any process, even in the most cash-strapped laboratories, it is advantageous if there is flexibility in manufacturing procedures allowing for a wide variety of equipment to be used. Other methods of applying uniform pressure have also been attempted in an effort to reduce the capital cost of setting up this bonding process.

Application of heat and pressure has been achieved by using an LPKF Multipress (LPKF Laser & Electronics AG), allowing for precise control of the temperature and pressure during bonding. An alternative method of applying heat is to use an oven. This method has been utilised many times during the course of this research and no noticeable difference has been found between chips bonded in the press or in the lab oven. Temperature is not as well controlled and variation may be as much as ± 5 °C (estimated using a thermometer on multiple occasions).

In the following section characterisation of the bonding pressure is discussed and the effect shown to be small. This allows a number of methods of applying pressure to be used without the actual value of applied pressure needing to be known. Figure B.3 shows two possible methods. By using a G-clamp an initial compression of the device is used to apply a pressure to the bonded joint. After heating and cooling in an oven it was noted that the force required to undo the G-clamp was greatly reduced and the applied force became very little. It is thought that the heating and cooling of the

material causes some plastic deformation of the substrates. This makes this particular method of pressure application useful when a limited deformation of the substrates is needed during the bonding process as the final deformation can be limited by limiting the initial torque on the clamp. In contrast the second method presented (Figure B.3) allows an almost constant pressure (as the modulus change in the steel springs is negligible in the temperature range utilised) to be applied throughout the heating and cooling cycles. This provides a useful low-cost method of bonding chips so long as the applied pressure is great enough to overcome any large scale deformation of the substrates reliable bonds can be achieved. During a period when the LPKF Multipress was being maintained in our lab this method was utilised with no detrimental effect to the quality of the chips produced.

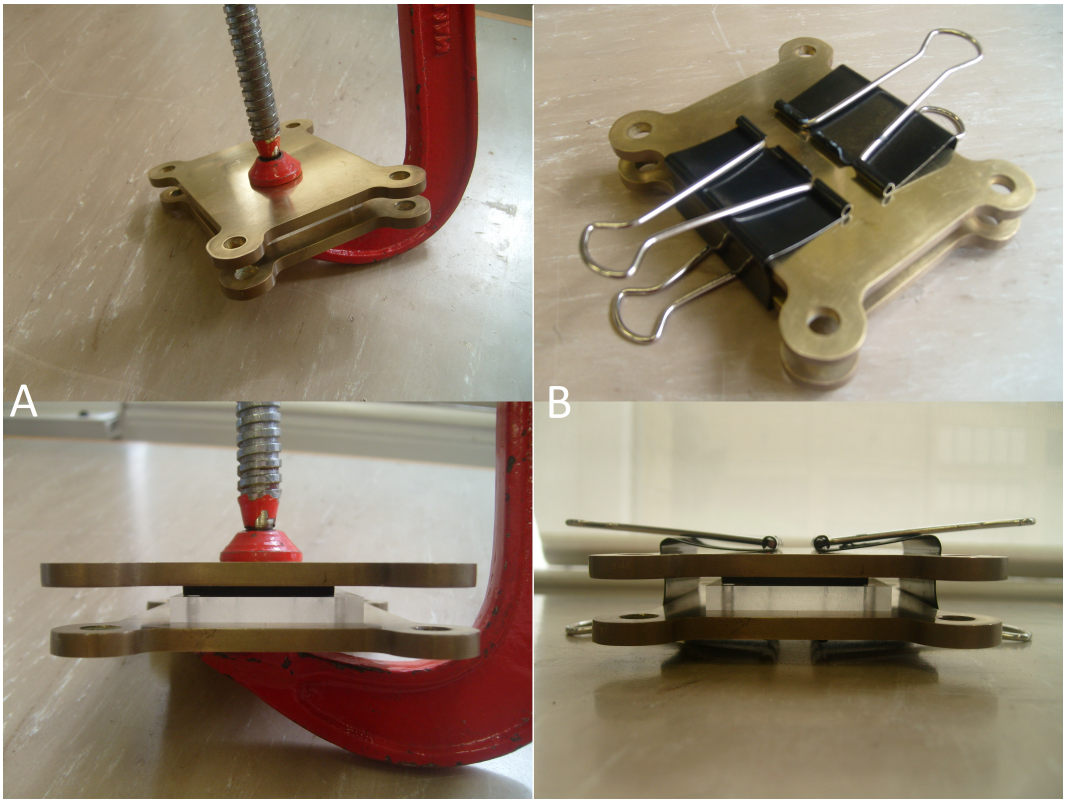

FIGURE B.3: Methods for applying pressure without a press, clear and tinted substrates used for added contrast, the 2 brass plates are used to distribute pressure, A. Using a G-clamp, B. Using 2 'bulldog' clips

B.3.5 Alignment

In order to create microfluidic chips with multi-layer aligned features (essential when producing micromixers) the assembly of aligned substrates prior to the final bonding steps is required. Simple corner alignment was attempted by machining a 90° corner on substrates to be aligned and these were used during assembly with a right angled jig (Figure B.4). This method produced chips that were aligned well visually (estimate

<20 μm misalignment) but after the pressing stage the final chips lost their accuracy. It appeared that the application of pressure in the LPKF Multipress also included application of some shear force (due to the internal design) causing the substrates to shear out of alignment. To counteract this effect a pin alignment method has been used where multiple alignment holes are machined into substrates prior to bonding and then ground steel pins which are slightly smaller (alignment holes ϕ3.00 mm, pins ϕ2.99 mm) are fitted into the holes. Final alignment is typically better than 20 μm, limited by the machining accuracy of the micromill and temperature induced distortion of the substrates in the press.

It is recommended that only two pins are used and that these are placed along an edge parallel to and at the front of the press. The LPKF Laser & Electronics AG Multipress appears to apply a shear force perpendicular to the door at the front, but when the pins are aligned as described any shear effects present in the press do not appear in the final device.

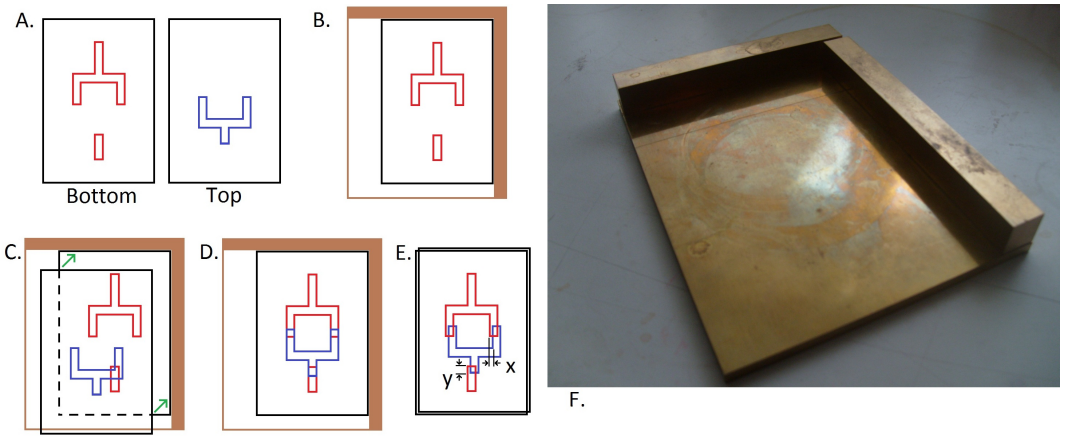

FIGURE B.4: A. Top and Bottom substrates are machined and prepared for bonding, B. Bottom substrate is placed on jig and aligned with the corner, C. Top substrate is pushed into jig without touching the bottom, D. Pressure is applied with both substrates pushed into the corner to bond them, E. Mis-alignment can be measured by viewing channels, F. A brass jig used for corner alignment of substrates

B.4 Choice of optical detector: TAOS TSL257 series

The TSL257 is a low-noise light-to-voltage optical converter chosen for use by CMM due to its high sensitivity and low price ($\sim$ £ 1 at the time of writing (RS Components Ltd)). It combines a photodiode and a transimpedance amplifier in a single package reducing the need for external components. At CMM these devices are supplied with 6 volts and give and output voltage from 0 - 5 volts proportional to light intensity received. This is easily recorded using National Instruments Corp. interfaces and Labview software or the in-house CMM datalogger; making it flexible for bench and deployment uses.

Other optical detectors are used at CMM but this is by far the most popular due to its simplicity and high sensitivity.

The first page of the datasheet for this device has been included on the following page (for the interest of the reader). Further information is available online or from suppliers such as RS Components Ltd.

TSL257
HIGH-SENSITIVITY LIGHT-TO-VOLTAGE CONVERTER

TAOS023C − NOVEMBER 2005

- **Converts Light Intensity to Output Voltage**
- **Monolithic Silicon IC Containing Photodiode, Operational Amplifier, and Feedback Components**
- **High Sensitivity**
- **Single Voltage Supply Operation (2.7 V to 5.5 V)**
- **Low Noise (200 μVrms Typ to 1 kHz)**
- **Rail-to-Rail Output**
- **High Power-Supply Rejection (35 dB at 1 kHz)**
- **Compact 3-Leaded Plastic Package**
- **RoHS Compliant (−LF Package Only)**

PACKAGE S
SIDELOOKER
(FRONT VIEW)

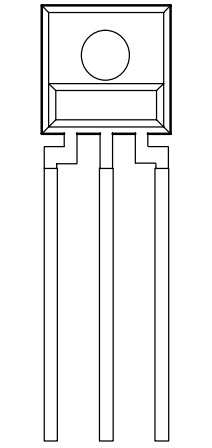

PACKAGE SM
SURFACE MOUNT
SIDELOOKER
(FRONT VIEW)

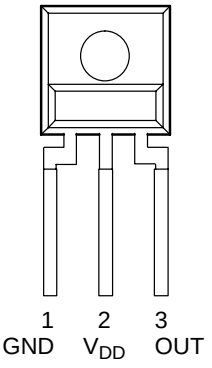

Description

The TSL257 is a high-sensitivity low-noise light-to-voltage optical converter that combines a photodiode and a transimpedance amplifier on a single monolithic CMOS integrated circuit. Output voltage is directly proportional to light intensity (irradiance) on the photodiode. The TSL257 has a transimpedance gain of 320 MΩ. The device has improved offset voltage stability and low power consumption and is supplied in a 3-lead clear plastic sidelooker package with an integral lens. When supplied in the lead (Pb) free package, the device is RoHS compliant.

Functional Block Diagram

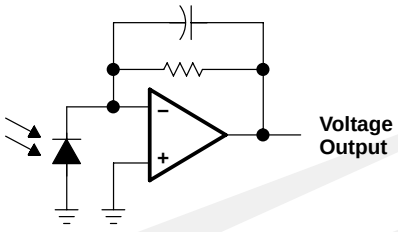

Available Options

DEVICE	T_A	PACKAGE − LEADS	PACKAGE DESIGNATOR	ORDERING NUMBER
TSL257	0°C to 70°C	3-lead Sidelooker	S	TSL257
TSL257	0°C to 70°C	3-lead Sidelooker — Lead (Pb) Free	S	TSL257−LF
TSL257	0°C to 70°C	3-lead Surface-Mount Sidelooker — Lead (Pb) Free	SM	TSL257SM−LF

Terminal Functions

TERMINAL NAME	TERMINAL NO.	DESCRIPTION
GND	1	Ground (substrate). All voltages are referenced to GND.
OUT	3	Output voltage
V_{DD}	2	Supply voltage

Texas Advanced Optoelectronic Solutions Inc.
1001 Klein Road • Suite 300 • Plano, TX 75074 • (972) 673-0759
www.taosinc.com

B.5 The Bouger-Beer-Lambert Law equations

The description of the Bouguer-Beer-Lambert law given in this section is based upon early unpublished work by Dr. Cedric Floquet and Dr. Matthew Mowlem. This author has made appropriate corrections and amended it for additional clarity for the reader.

The idealised relationship between the measured optical power, absorbance and chemical concentration is described by the Bouguer-Beer-Lambert law (Bouguer (1729), Lambert (1760), Beer (1852)) but for mathematical simplicity the exponential form of Beers law is given in equation B.8 (Beer (1852)).

$$P_{sample} = P_0 e^{-\alpha c l} \tag{B.8}$$

Where P_{sample} is the optical power at the detector, P_0 is the optical source power, α the absorption coefficient of the absorbing species, c is the concentration of the absorbing species and l the effective length of the absorption cell. The Bouguer-Beer-Lambert law only applies if a monochromatic light source is used (i.e. α is assumed wavelength independant), and for low concentrations (no interaction between molecules of the absorbing species). In this case, the absorbance due to the presence of the analyte, A, and hence the concentration, is determined using equation B.9.

$$A = \alpha c l = ln \frac{P_{ref}}{P_{sample}} \tag{B.9}$$

P_{ref} can be determined by measurement of a sample with no absorbing species (i.e. a blank). Equation B.9 tells us that the sensitivity of an idealised optical cell is maximised when the absorbance is equal to unity. This implies that an optimal cell length for maximum sensitivity (for a given absorption coefficient and concentration), can be determined by equation B.10.

$$\frac{d(\frac{dP_{sample}}{dc})}{dl} = -\alpha^2 l c P_0 e^{(-\alpha l c)} + \alpha P_0 e^{(-\alpha l c)} = 0 \rightarrow \alpha = \alpha^2 l c \rightarrow \alpha l c = 1 \tag{B.10}$$

In systems utilising these principals monochromatic light sources are not often used so P_0 and α are wavelength dependent. In addition there will be an offset at the detector due to ambient and stray light not passing through the optical detection volume. Therefore the measured power is given by equation B.11.

$$P = \int P_0(\lambda) e^{-\alpha(\lambda) c l} d\lambda + P_{offset} \tag{B.11}$$

If the the spectral characteristics of the source and the extinction coefficient are not

identical then, even in the absence of stray light, equation B.9 is not applicable and if used incorrectly will result in a non-linear absorption measurement. Galli (2001) demonstrated this non-linearity by developing an analytical solution for a Gaussian source spectrum and a linear slope molecular extinction coefficient spectrum. Even neglecting spectral effects, ambient and stray light cause non-linearity and must be considered by adding P_{offset} to equation B.9 giving equation B.12.

$$A = ln\frac{P_{ref}}{P_{sample}} = ln\frac{(P_0 + P_{offset})}{(P_0 e^{-\alpha cl} + P_{offset})} \tag{B.12}$$

P_{offset} can be determined directly by measuring the optical power when an opaque sample is placed in the absorption cell enabling the correction of recorded results. By eliminating stray light as much as possible, measuring its effect through opaque samples and standards it is possible to obtain a calibration curve for optical flow cells to obtain highly accurate measurements. If wavelength independence can be maintained through careful choice of light source and detector (to ensure the spectral responses convolve) linearity of system response and in turn the accuracy can be even further improved.

B.6 Example calculation of optical cell efficiency with tinted PMMA

For Nitrite measurement with the Griess reaction the molar absorptivity is **39,000 M^{-1} cm^{-1}** (Sieben et al. (2010));

Using equation B.9 gives a absorption length of **2.56 cm** for maximum sensitivity (absorption = 1) at 10 μM concentration.

For maximum power efficiency during blank measurements window thickness should be minimised. In practice windows should each be at least 300 μm thick to allow for any misalignments during manufacturing.

Therefore the **in path** absorption length (for a blank) is **600 μm**

The **out of path** absorption length (from source light) is 600 μm + 2.56 cm = **2.62 cm**

From Table 2.1 the excitation/detection wavelength for the Griess reaction is 525 nm.

Assuming 7c14 light grey PMMA is the chosen build material, from Figure 4.3 the optical density for a 1 mm sample at 525 nm is 0.3; therefore the absorbance is **3 cm^{-1}**.

With 7c14 PMMA the **through channel** absorption (A_{in}) is **1.8**.

The **out of channel** absorption (A_{out}) is **7.86**.

In analytical chemistry absorbance is given by equation B.13 where I_0 is the intensity of the light at the source and I_1 is the intensity of the light at the detector (Grasshoff et al. (1999)).

$$A = log_{10}\frac{I_0}{I_1} \tag{B.13}$$

Assuming a large, poorly matched light source is used (and detector of equal dimensions) and only 1% of light goes into channel (i.e. $I_{0out} = 99I_{0in}$), using equation B.13 the noise at the detector as a proportion of the total signal is

$$\frac{I_{1out}}{I_{1in} + I_{1out}} = \frac{99}{\frac{10^{A_{out}}}{10^{A_{in}}} + 99} = 0.01\% \tag{B.14}$$

Using a light source that only excites within the channel and a detector which only detects within the channel area would improve this further.

B.7 Integration of Membranes: Attempts to copy literature

Although the use of PDMS is not optimal for the development of wet chemical sensors due to the porous nature of the material a number of attempts were made at bonding this material to polymer substrates for the inclusion of elastomeric actuators. Solvent vapour bonding, by the method mentioned previously, was attempted with two PMMA substrates and both PDMS and Teflon membranes. An example of a chip produced with this method is shown in Figure B.5. This method produced a weak bond between the PMMA and membrane. PDMS was not usable due to the very weak bonding but Teflon did provide some promising results although the weakness meant very careful handling was needed not to delaminate the chips produced. This method was also attempted with COC substrates without improvement.

Following the work by Duffy et al. (1998) oxygen plasma treatment was also attempted with PDMS and polymer substrates. Successful bonding of PDMS to itself was possible (as one might expect) but bonding to PMMA was not possible as oxygen plasma does not appear to activate the surface sufficiently. Using a short exposure to oxygen plasma (15 sec) with a low power (50 W) it was possible to adhere PDMS to COC. Although it was possible to obtain a fairly strong bond if a post-exposure heat treatment of 80°C for 1 hour was performed, the bond was not permanent and the materials would come apart after 24 hrs. This process has been further attempted in a cleanroom by members of CMM who have been able to produce longer stability with cleaner substrates.

B.8 Novel integration of cast membranes

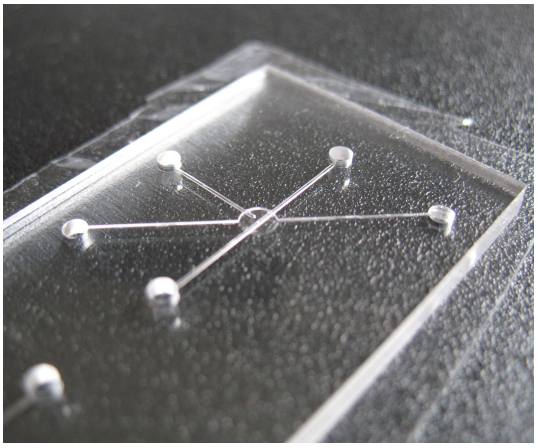

FIGURE B.5: A PMMA microfluidic chip bonded with a Teflon membrane

Taking a different approach to the previous experiments to integrate membranes, the casting of integral components was attempted. First attempts utilised a polyurethane (PU) based sealent/adhesive (Terostat PU 92, available from RS Components Ltd) manufactured by Loctite. Following the method detailed in Figure B.6 a series of membranes were cast. The cast membrane appeared to be strong but while cleaning with solvents (ethanol and isopropanol) it was noted that some of the black colour was transferred away. As cleaning of parts with these solvents is part of our standard processes a more appropriate elastomer was searched for.

Following investigation Viton® elastomers (a range of polymers manufactured by Dupont) appeared to be a useful alternative to PU based materials. These materials have a good resistance to almost all acids, bases and solvents and swell only in the presence of ketones. A sheet of FKM 0.5 mm thick was obtained from Goodfellows and tested for resistance to our lab solvents and (as datasheets suggested) only swelled in the presence of ketones (Acetone and 2-Butanone were used) after 10-12 hours soaking. Attempts to bond the FKM sheet with the PU adhesive were at first successful although under strain (estimated >100%) the materials separated. Long term strain cycling which occurs in the operation of valves is likely to also cause this failure so further investigation into adhesives for Viton® materials was undertaken.

A Viton® based adhesive used in high temperature applications is THA3000 manufactured by Thermodyn Corp.. This material was obtained and a series of test pieces created. The formulation is suitable for the adhesion of a range of materials as can be seen in Table B.2. The finished material is also very elastomeric and being Viton® based has the same chemical resistance. No noticeable effect has been noted using ethanol or isopropanol to clean the material once cured, swelling only being present when acetone and 2-butanone are used. During the casting process it is apparent that there is significant shrinkage of the elastomer throughout the cure which was recorded. This has been noted to be 85%, measured by curing a 100 ml sample for 2 weeks and noting the final volume. When membranes are cast from this material they are strong and flexible and have been used to create a working valve structure (Figure B.7).

The difficulty with this method is the unreliability of the casting process; approximately

20% of the cast membranes were of usable quality (i.e. flat without inclusions). During the process out-gassing of solvent occurs and presumably this causes the inclusions. Because of this reliability problem further research into the inclusion of commercially available membranes was pursued.

TABLE B.2: Adhesion of THA3000 adhesive to substrate materials

Material	Adhesion
Poly(methyl methacrylate) (PMMA)	Good
Polytetrafluoroethylene (PTFE)	Weak
Polypropylene (PP)	very Weak
Polyether ether ketone (PEEK)	Good
FKM sheet	Good
Glass	Strong
Polydimethylsiloxane (PDMS)	VERY Strong
Cyclic Olefin Copolymer (COC)	Good

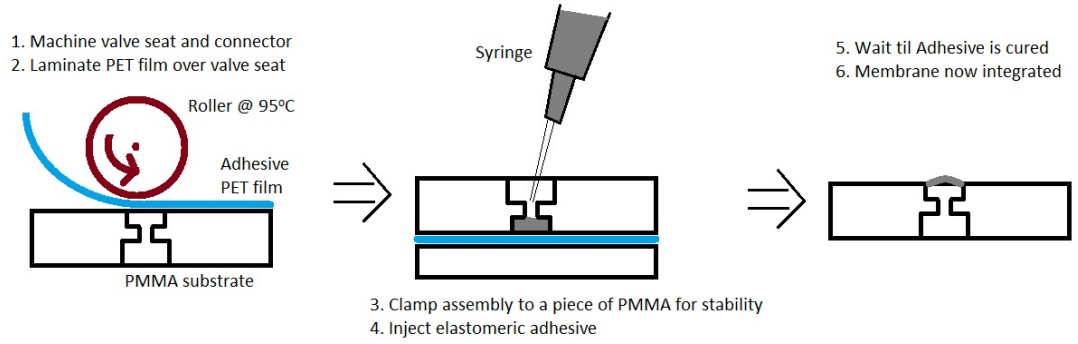

FIGURE B.6: Method for casting elastomeric membranes using common adhesives

B.9 Optimisation of oxygen plasma exposure

Shown in Figure B.8 and Figure B.9 are photographs taken of droplets of MilliQ water on PMMA and Viton® polymer surfaces exposed to oxygen plasma. Contact angles were assessed from these pictures and used to refine the process in 5.

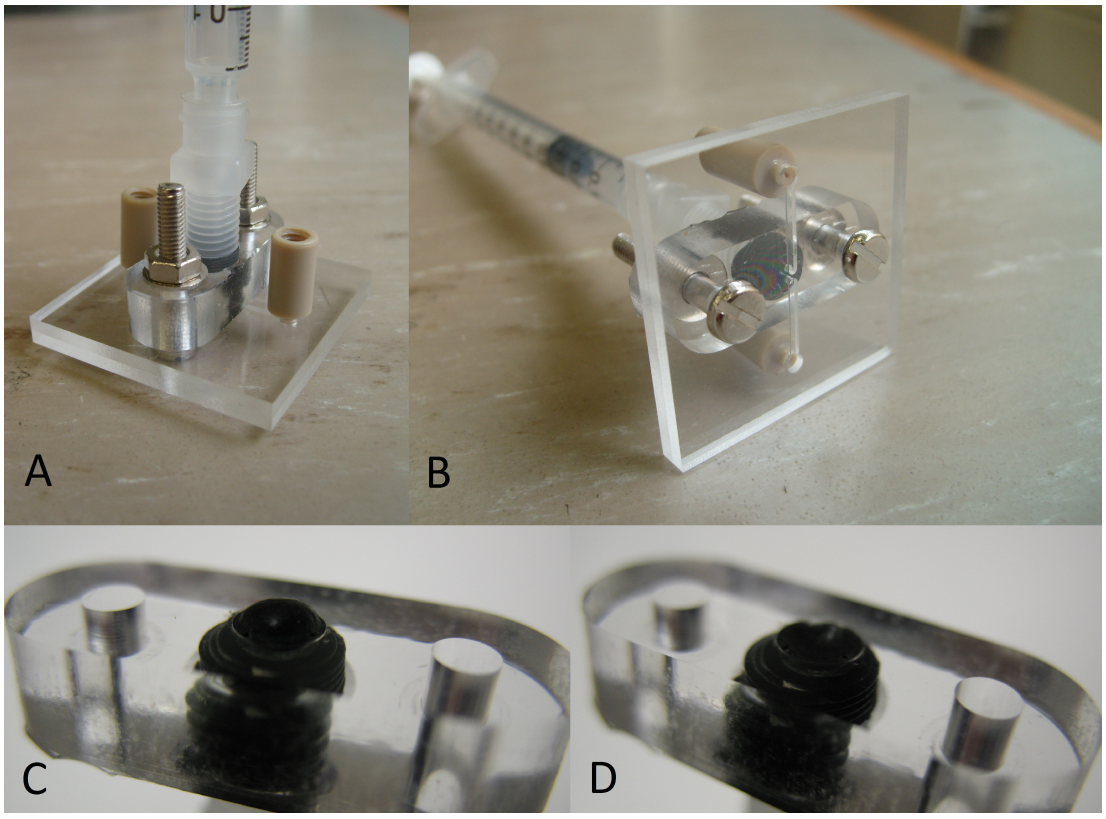

FIGURE B.7: A & B. Valve Test assembly using cast Viton® (THA3000) valve membrane. Syringe is used as a hydraulic actuator. Connectors into and out of chip are made from PEEK, C. Membrane deflection under positive pressure, D. Membrane deflection under negative pressure

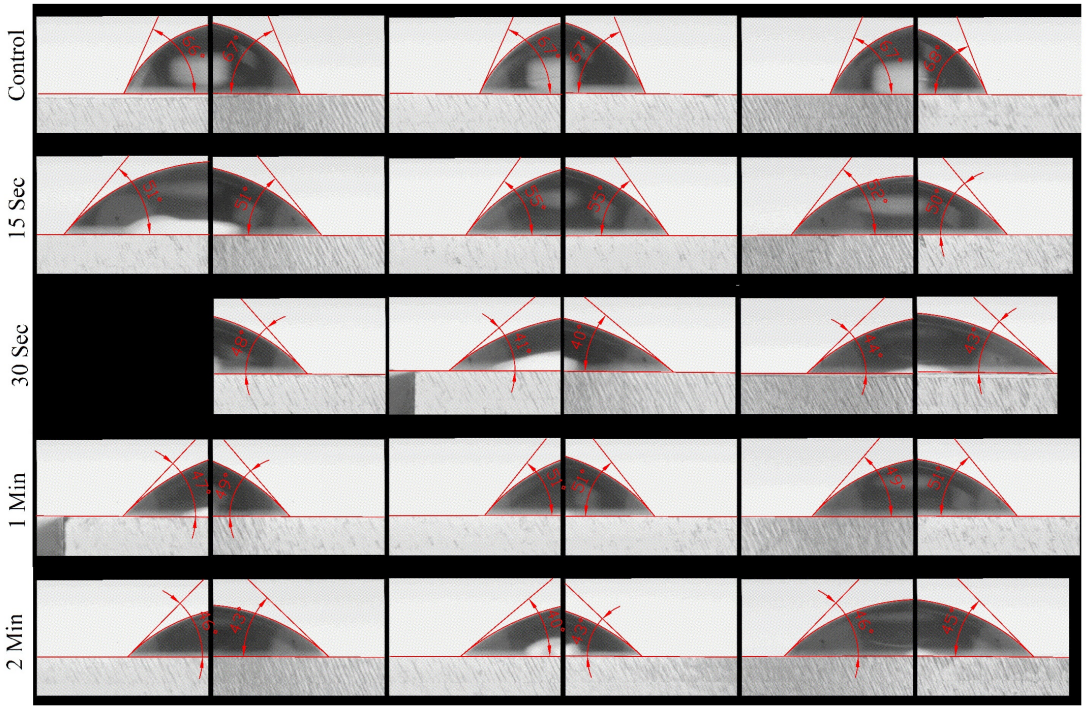

FIGURE B.8: Measurement of droplet contact angle on oxygen plasma treated PMMA

FIGURE B.9: Measurement of droplet contact angle on oxygen plasma treated Viton®

Bibliography

Samer Abi Kaed Bey. Series 300-2 way micro inert valve testing: Leakage determination and power optimization: Report i, 2011. internal report, Centre for Marine Microsystems, National Oceanography Centre, Southampton, UK.

M. L. Adams, M. L. Johnston, A. Scherer, and S. R. Quake. Polydimethylsiloxane based microfluidic diode. *J. Micromech. Microeng*, 15:1517, 2005.

L. R. Adornato, E. A. Kaltenbacher, T. A. Villareal, and R. H. Byrne. Continuous in situ determinations of nitrite at nanomolar concentrations. *Deep Sea Research Part I: Oceanographic Research Papers*, 52(3):543–551, 2005.

A. Ajdari, N. Bontoux, and H. A. Stone. Hydrodynamic dispersion in shallow mirochannels: the effect of cross-sectional shape. *Analytical Chemistry*, 78(2):387–392, 2006. ISI Document Delivery No.: 005MJ Times Cited: 33 Cited Reference Count: 13 AMER CHEMICAL SOC.

Natchanon Amornthammarong, Jaroon Jakmunee, Jianzhong Li, and Purnendu K. Dasgupta. Hybrid fluorometric flow analyzer for ammonia. *Analytical Chemistry*, 78: 1890–1896, 2006.

Argo. Argo Information Center, JCOMMOPS, 8-10, rue Hermes, Parc technologique du Canal, 31526 Ramonville cedex, France www.argo.ucsd.edu.

R. Aris. On the dispersion of a solute in a fluid flowing through a tube. *Proceedings of the Royal Society of London. Series A, Mathematical and Physical Sciences*, 235 (1200):67–77, 1956. ArticleType: research-article / Full publication date: Apr. 10, 1956 / Copyright 1956 The Royal Society.

R. Aris. On the dispersion of a solute in pulsating flow through a tube. *Proceedings of the Royal Society of London. Series A, Mathematical and Physical Sciences*, 259 (1298):370–376, 1960. ArticleType: research-article / Full publication date: Dec. 29, 1960 / Copyright 1960 The Royal Society.

F. A. J. Armstrong, C. R. Stearns, and J. D. H. Strickland. The measurement of upwelling and subsequent biological process by means of the technicon autoanalyzer and associated equipment. *Deep Sea Research and Oceanographic Abstracts*, 14(3): 381–389, 1967.

ASTM. Standard d1876 standard test method for peel resistance of adhesives (t-peel test), 2008.

W.R.G. Atkins. The phosphate content of fresh and salt waters in its relationship to the growth of the algal plankton. *Journal of the Marine Biological Association of the United Kingdom*, 13(1):119–150, 1923.

M. Bahrami, M. M. Yovanovich, and J. R. Culham. Pressure drop of fully-developed, laminar flow in microchannels of arbitrary cross-section. *Journal of Fluids Engineering*, 128(5):1036–1044, 2006.

Bartels Mikrotechnik GmbH. Emil-Figge-Str. 76a D-44227 Dortmund, Germany www.bartels.mikrotechnik.de.

R. C. Batra, M. Porfiri, and D. Spinello. Review of modeling electrostatically actuated microelectromechanical systems. *Smart Materials and Structures*, 16(6):R23, 2007.

Alexander D. Beaton, Vincent J. Sieben, Cedric F. A. Floquet, Edward M. Waugh, Samer Abi Kaed Bey, Iain R. G. Ogilvie, Matthew C. Mowlem, and Hywel Morgan. An automated microfluidic colourimetric sensor applied in situ to determine nitrite concentration. *Sensors and Actuators B: Chemical*, 156(2):1009–1014, 2011.

Holger Becker and Claudia Gärtner. Polymer microfabrication methods for microfluidic analytical applications. *Electrophoresis*, 21(1):12–26, 2000.

Holger Becker and Ulf Heim. Hot embossing as a method for the fabrication of polymer high aspect ratio structures. *Sensors and Actuators A: Physical*, 83(1-3):130–135, 2000. 0924-4247 doi: DOI: 10.1016/S0924-4247(00)00296-X.

Beer. Bestimmung der absorption des rothen lichts in farbigen flüssigkeiten. *Annalen der Physik*, 162:78–88, 1852.

D. Belder and M. Ludwig. Surface modification in microchip electrophoresis. *Electrophoresis*, 24(21):3595–3606, 2003.

A. Bertsch, H. Lorenz, and P. Renaud. 3d microfabrication by combining microstereolithography and thick resist uv lithography. *Sensors and Actuators A: Physical*, 73 (1-2):14–23, 1999. 0924-4247 doi: DOI: 10.1016/S0924-4247(98)00249-0.

Ali Asgar S. Bhagat, Erik T. K. Peterson, and Ian Papautsky. A passive planar micromixer with obstructions for mixing at low reynolds numbers. *Journal of Micromechanics and Microengineering*, 17:1017–1024, 2007. doi:10.1088/0960-1317/17/5/023.

Li Biao, Schwarz Thomas, and Sharon Andre. Implementation of microfluidic devices at a transparency. *Journal of Micromechanics and Microengineering*, 16(12):2639, 2006.

C. L. Bliss, J. N. McMullin, and C. J. Backhouse. Integrated wavelength-selective optical waveguides for microfluidic-based laser-induced fluorescence detection. *Lab on a Chip*, 8(1):143–151, 2008.

Blue White Industries Ltd. Blue-white industries. 5300 Business Drive, Huntington Beach, California, 92649 http://www.bluwhite.com/.

R. Boden, U. Simu, J. Margell, M. Lehto, K. Hjort, G. Thornell, and J. A. Schweitz. Metallic high-pressure microfluidic pump with active valves. In *Solid-State Sensors, Actuators and Microsystems Conference, 2007. TRANSDUCERS 2007. International*, pages 2429–2432, 2007.

Roger Boden, Marcus Lehto, Urban Simu, Greger Thornell, Klas Hjort, and Jan-ke Schweitz. A polymeric paraffin actuated high-pressure micropump. *Sensors and Actuators A: Physical*, 127(1):88–93, 2006. 0924-4247 doi: DOI: 10.1016/j.sna.2005.11.068.

Sebastian Böhm, Wouter Olthuis, and Piet Bergveld. A plastic micropump constructed with conventional techniques and materials. *Sensors and Actuators A: Physical*, 77 (3):223–228, 1999. 0924-4247 doi: DOI: 10.1016/S0924-4247(99)00192-2.

Bouguer. *Essai d'optique sur la gradation de la lumiere*, a paris, chez claude jombert ..., 1729.

M. Bowden and D. Diamond. The determination of phosphorus in a microfluidic manifold demonstrating long-term reagent lifetime and chemical stability utilising a colorimetric method. *Sensors and Actuators B (Chemical)*, B90(1-3):170–4, 2003. Times Cited: 0 6th European Conference on Optical Chemical Sensors and Biosensors. EUROPT(R)ODE VI Manchester UK.

M. Bowden, M. Sequeira, J. P. Krog, P. Gravesen, and D. Diamond. A prototype industrial sensing system for phosphorus based on micro system technology. *Analyst*, 127(1):1–4, 2002a. Times Cited: 14.

M. Bowden, M. Sequiera, J. P. Krog, P. Gravesen, and D. Diamond. Analysis of river water samples utilising a prototype industrial sensing system for phosphorus based on micro-system technology. *Journal of Environmental Monitoring*, 4(5):767–771, 2002b. Times Cited: 11.

Laurie Brown, Terry Koerner, J. Hugh Horton, and Richard D. Oleschuk. Fabrication and characterization of poly(methylmethacrylate) microfluidic devices bonded using surface modifications and solvents. *Lab on a Chip*, 6(1):66–73, 2006.

F. Bundgaard, T. Nielsen, D. Nilsson, P. X. Shi, G. Perozziello, A. Kristensen, and O. Geschke. Cyclic olefin copolymer (coc/topas ®) - an exceptional material for exceptional lab-on-a-chip systems. *Micro Total Analysis Systems*, 2(297):372–374, 2004.

F. Bundgaard, G. Perozziello, and O. Geschke. Rapid prototyping tools and methods for all-topas (r) cyclic olefin copolymer fluidic microsystems. *Proceedings of the I MECH E Part C Journal of Mechanical Engineering Science*, 220:1625–1632, 2006. doi:10.1243/09544062JMES295.

K. Carlsson, H. S. Jacobsen, A. L. Jensen, T. Stenstrom, and B. Karlberg. Micro-continuous flow system for wet chemical analysis. *Analytica Chimica Acta*, 354(1-3): 35–42, 1997.

P. C. Chatwin and P. J. Sullivan. The effect of aspect ratio on longitudinal diffusivity in rectangular channels. *Journal of Fluid Mechanics*, 120(JUL):347–358, 1982. ISI Document Delivery No.: PB900 Times Cited: 49 Cited Reference Count: 25 CAMBRIDGE UNIV PRESS.

Chelsea Instruments. Aqualine ferrybox system. http://www.chelsea.co.uk/FerryBox.htm.

Chang-Yu Chen, Chang-Hung Chen, Ting-Yuan Tu, Cheng-Ming Lin, and Andrew M. Wo. Electrical isolation and characteristics of permanent magnet-actuated valves for pdms microfluidics. *Lab on a Chip*, 11:733–737, 2011.

Hao Chen and Jens-Christian Meiners. Topologic mixing on a microfluidic chip. *Applied Physics Letters*, 84(12):2193–2195, 2004.

Qiang Chen, Gang Li, Qing-Hui Jin, Jian-Long Zhao, Qiu-Shi Ren, and Yuan-Sen Xu. A rapid and low-cost procedure for fabrication of glass microfluidic devices. *Microelectromechanical Systems, Journal of*, 16(5):1193–1200, 2007. 1057-7157.

Z. F. Chen, Y. H. Gao, J. M. Lin, R. G. Su, and Y. Xie. Vacuum-assisted thermal bonding of plastic capillary electrophoresis microchip imprinted with stainless steel template. *Journal of Chromatography A*, 1038(1-2):239–245, 2004.

H. P. Cheng and C. P. Chien. Ejection interaction of two adjacent micropumps. *Journal of Fluids Engineering*, 128(4):742–750, 2006.

C. S. Chin, K. S. Johnson, and K. H. Coale. Spectrophotometric determination of dissolved manganese in natural-waters with 1-(2-pyridylazo)-2-naphthol - application to analysis in situ in hydrothermal plumes. *Marine Chemistry*, 37(1-2):65–82, 1992.

K. L. Tan Christabel, C. Tracey Mark, B. Davis John, and D. Johnston Ian. Continuously variable mixing-ratio micromixer with elastomer valves. *Journal of Micromechanics and Microengineering*, 15(10):1885, 2005.

Huang Chun-Wei, Huang Song-Bin, and Lee Gwo-Bin. Pneumatic micropumps with serially connected actuation chambers. *Journal of Micromechanics and Microengineering*, 16(11):2265, 2006.

J. Cleary, C. Slater, and D. Diamond. Analysis of phosphate in wastewater using an autonomous microfluidics-based analyser. *International Journal of Civil and Environmental Engineering*, 2(3):145–148, 2010.

J. Cleary, C. Slater, C. McGraw, and D. Diamond. An autonomous microfluidic sensor for phosphate: On-site analysis of treated wastewater. *Ieee Sensors Journal*, 8(5-6): 508–515, 2008. Times Cited: 0.

Hitachi High-Technologies Corporation. Whitebrook Park, Lower Cookham Road, Maidenhead, Berkshire, SL6 8YA, U.K www.hitachi-hitec.com.

C. Cupelli, P. Koltay, Jens Ducree, Roland Zengerle, and M. Santer. Towards a modular split & recombine micro mixer, 2005. IMTEK - University of Freiburg, Laboratory for MEMS Applications, Georges-Koehler-Allee 103, D-79110 Freiburg, Germany, http://www.imtek.de/content/pdf/public/2005/2004-04-05_simod@imret.pdf, Accessed 15th May 2010.

Arindom Datta, In-Yong Eom, Achintya Dhar, Petr Kuban, Rosalynn Manor, Iftikhar Ahmad, Shubhra Gangopadhyay, Tim Dallas, Mark Holtz, Henryk Temkin, and Purnendu K. Dasgupta. Microfabrication and characterization of teflon af-coated liquid core waveguide channels in silicon. *IEEE sensors journal*, 3(6):8, 2003.

Dolomite. Unit 1, Anglian Business Park, Orchard Road, Royston, SG8 5TW, United Kingdom www.dolomite-microfluidics.com.

K. D. Dorfman and H. Brenner. Comment on "taylor dispersion of a solute in a microfluidic channel" [j. appl. phys. 89, 4667 (2001)]. *Journal of Applied Physics*, 90(12): 6553–6554, 2001. ISI Document Delivery No.: 498BK Times Cited: 8 Cited Reference Count: 10 AMER INST PHYSICS.

John F. Douglas, Janusz M. Gasiorek, and John A. Swaffield. *Fluid Mechanics*. Pearson Education, 4th edition, 2001.

Wen-Bin Du, Qun Fang, Qiao-Hong He, and Zhao-Lun Fang. High-throughput nanoliter sample introduction microfluidic chip-based flow injection analysis system with gravity-driven flows. 77(5):8, 2005.

D. C. Duffy, J. C. McDonald, O. J. A. Schueller, and G. M. Whitesides. Rapid prototyping of microfluidic systems in poly(dimethylsiloxane). *Analytical Chemistry*, 70 (23):4974–4984, 1998.

M. P. Duggan, Tom McCreedy, and J. W. Aylott. A non-invasive analysis method for on-chip spectrophotometric detection using liquid-core waveguiding within a 3d architecture. *The Analyst*, 128(11):5, 2003.

J. Dutt and J. Davis. Current strategies in nitrite detection and their application to field analysis. *Journal of Environmental Monitoring*, 4(3):465–471, 2002.

D. Dutta and D. T. Leighton. Dispersion reduction in pressure driven flow through microetched channels. *Analytical Chemistry*, 73(3):504–513, 2001.

D. Dutta, A. Ramachandran, and D. T. Leighton. Effect of channel geometry on solute dispersion in pressure-driven microfluidic systems. *Microfluidics and Nanofluidics*, 2 (4):275–290, 2006.

C. S. Effenhauser, G. J. M. Bruin, A. Paulus, and M. Ehrat. Integrated capillary electrophoresis on flexible silicone microdevices: Analysis of dna restriction fragments and detection of single dna molecules on microchips. *Analytical Chemistry*, 69(17): 3451–3457, 1997.

Albert Einstein. On the movement of small particles suspended in stationary liquids required by the molecular-kinetic theory of heat. *Annalen der Physik*, 17:549–560, 1905.

Elga Europe. via della Merlata 8, 20014 Nerviano, Milano, Italy www.elgaeurope.it.

M. Esashi, S. Shoji, and A. Nakano. Normally close microvalve and micropump fabricated on a silicon wafer. In *Micro Electro Mechanical Systems, 1989, Proceedings, An Investigation of Micro Structures, Sensors, Actuators, Machines and Robots. IEEE*, pages 29–34, 1989.

Evonik Röhm Gmbh. Evonik Industries AG, Rellinghauser Strae 1-11, 45128 Essen http://corporate.evonik.com Plexiglass GS and XT Product Description Datasheets give Tg information.

Adolf Fick. Ueber diffusion. *Annalen der Physik*, 170(1):59–86, 1855.

M. S. Finch, D. J. Hydes, and C. H. Clayson. A low power ultra violet spectrophotometer for measurement of nitrate in seawater: introduction, calibration and initial sea trials. *Analytica Chimica Acta*, 377(2-3):167–177, 1998.

Fisher Scientific UK Ltd. Fisher scientific. Bishop Meadow Road, Loughborough, Leicestershire, LE11 5RG http://www.fisher.co.uk/.

Leanne J. Flewelling, Jerome P. Naar, Jay P. Abbott, Daniel G. Baden, Nelio B. Barros, Gregory D. Bossart, Marie-Yasmine D. Bottein, Daniel G. Hammond, Elsa M. Haubold, Cynthia A. Heil, Michael S. Henry, Henry M. Jacocks, Tod A. Leighfield, Richard H. Pierce, Thomas D. Pitchford, Sentiel A. Rommel, Paula S. Scott, Karen A. Steidinger, Earnest W. Truby, Frances M. Van Dolah, and Jan H. Landsberg. Brevetoxicosis red tides and marine mammal mortalities. *Nature*, 435(7043):755–756, 2005. 10.1038/435755a.

Cedric F. A. Floquet, Vincent J. Sieben, Ambra Milani, Etienne P. Joly, Iain R. G. Ogilvie, Hywel Morgan, and Matthew C. Mowlem. Nanomolar detection with high sensitivity microfluidic absorption cells manufactured in tinted pmma for chemical analysis. *Talanta*, 84(1):235–239, 2011. doi: DOI: 10.1016/j.talanta.2010.12.026.

C. R. Friedrich and M. J. Vasile. Development of the micromilling process for high-aspect-ratio microstructures. *Journal of Microelectromechanical Systems*, 5(1):33–38, 1996. Times Cited: 61.

Lung-Ming Fu and Ruey-Jen Yang Che-Hsin Lin Yu-Sheng Chien. A novel microfluidic mixer utilizing electrokinetic driving forces under low switching frequency. *Electrophoresis*, 26(9):1814–1824, 2005.

C. Galli. Modeling systematic errors: polychromatic sources of beer-lambert deviations in hplc/uv and nonchromatographic spectrophotometric assays. *Journal of Pharmaceutical and Biomedical Analysis*, 25(5-6):803–809, 2001.

Y. Ganor, D. Shilo, J. Messier, T. W. Shield, and R. D. James. Testing system for ferromagnetic shape memory micro-actuators. *Review of Scientific Instruments*, 78 (073907-1):379–380, 2007. 10.1007/978-1-4020-6239-1_188.

Wayne S. Gardner and John M. Malczyk. Discrete injection segmented flow analysis of nutrients in small-volume water samples. *Analytical Chemistry*, 55(9):1645–1647, 1983. doi: 10.1021/ac00260a055.

A. Geipel, A. Doll, P. Jantscheff, N. Esser, U. Massing, P. Woias, and F. Goldschmidtboeing. A novel two-stage backpressure-independent micropump: modeling and characterization. *Journal of Micromechanics and Microengineering*, 17(5):949, 2007.

A. Geipel, F. Goldschmidtbing, A. Doll, P. Jantscheff, N. Esser, U. Massing, and P. Woias. An implantable active microport based on a self-priming high-performance two-stage micropump. *Sensors and Actuators A: Physical*, 145-146:414–422, 2008. doi: 10.1016/j.sna.2007.11.024.

T. Gerlach, M. Schuenemann, and H. Wurmus. A new micropump principle of the reciprocating type using pyramidic micro flowchannels as passive valves. *Journal of Micromechanics and Microengineering*, 5(2):199, 1995.

G.Kisker. Ochtruper Straße 18, D-48543 Steinfurt, Germany www.kisker-biotech.com.

Brian T. Good, Christopher N. Bowman, and Robert H. Davis. An effervescent reaction micropump for portable microfluidic systems. *Lab on a Chip*, 6(5):659–666, 2006.

Goodfellow Cambridge Ltd. Ermine Business Park, Huntingdon, England PE29 6WR www.goodfellow.com.

J. Gould, D. Roemmich, S. Wijffels, H. Freeland, M. Ignaszewsky, X. Jianping, S. Pouliquen, Y. Desaubies, U. Send, K. Radhakrishnan, K. Takeuchi, K. Kim, M. Danchenkov, P. Sutton, B. King, B. Owens, and S. Riser. Argo profiling floats bring new era of in situ ocean observations. *EOS, Transactions American Geophysical Union*, 85(19):185, 2004.

Jacques Goulpeau, Daniel Trouchet, Armand Ajdari, and Patrick Tabeling. Experimental study and modeling of polydimethylsiloxane peristaltic micropumps. *Journal of Applied Physics*, 98(4):044914–9, 2005.

Klaus Grasshoff, Klaus Kremling, and Manfred Ehrhardt. *Methods of Seawater Analysis (Third Edition)*. Wiley-VCH, Weinheim (Federal Republic of Germany), 1999.

James Green, Hold, Arne E., and Aman Khan. A review of passive and active mixing systems in microfluidic devices. *The International Journal of Multiphysics*, 1:1–32, 2007. doi:10.1260/175095407780130544.

G. M. Greenway, S. J. Haswell, and P. H. Petsul. Characterisation of a micro-total analytical system for the determination of nitrite with spectrophotometric detection. *Analytica Chimica Acta*, 387(1):1–10, 1999.

Anja Griebel, Sabine Rund, Friedhelm Schonfeld, Wolfgang Dorner, Renate Konrad, and Steffen Hardt. Integrated polymer chip for two-dimensional capillary gel electrophoresis. *Lab on a Chip*, 4(1):18–23, 2004.

Peter Griess. Bemerkungen zu der abhandlung der hh. weselsky und benedikt ;ueber einige azoverbindungen. *Berichte der deutschen chemischen Gesellschaft*, 12(1):426–428, 1879.

Anthony Grimes, David N. Breslauer, Maureen Long, Jonathan Pegan, Luke P. Lee, and Michelle Khine. Shrinky-dink microfluidics: rapid generation of deep and rounded patterns. *Lab on a Chip*, 8(1):170–172, 2008.

W. H. Grover, A. M. Skelley, C. N. Liu, E. T. Lagally, and R. A. Mathies. Monolithic membrane valves and diaphragm pumps for practical large-scale integration into glass microfluidic devices. *Sensors and Actuators B-Chemical*, 89(3):315–323, 2003.

W. H. Grover, M. G. von Muhlen, and S. R. Manalis. Teflon films for chemically-inert microfluidic valves and pumps. *Lab on a Chip*, 8(6):913–918, 2008. Grover, William H. von Muhlen, Marcio G. Manalis, Scott R.

M. Grumann, J. Steigert, L. Riegger, I. Moser, B. Enderle, K. Riebeseel, G. Urban, R. Zengerle, and J. Ducre. Sensitivity enhancement for colorimetric glucose assays on whole blood by on-chip beam-guidance. *Biomedical Microdevices*, 8(3):209–214, 2006.

Pan Gu, Ke Liu, Hong Chen, Toshikazu Nishida, and Z. Hugh Fan. Chemical-assisted bonding of thermoplastics/elastomer for fabricating microfluidic valves. *Analytical Chemistry*, 83(1):446–452, 2010. doi: 10.1021/ac101999w.

W. Gu, H. Chen, Y. C. Tung, J. C. Meiners, and S. Takayama. Multiplexed hydraulic valve actuation using ionic liquid filled soft channels and braille displays. *Applied Physics Letters*, 90(3):3, 2007. ISI Document Delivery No.: 127JR Times Cited:

3 Cited Reference Count: 17 Gu, Wei Chen, Hao Tung, Yi-Chung Meiners, Jens-Christian Takayama, Shuichi AMER INST PHYSICS.

Wei Gu, Xiaoyue Zhu, Nobuyuki Futai, Brenda S. Cho, and Shuichi Takayama. Computerized microfluidic cell culture using elastomeric channels and braille displays. *Proceedings of the National Academy of Sciences of the United States of America*, 101 (45):15861–15866, 2004. 10.1073/pnas.0404353101.

Hamilton Company. P.O. Box 26, CH-7402 Bonaduz, GR, Switzerland www.hamiltoncompany.com.

C. M. Hansen and L. Just. *Prediction of environmental stress cracking in plastics with Hansen solubility parameters*, volume 40. American Chemical Society, Washington, DC, ETATS-UNIS, 2001.

A. K. Hanson. A new in situ chemical analyzer for mapping coastal nutrient distributions in real time, 2000. OCEANS 2000 MTS/IEEE Conference and Exhibition, 3:1975-1982.

A. K. Hanson. Cabled and autonomous submersible chemical analyzers for coastal observations. *Abstracts of Papers of the American Chemical Society*, 229:U152–U153, 2005. ISI Document Delivery No.: 913TZ Times Cited: 0 Cited Reference Count: 0 Part 1.

S. Hardt, H. Pennemann, and F. Schnfeld. Theoretical and experimental characterization of a low-reynolds number split-and-recombine mixer. *Microfluidics and Nanofluidics*, 2(3):237–248, 2006. 10.1007/s10404-005-0071-6.

Herb Hartshorne, Christopher J. Backhouse, and William E. Lee. Ferrofluid-based microchip pump and valve. *Sensors and Actuators B: Chemical*, 99(2-3):592–600, 2004.

Harvard Apparatus. 84 October Hill Road, Holliston, Massachusetts 01746, United States www.harvardapparatus.com.

D. Y. He, Z. J. Zhang, Y. Huang, and Y. F. Hu. Chemiluminescence microflow injection analysis system on a chip for the determination of nitrite in food. *Food Chemistry*, 101(2):667–672, 2007.

Qi Heng, Chen Tao, and Zuo Tie-chuan. Surface roughness analysis and improvement of micro-fluidic channel with excimer laser. *Microfluidics and Nanofluidics*, 2(4):357–360, 2006. 10.1007/s10404-006-0078-7.

Henniker Scientific Ltd. Cavendish House, Birchwood Park, Warrington, Cheshire, WA3 6BU UK www.henniker-scientific.com.

Volker Hessel, Holger Lwe, and Friedhelm Schnfeld. Micromixers–a review on passive and active mixing principles. *Chemical Engineering Science*, 60(8-9):2479–2501, 2005. 0009-2509 doi: DOI: 10.1016/j.ces.2004.11.033.

O. Hofmann, X. H. Wang, A. Cornwell, S. Beecher, A. Raja, D. D. C. Bradley, A. J. deMello, and J. C. deMello. Monolithically integrated dye-doped pdms long-pass filters for disposable on-chip fluorescence detection. *Lab on a Chip*, 6(8):981–987, 2006.

Alexandra Homsy, Sander Koster, Jan C. T. Eijkel, Albert van den Berg, F. Lucklum, E. Verpoorte, and Nico F. de Rooij. A high current density dc magnetohydrodynamic (mhd) micropump. *Lab on a Chip*, 5(4):466–471, 2005.

Chien-Chong Hong, Jin-Woo Choi, and Chong H. Ahn. A novel in-plane passive microfluidic mixer with modified tesla structures. *Lab on a Chip*, 4(2):109–113, 2004.

Peter B. (Jr.) Howell, David R. Mott, Stephanie Fertig, Carolyn R. Kaplan, Joel P. Golden, Elaine S. Oran, and Frances S. Ligler. A microfluidic mixer with grooves placed on the top and bottom of the channel. *Lab on a Chip*, 5(5):524–530, 2005.

Yi-Chu Hsu and Tang-Yuan Chen. Applying taguchi methods for solvent-assisted pmma bonding technique for static and dynamic -tas devices. *Biomedical Microdevices*, 9(4): 513–522, 2007. 10.1007/s10544-007-9059-1.

J. S. Hu and Christopher Y. H. Chao. A study of the performance of microfabricated electroosmotic pump. *Sensors and Actuators A: Physical*, 135(1):273–282, 2007. 0924-4247 doi: DOI: 10.1016/j.sna.2006.07.007.

Yongguang Huang, Shibing Liu, Wei Yang, and Chengxin Yu. Surface roughness analysis and improvement of pmma-based microfluidic chip chambers by co2 laser cutting. *Applied Surface Science*, In Press, Corrected Proof, 2010. doi: 10.1016/j.apsusc.2009.09.092.

S. E. Hulme, S. S. Shevkoplyas, and G. M. Whitesides. Incorporation of prefabricated screw, pneumatic, and solenoid valves into microfluidic devices. *Lab on a Chip*, 9(1): 79–86, 2009. Hulme, S. Elizabeth Shevkoplyas, Sergey S. Whitesides, George M.

Chen-I. Hung, Ke-Chin Wang, and Chin-Kwun Chyou. Design and flow simulation of a new micromixer. *JSME International Journal Series B Fluids and Thermal Engineering*, 48(1):17–24, 2005.

Hamish Hunt and James Wilkinson. Optofluidic integration for microanalysis. *Microfluidics and Nanofluidics*, 4(1):53–79, 2008.

D. J. Hydes, M. C. Hartman, J. Kaiser, and J. M. Campbell. Measurement of dissolved oxygen using optodes in a ferrybox system. *Estuarine, Coastal and Shelf Science*, 83 (4):485–490, 2009.

Instron. Coronation Road, High Wycombe, Bucks HP12 3SY, United Kingdom www.instron.co.uk.

Kazuyoshi Itoga, Jun Kobayashi, Yukiko Tsuda, Masayuki Yamato, and Teruo Okano. Second-generation maskless photolithography device for surface micropatterning and microfluidic channel fabrication. *Analytical Chemistry*, 80(4):1323–7, 2008.

J-Flex Rubber Products. Unit 1, London Road Business Park, Retford, Nottinghamshire, DN22 6HG UK www.j-flex.co.uk.

Jaesung Jang and Seung S. Lee. Theoretical and experimental study of mhd (magnetohydrodynamic) micropump. *Sensors and Actuators A: Physical*, 80(1):84–89, 2000. doi: 10.1016/S0924-4247(99)00302-7.

Ling-Sheng Jang and Yung-Chiang Yu. Peristaltic micropump system with piezoelectric actuators. *Microsystem Technologies*, 14(2):241–248, 2008. 10.1007/s00542-007-0428-8.

H. W. Jannasch, K. S. Johnson, and C. M. Sakamoto. Submersible, osmotically pumped analyzers for continuous determination of nitrate in-situ. *Analytical Chemistry*, 66(20): 3352–3361, 1994. ISI Document Delivery No.: PL230 Times Cited: 55 Cited Reference Count: 28 AMER CHEMICAL SOC.

Chang Nyung Kim Jin Jeong. A numerical simulation on diffuser-nozzle based piezoelectric micropumps with two different numerical models. *international Journal for Numerical Methods in Fluids*, 53(4):561–571, 2007.

K. S. Johnson and L. J. Coletti. In situ ultraviolet spectrophotometry for high resolution and long-term monitoring of nitrate, bromide and bisulfide in the ocean. *Deep-Sea Research Part I-Oceanographic Research Papers*, 49(7):1291–1305, 2002.

G. V. Kaigala, S. Ho, R. Penterman, and C. J. Backhouse. Rapid prototyping of microfluidic devices with a wax printer. *Lab on a Chip*, 7(3):384–387, 2007.

G. V. Kaigala, V. N. Hoang, and C. J. Backhouse. Electrically controlled microvalves to integrate microchip polymerase chain reaction and capillary electrophoresis. *Lab on a Chip*, 8(7):1071–1078, 2008. ISI Document Delivery No.: 320LT Times Cited: 6 Cited Reference Count: 32 Kaigala, Govind V. Hoang, Viet N. Backhouse, Christopher J. ROYAL SOC CHEMISTRY.

I. Kano, Y. Shii, and T. Nishina. Development of an electrohydrodynamic micropump. In *Industry Applications Conference, 2007. 42nd IAS Annual Meeting. Conference Record of the 2007 IEEE*, pages 38–44, 2007.

Ryan T. Kelly, Tao Pan, and Adam T. Woolley. Phase-changing sacrificial materials for solvent bonding of high-performance polymeric capillary electrophoresis microchips. *Analytical Chemistry*, 77(11):3536–3541, 2005. doi: 10.1021/ac0501083.

D. S. Kim, S. H. Lee, T. H. Kwon, and C. H. Ahn. A serpentine laminating micromixer combining splitting/recombination and advection. *Lab on a Chip*, 5(7):739–747, 2005a.

ISI Document Delivery No.: 937YJ Times Cited: 34 Cited Reference Count: 21 ROYAL SOC CHEMISTRY.

H. Kim, A. A. Astle, K. Najafi, L. P. Bernal, P. D. Washabaugh, and F. Cheng. Bidirectional electrostatic microspeaker with two large-deflection flexible membranes actuated by single/dual electrodes. In *Sensors, 2005 IEEE*, page 4 pp., 2005b.

K. Kim, S. W. Park, and S. S. Yang. The optimization of pdms-pmma bonding process using silane primer. *Biochip Journal*, 4(2):148–154, 2010. ISI Document Delivery No.: 613UP Times Cited: 0 Cited Reference Count: 14 Kim, Kangil Park, Sin Wook Yang, Sang Sik SPRINGER.

H. Klank, J.P. Kutter, and O. Geschke. Co2-laser micromachining and back-end processing for rapid production of pmma-based microfluidic systems. *Lab Chip*, 2:242 – 246, 2002.

Kloehn Inc. 10000 Banburry Cross Drive, Las Vegas, NV 89144, USA www.kloehn.com.

Michael Koch, Nick Harris, Alan G. R. Evans, Neil M. White, and Arthur Brunnschweiler. A novel micromachined pump based on thick-film piezoelectric actuation. *Sensors and Actuators A: Physical*, 70(1-2):98–103, 1998. doi: 10.1016/S0924-4247(98)00120-4.

Myra T. Koesdjojo, Corey R. Koch, and Vincent T. Remcho. Technique for microfabrication of polymeric-based microchips from an su-8 master with temperature-assisted vaporized organic solvent bonding. *Analytical Chemistry*, 81(4):1652–1659, 2009. doi: 10.1021/ac802450u.

Myra T. Koesdjojo, Yolanda H. Tennico, and Vincent T. Remcho. Fabrication of a microfluidic system for capillary electrophoresis using a two-stage embossing technique and solvent welding on poly(methyl methacrylate) with water as a sacrificial layer. *Analytical Chemistry*, 80(7):2311–2318, 2008. doi: 10.1021/ac7021647.

S. D. Kolev. Mathematical-modeling of flow-injection systems. *Analytica Chimica Acta*, 308(1-3):36–66, 1995.

M. Kraft, C. P. Lewis, and T. G. Hesketh. Closed-loop silicon accelerometers. *Circuits, Devices and Systems, IEE Proceedings* -, 145(5):325–331, 1998.

L. J. Kricka, P. Fortina, N. J. Panaro, P. Wilding, G. Alonso-Amigo, and H. Becker. Fabrication of plastic microchips by hot embossing. *Lab on a Chip*, 2(1):1–4, 2002.

Hung Kuo Yung, Liao Jung Chiang, Tseng Fan Gang, H. P. Feng, and H. H. Tsai. Optimal fabricate technology of polymer micro optical mirror. In *Industrial Technology, 2008. ICIT 2008. IEEE International Conference on*, pages 1–6, 2008.

Bambang Kuswandi, Nuriman, Jurriaan Huskens, and Willem Verboom. Optical sensing systems for microfluidic devices: A review. *Analytica Chimica Acta*, 601(2):141–155, 2007.

Hoyin Lai and Albert Folch. Design and dynamic characterization of "single-stroke" peristaltic pdms micropumps. *Lab on a Chip*, 11(2):336–342, 2011.

Johann Heinrich Lambert. *I.H. Lambert Photometria, sive, De mensura et gradibus luminis, colorum et umbrae [microform].* Landmarks of science. V.E. Klett, Augustae Vindelicorum, 1760. Includes index. Master microform held by: Readex.

Dong Gun Lee, Daniel D. Shin, and Gregory P. Carman. Large flow rate/high frequency microvalve array for high performance actuators. *Sensors and Actuators A: Physical*, 134(1):257–263, 2007. doi: 10.1016/j.sna.2006.06.036.

K. S. Lee and R. J. Ram. Plastic-pdms bonding for high pressure hydrolytically stable active microfluidics. *Lab on a Chip*, 9(11):1618–1624, 2009. ISI Document Delivery No.: 448NN Times Cited: 9 Cited Reference Count: 21 Lee, Kevin S. Ram, Rajeev J. ROYAL SOC CHEMISTRY.

Kiha Lee and David A. Dornfeld. A study of surface roughness in the micro-end-milling process, 2004. University of California eScholarship Repository [http://repositories.cdlib.org/cgi/oai2.cgi] (United States) ER, accessed 15th May 2010.

N. Y. Lee and B. H. Chung. Novel poly(dimethylsiloxane) bonding strategy via room temperature "chemical gluing". *Langmuir*, 25(6):3861–3866, 2009. ISI Document Delivery No.: 418JR Times Cited: 4 Cited Reference Count: 28 Lee, Nae Yoon Chung, Bong Hyun AMER CHEMICAL SOC.

Seok Woo Lee, Kim Dong Sung, S. Lee Seung, and Kwon Tai Hun. A split and re-combination micromixer fabricated in a pdms three-dimensional structure. *Journal of Micromechanics and Microengineering*, 16(5):1067, 2006.

K. F. Lei, S. Ahsan, N. Budraa, W. J. Li, and J. D. Mai. Microwave bonding of polymer-based substrates for potential encapsulated micro/nanofluidic device fabrication. *Sensors and Actuators a-Physical*, 114(2-3):340–346, 2004.

Asuncion V. Lemoff and Abraham P. Lee. An ac magnetohydrodynamic micropump. *Sensors and Actuators B: Chemical*, 63(3):178–185, 2000. doi: 10.1016/S0925-4005(00)00355-5.

Kun Lian and Zhong-Geng Ling. Post-exposure heat treatment to reduce surface roughness of pmma surfaces formed by radiation lithography, 2002. Board of Supervisors of Louisiana State University and Agricultural and Mechanical College, USA, US Patent Number 2000-566261 6387578.

Zhenhua Liang, Nghia Chiem, Gregor Ocvirk, Thompson Tang, Karl Fluri, and D. Jed Harrison. Microfabrication of a planar absorbance and fluorescence cell for integrated capillary electrophoresis devices. *Analytical Chemistry*, 68(6):1040–1046, 1996.

Che-Hsin Lin, Chien-Hsiang Chao, and Che-Wei Lan. Low azeotropic solvent for bonding of pmma microfluidic devices. *Sensors and Actuators B: Chemical*, 121(2):698–705, 2007. doi: 10.1016/j.snb.2006.04.086.

Jian Liu, Kyung-Won Ro, Ranu Nayak, and Daniel R. Knapp. Monolithic column plastic microfluidic device for peptide analysis using electrospray from a channel opening on the edge of the device. *International Journal of Mass Spectrometry*, 259(1-3):65–72, 2007. doi: 10.1016/j.ijms.2006.08.017.

Liyu Liu, Xiaoqing Chen, Xize Niu, Weijia Wen, and Ping Sheng. Electrorheological fluid-actuated microfluidic pump. *Applied Physics Letters*, 89(8):083505–3, 2006.

H. Lorenz, M. Despont, N. Fahrni, N. LaBianca, P. Renaud, and P. Vettiger. Su-8: a low-cost negative resist for mems. *Journal of Micromechanics and Microengineering*, 7:121–124, 1997.

J. J. Loverich, I. Kanno, and H. Kotera. Concepts for a new class of all-polymer micropumps. *Lab on a Chip*, 6(9):1147–1154, 2006.

LPKF Laser & Electronics AG. Osteriede 7, 30827 Garbsen, Germany, www.lpkf.com.

Liang-Hsuan Lu, Ryu Kee Suk, and Liu Chang. A magnetic microstirrer and array for microfluidic mixing. *Microelectromechanical Systems, Journal of*, 11(5):462–469, 2002. 1057-7157.

Dieudonne A. Mair, Marco Rolandi, Marian Snauko, Richard Noroski, Frantisek Svec, and Jean M. J. Frechet. Room-temperature bonding for plastic high-pressure microfluidic chips. *Analytical Chemistry*, 79(13):5097–5102, 2007. doi: 10.1021/ac070220w.

Rosalynn Manor, Arindom Datta, Iftikar Ahmad, Mark Holtz, Shubhra Gangopadhyay, and Tim Dallas. Microfabrication and characterization of liquid core waveguide glass channels coated with teflon af. *IEEE sensors journal*, 3(6):6, 2003.

L. Martynova, L. E. Locascio, M. Gaitan, G. W. Kramer, R. G. Christensen, and W. A. MacCrehan. Fabrication of plastic microfluid channels by imprinting methods. *Analytical Chemistry*, 69(23):4783–4789, 1997.

C. M. McGraw, S. E. Stitzel, J. Cleary, C. Slater, and D. Diamond. Autonomous microfluidic system for phosphate detection. *Talanta*, 71(3):1180–1185, 2007. Times Cited: 8.

A. Mercanzini, M. Bachmann, A. Jordan, Y. Amstutz, N. De Rooij, and N. Stergiopulos. A low power, polyimide valved micropump for precision drug delivery. In *Microtechnology in Medicine and Biology, 2005. 3rd IEEE/EMBS Special Topic Conference on*, pages 146–149, 2005.

Met Office. FitzRoy Road, Exeter, Devon, EX1 3PB, United Kingdom www.metoffice.gov.uk.

O. B. Michelsen. Photometric determination of phosphorus as molybdovanadophosphoric acid. *Analytical Chemistry*, 29(1):60–62, 1957. doi: 10.1021/ac60121a017.

MicroChem Corp. Microchem. 90 Oak St. Newton, MA 02464 USA http://www.microchem.com/.

Microfluidica. 6901 N. Rockledge Ave., Milwaukee, WI 53209 USA www.microfluidica.info.

G. Misson. *Chem.-Ztg*, 32:633, 1908.

M. J. Moorcroft, J. Davis, and R. G. Compton. Detection and determination of nitrate and nitrite: a review. *Talanta*, 54(5):785–803, 2001.

T. S. Moore, K. M. Mullaugh, R. R. Holyoke, A. N. S. Madison, M. Yucel, and G. W. Luther. Marine chemical technology and sensors for marine waters: Potentials and limits. *Annual Review of Marine Science*, 1:91–115, 2009.

C. J. Morris and F. K. Forster. Low-order modeling of resonance for fixed-valve micropumps based on first principles. *Microelectromechanical Systems, Journal of*, 12 (3):325–334, 2003. 1057-7157.

Bobak Mosadegh, Hossein Tavana, Sasha Cai Lesher-Perez, and Shuichi Takayama. High-density fabrication of normally closed microfluidic valves by patterned deactivation of oxidized polydimethylsiloxane. *Lab on a Chip*, 11:738–742, 2011.

J. Murphy and J. P. Riley. A modified single solution method for the determination of phosphate in natural waters. *Analytica Chimica Acta*, 27(0):31–36, 1962.

Akira Nakajima, Kazuhito Hashimoto, and Toshiya Watanabe. Recent studies on superhydrophobic films. *Monatshefte fr Chemie / Chemical Monthly*, 132(1):31–41, 2001. 10.1007/s007060170142.

Nguyen Nam-Trung and Wu Zhigang. Micromixers-a review. *Journal of Micromechanics and Microengineering*, 15:R1–R16, 2005. doi:10.1088/0960-1317/15/2/R01.

National Instruments Corp. 11500 N Mopac Expwy, Austin, TX 78759-3504 USA www.ni.com.

NERC. Natural Environment Research Council, Polaris House, North Star Avenue, Swindon, SN2 1EU, Wiltshire, UK. www.nerc.ac.uk Accounts Taken from; http://www.nerc.ac.uk/publications/annualreport/2010/annualreport.pdf on 25th September 2011.

Chiu-On Ng. Dispersion in steady and oscillatory flows through a tube with reversible and irreversible wall reactions. *Proceedings: Mathematical, Physical and Engineering Sciences*, 462(2066):481–515, 2006. ArticleType: research-article / Full publication date: Feb. 8, 2006 / Copyright 2006 The Royal Society.

S. Ng, R. Tjeung, Z. Wang, A. Lu, I. Rodriguez, and N. de Rooij. Thermally activated solvent bonding of polymers. *Microsystem Technologies*, 14(6):753–759, 2008. 10.1007/s00542-007-0459-1.

Nam-Trung Nguyen and Thai-Quang Truong. A fully polymeric micropump with piezoelectric actuator. *Sensors and Actuators B: Chemical*, 97(1):137–143, 2004. doi: 10.1016/S0925-4005(03)00521-5.

Thanh Tung Nguyen, Nam Seo Goo, Vinh Khanh Nguyen, Youngtai Yoo, and Seungbae Park. Design, fabrication, and experimental characterization of a flap valve ipmc micropump with a flexibly supported diaphragm. *Sensors and Actuators A: Physical*, 141(2):640–648, 2008. doi: 10.1016/j.sna.2007.09.017.

Hong-Seok Noh, Yong Huang, and Peter J. Hesketh. Parylene micromolding, a rapid and low-cost fabrication method for parylene microchannel. *Sensors and Actuators B: Chemical*, 102(1):78–85, 2004. doi: 10.1016/j.snb.2003.09.038.

Norland Products Inc. 2540 Route 130, Suite 100, Cranbury, NJ 08512 www.norlandprod.com.

D. Ogonczyk, J. Wegrzyn, P. Jankowski, B. Dabrowski, and P. Garstecki. Bonding of microfluidic devices fabricated in polycarbonate. *Lab on a Chip*, 10(10):1324–1327, 2010.

K. W. Oh and C. H. Ahn. A review of microvalves. *Journal of Micromechanics and Microengineering*, 16(5):R13–R39, 2006.

Oxford Nutrition. Unit 5 Western Units, Pottery Road. Bovey Tracey. Devon. TQ13 9JJ UK www.nutrinox.com.

Jeng-Hao Pai, Yuli Wang, Gina ToA Salazar, Christopher E. Sims, Mark Bachman, G. P. Li, and Nancy L. Allbritton. Photoresist with low fluorescence for bioanalytical applications. *Analytical Chemistry*, 79(22):8774–80, 2007.

C. T. Pan, J. Shiea, and S. C. Shen. Fabrication of an integrated piezo-electric micronebulizer for biochemical sample analysis. *Journal of Micromechanics and Microengineering*, 17:659–669, 2007. doi:10.1088/0960-1317/17/3/031.

Tingrui Pan, J. McDonald Scott, M. Kai Eleanor, and Ziaie Babak. A magnetically driven pdms micropump with ball check-valves. *Journal of Micromechanics and Microengineering*, 15(5):1021, 2005.

Vaibhav Patel and Samuel Kinde Kassegne. Electroosmosis and thermal effects in magnetohydrodynamic (mhd) micropumps using 3d mhd equations. *Sensors and Actuators B: Chemical*, 122(1):42–52, 2007. doi: 10.1016/j.snb.2006.05.015.

M. D. Patey, M. J. A. Rijkenberg, P. J. Statham, M. C. Stinchcombe, E. P. Achterberg, and M. Mowlem. Determination of nitrate and phosphate in seawater at nanomolar concentrations. *Trac-Trends in Analytical Chemistry*, 27(2):169–182, 2008.

David Payne. Modelling and simulation of passive microfuidic mixers, 19th September 2008. University of Southampton, Electronics and Computer Science Department, Supervisor; Hywel Morgan.

Wilhelm Petersen, Michail Petschatnikov, Friedhelm Schroeder, and Franciscus Colijn. Ferrybox systems for monitoring coastal waters. In N. C. Flemming K. Nittis H. Dahlin and S. E. Petersson, editors, *Elsevier Oceanography Series*, volume Volume 69, pages 325–333. Elsevier, 2003.

Power Technology Inc., 2010. P. O. Box 191117, Little Rock, AR 72219-1117, USA www.powertechnology.com.

A. R. Prakash, S. Adamia, V. Sieben, P. Pilarski, L. M. Pilarski, and C. J. Backhouse. Small volume pcr in pdms biochips with integrated fluid control and vapour barrier. *Sensors and Actuators B-Chemical*, 113(1):398–409, 2006.

D. E. Prober, M. D. Feuer, and N. Giordano. Fabrication of 300- å metal lines with substrate-step techniques. *Applied Physics Letters*, 37(1):94–96, 1980.

S. A. Prokhorova, A. Kopyshev, A. Ramakrishnan, H. Zhang, and J. Ruhe. Can polymer brushes induce motion of nano-objects? *Nanotechnology*, 14(10):1098–1108, 2003. 0957-4484.

Shize Qi, Xuezhu Liu, Sean Ford, James Barrows, Gloria Thomas, Kevin Kelly, Andrew McCandless, Kun Lian, Jost Goettertc Soper, and Steven A. Microfluidic devices fabricated in poly(methyl methacrylate) using hot-embossing with integrated sampling capillary and fiber optics for fluorescence detection. *Lab on a Chip*, 2:88–95, 2002.

S. R. Quake and A. Scherer. From micro- to nanofabrication with soft materials. *Science*, 290(5496):1536–1540, 2000.

K. P. Quinlan and M. A. DeSesa. Spectrophotometric determination of phosphorus as molybdovanadophosphoric acid. *Analytical Chemistry*, 27(10):1626–1629, 1955. doi: 10.1021/ac60106a039.

A. Rainelli, R. Stratz, K. Schweizer, and P. C. Hauser. Miniature flow-injection analysis manifold created by micromilling. *Talanta*, 61(5):659–665, 2003.

Osborne Reynolds. An experimental investigation of the circumstances which determine whether the motion of water shall be direct or sinuous, and of the law of resistance in parallel channels. *Philosophical Transactions of the Royal Society of London*, 174 (ArticleType: research-article / Full publication date: 1883 / Copyright 1883 The Royal Society):935–982, 1883.

Kyung Won Ro, Kwanseop Lim, Bong Chu Shim, and Jong Hoon Hahn. Integrated light collimating system for extended optical-path-length absorbance detection in microchip-based capillary electrophoresis. *Analytical Chemistry*, 77(16):5160–5166, 2005.

Kyung Won Ro, Jian Liu, and Daniel R. Knapp. Plastic microchip liquid chromatography-matrix-assisted laser desorption/ionization mass spectrometry using monolithic columns. *Journal of Chromatography A*, 1111(1):40–47, 2006. doi: 10.1016/j.chroma.2006.01.105.

Roithner Lasertechnik GmbH. Wiedner Hauptstrae 76, A-1040 Vienna, Austria www.roithner-laser.com.

RS Components Ltd. rswww.com. Birchington Road, Corby, Northants, NN17 9RS, UK http://uk.rs-online.com/web/.

Daniel L. Rudnick, Russ E. Davis, Charles C. Eriksen, David M. Fratantoni, and Mary Jane Perry. Underwater gliders for ocean research. *Marine Technology Society Journal*, 38(2):73–84, 2004.

J. Ruzicka and G. D. Marshall. Sequential injection - a new concept for chemical sensors, process analysis and laboratory assays. *Analytica Chimica Acta*, 237(2):329–343, 1990.

Satlantic Inc. Satlantic Inc. Richmond Terminal, Pier 9, 3481 North Marginal Road, Halifax, Nova Scotia, Canada, www.satlantic.com.

Alexis F. Sauer-Budge, Paul Mirer, Anirban Chatterjee, Catherine M. Klapperich, David Chargin, and Andre Sharon. Low cost and manufacturable complete microtas for detecting bacteria. *Lab on a Chip*, 9:2803–2810, 2009.

Sea-Bird Electronics Inc. www.seabird.com. 13431 NE 20th Street, Bellevue, Washington 98005, USA www.seabird.com.

Kevin G. Sellner, Gregory J. Doucette, and Gary J. Kirkpatrick. Harmful algal blooms: causes, impacts and detection. *Journal of Industrial Microbiology and Biotechnology*, 30(7):383–406, 2003.

M. Sequeira, M. Bowden, E. Minogue, and D. Diamond. Towards autonomous environmental monitoring systems. *Talanta*, 56(2):355–363, 2002. Times Cited: 29.

Jayna J. Shah, Jon Geist, Laurie E. Locascio, Michael Gaitan, Mulpuri V. Rao, and Wyatt N. Vreeland. Capillarity induced solvent-actuated bonding of polymeric microfluidic devices. *Analytical Chemistry*, 78(10):3348–3353, 2006. doi: 10.1021/ac051883l.

V. J. Sieben, C. S. Debes Marun, P. M. Pilarski, G. V. Kaigala, L. M. Pilarski, and C. J. Backhouse. Fish and chips: chromosomal analysis on microfluidic platforms. *IET Nanobiotechnology*, 1(3):27–35, 2007.

Vincent J. Sieben, Cedric F. A. Floquet, Iain R. G. Ogilvie, Matthew C. Mowlem, and Hywel Morgan. Microfluidic colourimetric chemical analysis system: Application to nitrite detection. *Analytical Methods*, 2:484–491, 2010. DOI: 10.1039/c002672g.

Sigma-Aldrich Company Ltd. The Old Brickyard, New Road, Gillingham, Dorset SP8 4XT www.sigmaaldrich.com.

Vishal Singhal and Suresh V. Garimella. Induction electrohydrodynamics micropump for high heat flux cooling. *Sensors and Actuators A: Physical*, 134(2):650–659, 2007. doi: 10.1016/j.sna.2006.05.007.

Vishal Singhal, Suresh V. Garimella, and Jayathi Y. Murthy. Low reynolds number flow through nozzle-diffuser elements in valveless micropumps. *Sensors and Actuators A: Physical*, 113(2):226–235, 2004. doi: 10.1016/j.sna.2004.03.002.

C. Slater, J. Cleary, K. T. Lau, D. Snakenborg, B. Corcoran, J. P. Kutter, and D. Diamond. Validation of a fully autonomous phosphate analyser based on a microfluidic lab-on-a-chip. *Water Science and Technology*, 61(7):1811–1818, 2010.

Kristian Smistrup and Howard A. Stone. A magnetically actuated ball valve applicable for small-scale fluid flows. *Physics of Fluids*, 19(6):063101–9, 2007.

Scott A. Socolofsky and Gerhard H. Jirka. *Environmental Fluid Mechanics Part I: Mass Transfer and Diffusion.* Institut fur Hydromechanik, Universitat Karlsruhe, Karlsruhe, Germany, 2nd edition edition, 2002.

W. H. Song and J. Lichtenberg. Thermo-pneumatic, single-stroke micropump. *Journal of Micromechanics and Microengineering*, 15(8):1425, 2005.

Southern California Coastal Ocean Observing System. Sccoos automated shore stations. http://www.sccoos.org/as-tech.html.

J. Steigert, S. Haeberle, T. Brenner, C. Muller, C. P. Steinert, P. Koltay, N. Gottschlich, H. Reinecke, J. Ruhe, R. Zengerle, and J. Ducree. Rapid prototyping of microfluidic chips in coc. *Journal of Micromechanics and Microengineering*, 17(2):333–341, 2007. Times Cited: 10.

L. L. Stookey. Ferrozine - a new spectrophotometric reagent for iron. *Analytical Chemistry*, 42(7):779–, 1970.

Marco Stubbe, Moritz Holtappels, and Jan Gimsa. A new working principle for ac electro-hydrodynamic on-chip micro-pumps. *Journal of Physics D: Applied Physics*, 40:6850–6856, 2007. doi:10.1088/0022-3727/40/21/055.

V. Studer, A. Pepin, and Y. Chen. Nanoembossing of thermoplastic polymers for microfluidic applications. *Applied Physics Letters*, 80(19):3614–3616, 2002.

SubChem Systems Inc. SubChem Systems Inc. 65 Pier Road, Narragansett, RI 02882 USA, www.subchem.com.

Xiuhua Sun, Bridget A. Peeni, Weichun Yang, Hector A. Becerril, and Adam T. Woolley. Rapid prototyping of poly(methyl methacrylate) microfluidic systems using solvent imprinting and bonding. *Journal of Chromatography A*, 1162(2):162–166, 2007. doi: 10.1016/j.chroma.2007.04.002.

W. C. Sung, G. B. Lee, C. C. Tzeng, and S. H. Chen. Plastic microchip electrophoresis for genetic screening: The analysis of polymerase chain reactions products of fragile x (cgg)n alleles. *Electrophoresis*, 22(6):1188–1193, 2001.

P. Svasek, E. Svasek, B. Lendl, and M. Vellekoop. Fabrication of miniaturized fluidic devices using su-8 based lithography and low temperature wafer bonding. *Sensors and Actuators A: Physical*, 115(2-3):591–599, 2004. doi: 10.1016/j.sna.2004.03.055.

Systea. Systea S.P.A. Via Paduni, 2A 03012 Anagni (FR) Italy, www.systea.it.

Patrick Tabeling. *Introduction to Microfluidics*. Oxford University Press, 2006.

A. Taberham, M. Kraft, M. Mowlem, and H. Morgan. The fabrication of lab-on-chip devices from fluoropolymers, 2008.

Alan Taberham. *Chemical analysis of nitrite in seawater using microfluidics*. Mphil/phd transfer thesis, University of Southampton, 2008.

L. Tang and N. Y. Lee. A facile route for irreversible bonding of plastic-pdms hybrid microdevices at room temperature. *Lab on a Chip*, 10(10):1274–1280, 2010. ISI Document Delivery No.: 592EP Times Cited: 1 Cited Reference Count: 35 Tang, Linzhi Lee, Nae Yoon ROYAL SOC CHEMISTRY.

TAOS. Texas Advanced Optoelectronic solutions, 1001 Klein Rd., Suite 300, Plano Texas 75074, USA www.taosinc.com.

Geoffrey Taylor. Dispersion of soluble matter in solvent flowing slowly through a tube. *Proceedings of the Royal Society of London. Series A, Mathematical and Physical Sciences*, 219(1137):186–203, 1953. ArticleType: research-article / Full publication date: Aug. 25, 1953 / Copyright 1953 The Royal Society.

Y. H. Tennico, M. T. Koesdjojo, S. Kondo, D. T. Mandrell, and V. T. Remcho. Surface modification-assisted bonding of polymer-based microfluidic devices. *Sensors and Actuators B-Chemical*, 143(2):799–804, 2010. ISI Document Delivery No.: 558UT Times Cited: 1 Cited Reference Count: 28 Tennico, Yolanda H. Koesdjojo, Myra T. Kondo, Saki Mandrell, David T. Remcho, Vincent T. ELSEVIER SCIENCE SA.

The International Seakeepers Society. The seakeeper 1000. http://www.seakeepers.com/.

The Lee Company USA. 2 Pettipaug Rd, PO Box 424, Westbrook, CT, 06498-0424 USA www.theleeco.com.

Thermodyn Corp. 3550 Silica Rd, Sylvania, Ohio 43560, USA www.thermodyn.com.

thinXXS Microtechnology AG. Amerikastrae 21, 66482 Zweibrcken, Germany www.thinxxs.com.

Thorlabs Ltd., 2010. 1 Saint Thomas Place, Ely, Cambridgeshire CB7 4EX, UK www.thorlabs.com.

T. Thorsen, S. J. Maerkl, and S. R. Quake. Microfluidic large-scale integration. *Science*, 298(5593):580–584, 2002.

Danile Thouron, Renaud Vuillemin, Xavier Philippon, Antonio Loureno, Christine Provost, Antonio Cruzado, and Vronique Garon. An autonomous nutrient analyzer for oceanic long-term in situ biogeochemical monitoring. *Analytical Chemistry*, 75 (11):2601–2609, 2003.

A. G. G. Toh, Z. F. Wang, and S. H. Ng. Fabrication of embedded microvalve on pmma microfluidic devices through surface functionalization. In V. M. Bright, T. Bourouina, B. Courtois, M. Desmulliez, J. M. Karam, and G. J. Wang, editors, *Symposium on Design, Test, Integration and Packaging of MEMS/MOEMS*, pages 267–272, Nice, FRANCE, 2008. Eda Publishing.

TOPAS Advanced Polymers GmbH. Industriepark Hchst, Gebude F821, 65926 Frankfurt-Hchst, Germany www.topas.com.

Jr-Hung Tsai and Liwei Lin. Active microfluidic mixer and gas bubble filter driven by thermal bubble micropump. *Sensors and Actuators A: Physical*, 97-98:665–671, 2002. doi: 10.1016/S0924-4247(02)00031-6.

C. W. Tsao and D. L. DeVoe. Bonding of thermoplastic polymer microfluidics. *Microfluidics and Nanofluidics*, 6(1):1–16, 2009.

C. W. Tsao, L. Hromada, J. Liu, P. Kumar, and D. L. DeVoe. Low temperature bonding of pmma and coc microfluidic substrates using uv/ozone surface treatment. *Lab on a Chip*, 7(4):499–505, 2007.

L. A. Tse, P. J. Hesketh, D. W. Rosen, and J. L. Gole. Stereolithography on silicon for microfluidics and microsensor packaging. *Microsystem Technologies*, 9(5):319–323, 2003. 10.1007/s00542-002-0254-y.

George A. Tsigdinos and Calvin J. Hallada. Solution properties of 12-heteropoly acids of molybdenum. *Inorganic Chemistry*, 9(11):2488–2492, 1970. doi: 10.1021/ic50093a022.

M. A. Unger, H. P. Chou, T. Thorsen, A. Scherer, and S. R. Quake. Monolithic microfabricated valves and pumps by multilayer soft lithography. *Science*, 288(5463): 113–116, 2000.

M. E. Vlachopoulou, A. Tserepi, P. Pavli, P. Argitis, M. Sanopoulou, and K. Misiakos. A low temperature surface modification assisted method for bonding plastic substrates. *Journal of Micromechanics and Microengineering*, 19(1):6, 2009. ISI Document Delivery No.: 393AW Times Cited: 12 Cited Reference Count: 19 Vlachopoulou, M-E Tserepi, A. Pavli, P. Argitis, P. Sanopoulou, M. Misiakos, K. IOP PUBLISHING LTD.

M. von Smoluchowski. Zur kinetischen theorie der brownschen molekularbewegung und der suspensionen. *Annalen der Physik*, 326(14):756–780, 1906.

P. Vulto, N. Glade, L. Altomare, J. Bablet, L. Del Tin, G. Medoro, I. Chartier, N. Manaresi, M. Tartagni, and R. Guerrieri. Microfluidic channel fabrication in dry film resist for production and prototyping of hybrid chips. *Lab on a Chip*, 5(2):158–162, 2005.

Inman Walker, Domansky Karel, Serdy James, Owens Bryan, Trumper David, and G. Griffith Linda. Design, modeling and fabrication of a constant flow pneumatic micropump. *Journal of Micromechanics and Microengineering*, 17(5):891, 2007.

Thomas I. Wallow, Alfredo M. Morales, Blake A. Simmons, Marion C. Hunter, Karen Lee Krafcik, Linda A. Domeier, Shane M. Sickafoose, Kamlesh D. Patel, and Andy Gardea. Low-distortion, high-strength bonding of thermoplastic microfluidic devices employing case-ii diffusion-mediated permeant activation. *Lab on a Chip*, 7(12):1825–1831, 2007.

S. H. Wang and J. M. Legare. Perfluoroelastomer and fluoroelastomer seals for semiconductor wafer processing equipment. *Journal of Fluorine Chemistry*, 122(1):113–119, 2003. ISI Document Delivery No.: 699CL Times Cited: 4 Cited Reference Count: 14 224th ACS National Meeting AUG, 2002 BOSTON, MASSACHUSETTS ACS ELSEVIER SCIENCE SA.

Douglas B. Weibel, Maarten Kruithof, Scott Potenta, Samuel K. Sia, Andrew Lee, and George M. Whitesides. Torque-actuated valves for microfluidics. *Analytical Chemistry*, 77(15):4726–4733, 2005.

WET Labs. WET Labs Instruments. 620 Applegate St., Philomath, OR 97370-0518 www.wetlabs.com/products.

Manda S. Williams, Kenneth J. Longmuir, and Paul Yager. A practical guide to the staggered herringbone mixer. *Lab on a Chip*, 8(7):1121–1129, 2008.

P. A. Willis, F. Greer, M. C. Lee, J. A. Smith, V. E. White, F. J. Grunthaner, J. J. Sprague, and J. P. Rolland. Monolithic photolithographically patterned fluorocur (tm) pfpe membrane valves and pumps for in situ planetary exploration. *Lab on a Chip*, 8 (7):1024–1026, 2008. Willis, Peter A. Greer, Frank Lee, Michael C. Smith, J. Anthony White, Victor E. Grunthaner, Frank J. Sprague, Jacob J. Rolland, Jason P.

P. A. Willis, B. D. Hunt, V. E. White, M. C. Lee, M. Ikeda, S. Bae, M. J. Pelletier, and F. J. Grunthaner. Monolithic teflon (r) membrane valves and pumps for harsh chemical and low-temperature use. *Lab on a Chip*, 7:1469–1474, 2007. Times Cited: 2.

Stephen A. Wilson, Renaud P. J. Jourdain, Qi Zhang, Robert A. Dorey, Chris R. Bowen, Magnus Willander, Qamar Ul Wahab, Magnus Willander, Safaa M. Al-hilli, Omer Nur, Eckhard Quandt, Christer Johansson, Emmanouel Pagounis, Manfred Kohl, Jovan Matovic, Bjrn Samel, Wouter van der Wijngaart, Edwin W. H. Jager, Daniel Carlsson, Zoran Djinovic, Michael Wegener, Carmen Moldovan, Rodica Iosub, Estefania Abad, Michael Wendlandt, Cristina Rusu, and Katrin Persson. New materials for micro-scale sensors and actuators: An engineering review. *Materials Science and Engineering: R: Reports*, 56(1-6):1–129, 2007. doi: 10.1016/j.mser.2007.03.001.

WMO. World Meteorological Organisation, 7bis, avenue de la Paix, Case postale No. 2300, CH-1211 Geneva 2, Switzerland www.wmo.int.

C. H. Wu and J. Ruzicka. Micro sequential injection: environmental monitoring of nitrogen and phosphate in water using a "lab-on-valve" system furnished with a microcolumn. *Analyst*, 126(11):1947–1952, 2001.

Huikai Xie and Gary K. Fedder. *Integrated Microelectromechanical Gyroscopes*, volume 16. ASCE, 2003.

J. Xie, J. Shih, Q. A. Lin, B. Z. Yang, and Y. C. Tai. Surface micromachined electrostatically actuated micro peristaltic pump. *Lab on a Chip*, 4(5):495–501, 2004.

Micah Yairi and Claudia Richter. Massively parallel microfluidic pump. *Sensors and Actuators A: Physical*, 137(2):350–356, 2007. doi: 10.1016/j.sna.2007.03.013.

Christophe Yamahata, Frdric Lacharme, Yves Burri, and Martin A. M. Gijs. A ball valve micropump in glass fabricated by powder blasting. *Sensors and Actuators B: Chemical*, 110(1):1–7, 2005. doi: 10.1016/j.snb.2005.01.005.

Jiwang Yan, Kazuyoshi Uchida, Nobuhito Yoshihara, and Tsunemoto Kuriyagawa. Fabrication of micro end mills by wire edm and some micro cutting tests. *Journal of Micromechanics and Microengineering*, 19(2):025004, 2009.

Zhen Yang, Sohei Matsumoto, Hiroshi Goto, Mikio Matsumoto, and Ryutaro Maeda. Ultrasonic micromixer for microfluidic systems. *Sensors and Actuators A: Physical*, 93(3):266–272, 2001. doi: 10.1016/S0924-4247(01)00654-9.

Mohammad Yaqoob, Abdul Nabi, and Paul J. Worsfold. Determination of nanomolar concentrations of phosphate in freshwaters using flow injection with luminol chemiluminescence detection. *Analytica Chimica Acta*, 510(2):213–218, 2004. doi: DOI: 10.1016/j.aca.2003.12.070.

Hung-Lin Yin, Yu-Che Huang, Weileun Fang, and Jerwei Hsieh. A novel electromagnetic elastomer membrane actuator with a semi-embedded coil. *Sensors and Actuators A: Physical*, 139(1-2):194–202, 2007. doi: 10.1016/j.sna.2007.01.003.

Zhizhong Yin and Andrea Prosperetti. A microfluidic 'blinking bubble' pump. *Journal of Micromechanics and Microengineering*, 15(3):643, 2005.

A. A. Yussuf, I. Sbarski, J. P. Hayes, M. Solomon, and N. Tran. Microwave welding of polymeric-microfluidic devices. *Journal of Micromechanics and Microengineering*, 15: 1692–1699, 2005. doi:10.1088/0960-1317/15/9/011.

R. Zengerle, S. Kluge, M. Richter, and A. Richter. A bidirectional silicon micropump. In *Micro Electro Mechanical Systems, 1995, MEMS '95, Proceedings. IEEE*, page 19, 1995.

Wenhua Zhang, Shuichao Lin, Chunming Wang, Jia Hu, Cong Li, Zhixia Zhuang, Yongliang Zhou, Richard A. Mathies, and Chaoyong James Yang. Pmma/pdms valves and pumps for disposable microfluidics. *Lab on a Chip*, 9(21):3088–3094, 2009. 10.1039/b907254c.